

FRACTURE TOUGHNESS TESTING OF SMALL  
CONCRETE BEAMS

by

Sheryl Rood

B.S., Kansas State University, 1983



A MASTER'S THESIS

submitted in partial fulfillment of the  
requirements for the degree of

MASTER OF SCIENCE

Department of Civil Engineering

KANSAS STATE UNIVERSITY

Manhattan, Kansas

1984

Approved:

  
Major Professor

LD  
2668  
.T4  
1984  
R66  
C.2

111202 670836

TABLE OF CONTENTS

ACKNOWLEDGEMENTS . . . . .	ii
LIST OF TABLES . . . . .	iii
LIST OF FIGURES. . . . .	iv
NOTATION . . . . .	v
CHAPTER 1 - INTROOUCTION . . . . .	1
CHAPTER 2 - LITERATURE REVIEW. . . . .	3
CHAPTER 3 - EXPERIMENTAL PROGRAM . . . . .	11
3.1 Test Specimens . . . . .	11
3.2 Testing Machine and Setup. . . . .	12
3.3 Testing Procedure. . . . .	14
(a) Compliance Calibration . . . . .	14
(b) Precracked Beams . . . . .	16
(c) Beams with Teflon Insert . . . . .	16
(d) Beam with Strain Gages . . . . .	16
CHAPTER 4 - EXPERIMENTAL RESULTS . . . . .	29
4.1 Compliance Beams . . . . .	29
4.2 Precracked Beams . . . . .	29
(a) Oetermination of Extended a/w. . . . .	29
(b) Stress intensity values. . . . .	30
(c) Energy Release Rates . . . . .	31
(d) CT00 . . . . .	33
4.3 Teflon Beams . . . . .	34
4.4 Strain Beam. . . . .	34
CHAPTER 5 - SUMMARY AND CONCLUSIONS. . . . .	56
APPENDIX I - REFERENCES . . . . .	58
APPENDIX II - SAND ANO AGGREGATE PROPERTIES. . . . .	59
APPENOIX III- STRAIN PROFILES. . . . .	64
APPENDIX IV - RAW OATA . . . . .	73

### Acknowledgements

The author would like to express her appreciation to Dr. Stuart E. Swartz for his guidance and assistance in the production of this thesis. Thanks also are given to Mr. Mojtaba Fartash and Mr. Russell Gillespie for their assistance during testing. Special thanks are given to my husband Dan for his moral support throughout this endeavor.

## LIST OF TABLES

Table 3.1	Mix Design . . . . .	28
Table 4.1	$K_I$ and $G_I$ Values for Unextended a/w in Precracked Beams. . .	47
Table 4.2	$K_{IC}$ and $G_{IC}$ Values for Extended a/w in Precracked Beams Based on CMOD. . . . .	48
Table 4.3	$K_{IC}$ and $G_{IC}$ Values for Extended a/w in Precracked Beams based on LPD . . . . .	49
Table 4.4	U and $G_{IC}$ Values in Precracked Beams . . . . .	50
Table 4.5	Summary of Average Values of $K_{IC}$ and $G_{IC}$ for Precracked Beams. . . . .	51
Table 4.6	CMOD and CTOD Values for Precracked Beams. . . . .	52
Table 4.7	$K_I$ and $G_I$ Values in Teflon Beams . . . . .	53
Table 4.8	U, $G_{IC}$ , CMOD and CTOD Values for Teflon Beams. . . . .	54
Table 4.9	Summary of Average Values of $K_{IC}$ and $G_{IC}$ for Teflon Beams. . . . .	55

## LIST OF FIGURES

Figure 2.1	Relationship between CTOD and CMOD for a Rigid Rotation about the Center of Rotation . . . . .	10
Figure 3.1	Three Point Bending Configuration. . . . .	18
Figure 3.2	Stress Versus Transverse Strain. . . . .	19
Figure 3.3	Stress Versus Longitudinal Strain . . . . .	20
Figure 3.4	CMOD Transducer Yokes. . . . .	21
Figure 3.5	Reverse Three Point Bending Configuration. . . . .	22
Figure 3.6	LPD Transducer Set Up. . . . .	23
Figure 3.7	Typical Failure Surfaces . . . . .	24
Figure 3.8	Typical CMOD Trace . . . . .	25
Figure 3.9	Typical LPD Trace. . . . .	26
Figure 3.10	Strain Gage Placement on Beam. . . . .	27
Figure 4.1	LPD Traces With and Without Slippage . . . . .	35
Figure 4.2	CMOD Compliance Calibration Curve. . . . .	36
Figure 4.3	LPD Compliance Calibration Curve . . . . .	37
Figure 4.4	$K_{IC}$ Versus $a/w$ for Unextended Crack Length. . . . .	38
Figure 4.5	$K_{IC}$ Versus $a/w$ for Extended Crack Length Based on CMOD. . . . .	39
Figure 4.6	$K_{IC}$ Versus $a/w$ for Extended Crack Length Based on LPD . . . . .	40
Figure 4.7	$G_{IC}$ Versus $a/w$ for Unextended Crack Length. . . . .	41
Figure 4.8	$G_{IC}$ Versus $a/w$ for Extended Crack Length Based on CMOD. . . . .	42
Figure 4.9	$G_{IC}$ Versus $a/w$ for Extended Crack Length Based on LPD . . . . .	43
Figure 4.10	$U$ Versus $a/w$ for Unextended Crack Length. . . . .	44
Figure 4.11	$U$ Versus $a/w$ for Extended Crack Length Based on CMOD. . . . .	45
Figure 4.12	$U$ Versus $a/w$ for <u>E</u> xtended Crack Length Based on LPD . . . . .	46

## Notation

a	- Crack Depth
b	- Beam Width
CMOD	- Crack Mouth Opening Displacement
CTOD	- Crack Tip Opening Displacement
E	- Modulus of Elasticity
G	- Energy Release Rate
$K_I$	- Stress Intensity Factor for Opening Mode
L	- Beam Length
M	- Moment
P	- Load
P-Max	- Maximum Load
R	- Rotation Factor
w	- Beam Depth
v	- Poisson's Ratio

## Chapter 1

### INTRODUCTION

The applicability of fracture mechanics to concrete has been under investigation for many years. Various test specimens and testing procedures have been used but few have had successful and consistent results. Concrete has proved to be a notch sensitive material, that is, it behaves differently when notched with teflon or a sawcut, than it does when it is precracked. This factor alone affects many of the previous investigations since many were done with notched beams. Many methods of analysis have been proposed, as have many testing procedures. In spite of the problems encountered it is still felt that fracture mechanics may be the best way to describe the fracture behavior of concrete.

An extensive study has been started in an attempt to verify the relationships between the fracture parameters for plain concrete in bending. The results presented here are representative of small beams with a width of 3 in., a depth of 4 in., and a span of 15 in. loaded in three-point bending. A modified compliance calibration technique was used to precrack the beams and load versus crack mouth opening displacement (CMOD) and load versus load point displacement (LPD) plots were obtained simultaneously. Five precracked beams of each crack depth to beam depth,  $a/w$ , ratio of 0.3, 0.5, and 0.7 were failed as well as two beams each of the same  $a/w$  ratios with teflon. A detailed description of the methods used is found in Chapter 3.

The results obtained included stress intensity factors ( $K_{IC}$ ), energy release rates based on  $K_{IC}$ , energy release rates based on the J-integral concept, energy release rates found from an energy method adapted from Petersson (4), and the crack tip opening displacement (CTOD). The use of the crack length at the point of instability was compared to the use of the precracked length as determined by the dye. These results are presented in Chapter 4.

Results obtained show fairly consistent energy release rates based on the energy approach and the J-integral approach, especially for larger crack lengths. Those based on the stress intensity factors tended to be much lower than those found by the other two methods. The CTOD values however, show consistent results for the extended crack lengths. The conclusions and summary are found in Chapter 5.



## Chapter 2

## LITERATURE REVIEW

Many experiments have been performed in an attempt to prove that the fracture toughness of concrete is a material property. Factors such as test specimen, testing procedure and method of analysis have been investigated and some of the pertinent investigations are described below.

An intensive study by Go and Swartz (3) investigated four criteria which were felt to be related to concrete failure. They were energy release rate, J-integral concept, stress intensity, and the crack tip opening displacement (CTOD). Their studies also included the feasibility of the compliance calibration technique and considered crack growth and the influence of the microcracking zone.

Studies on the stress intensity factor consisted of a comparison between the bending analogy, finite element method, and the Srawley formula in determining the stress intensity factor. An equation for estimating  $K_I$  was derived using the least squares method and is as follows (3):

$$K_I = \frac{M}{bw^{1.5}} (Az^2 + Bz + C + Dz^{-1} + Ez^{-2}) \dots \dots \dots (2.1)$$

M = moment at midspan

b = beam width

w = beam depth

z =  $1 - a/w$

A, B, C, D, E = Constants determined for different span/depth ratios

The applicability of the compliance calibration method as it relates to concrete was investigated by comparing crack length estimates found using the compliance curve with actual crack lengths revealed by the dye penetrant (3). Thirty specimens, made in two sets, were three inches wide, four inches deep and had a fifteen inch span. Two beams per set were notched at midspan to various depths and used to determine compliance and a plot of compliance versus  $a/w$  obtained. Fourteen of the beams had teflon inserts and were loaded to failure under load control. A load versus CMOD trace was obtained and the compliance found from the initial slope. Estimated crack lengths from the compliance curve were compared with the actual crack lengths. The remaining twelve specimens were notched 0.5 in. (12.7 mm) then loaded under strain control to generate a crack of desired length using the compliance curve. Dye was inserted and worked into the crack while the beam was in an inverted position. The beam was then righted and loaded to failure under load control. The estimated crack length was determined using the compliance curve and the slope of the trace after crack closure was overcome. This crack depth was compared with the actual crack depth revealed by dye.

Go and Swartz (3) concluded that application of the compliance calibration technique should be associated with the real crack length of a precracked beam instead of a sawcut depth. To determine energy release rates, sixteen specimens were tested in three-point-bending and a trace of either load versus CMOD or load versus LPD and a compliance curve based on LPD was obtained.

The stress intensity approach considered the specimen to be in plane strain and assumed that the sliding mode and tearing mode stress intensity

factors were negligible compared to the opening mode. The equation for plane strain then reduced to:

$$G = \frac{1-\nu^2}{E} K_I^2 \dots \dots \dots (2.2)$$

in which  $K_I$  was based on the extended crack length.

The J-integral approach is based on the concept that for an infinitesimal amount of crack extension, the decrease in stored elastic energy of a cracked body loaded under displacement control is identical to the decrease in potential energy when loaded under load control. To use this concept experimentally, a plot of the energy required to trigger the instability versus the unextended  $a/w$  was made and the slope of this straight line gave the energy change per change in  $a/w$ . This energy rate was then divided by the effective remaining area, that is, a surface 15% larger than the area revealed by dye to account for the roughness of the surface (3). A modification of Petersson's (4) approach was also investigated. The total energy consumed was calculated by finding the area up to the point of instability of the failure plot. The energy release rate was then calculated by dividing the energy by the effective remaining area at the point of unstable crack growth.

Conclusions reached by Go and Swartz were that the average energy release rate for the J-integral and stress intensity approaches based on stable crack growth and microcracking extension were in good agreement. Petersson's method, when not considering stable crack growth, gave lower values. However, good agreement with the other two methods was found when Petersson's method was applied considering crack extension. The results

based on the assumption of zero crack growth are clearly a lower bound on the actual failure results either in terms of energy release rate or stress intensity according to Go and Swartz. It was also determined that linear-elastic fracture mechanics concepts are valid in the study of concrete fracture.

The COD approach for specifying fracture toughness was examined. Based on the concept that the rotating center of the crack is at the strain reversal point (i.e. neutral axis), Go and Swartz used William's stress function to evaluate the rotation factor R for the 3 point bending specimen (3). The rotation factor, R, is defined as shown in Figure 2.1. For span/depth ratios equal to 3.75, the average value of R was 0.45 with maximum deviation less than 5%. Using this rotation factor, the relationship between the CMOD and CTOD was found to be

$$S(CTOD) = \frac{R(w-a)}{R(w-a)+a+z} v(CMOD) \dots \dots \dots (2.3)$$

for beams in three point bending. The constant, z, is the thickness of the knife edge as shown in Figure 2.1. It was concluded that the CTOD showed promise as a fracture criterion for concrete. It may be a valid alternative treatment instead of  $G_I$  or  $K_I$ .

A study done by Fartash (2) was conducted to compare the behavior of beams with notches to those with natural cracks. A total of ninety six beams with a width of 3 in., a depth of 4 in. and a span of 15 in. were made and tested in 3 and 4 point bending. Twelve beams were used for compliance curves, forty-eight had teflon inserts, and forty-eight were precracked. The crack lengths used in this study gave a/w ratios of 0.3,

0.5, 0.7. Of the specimens used in this investigation half of them had a strength of 3200 psi and half had a compressive strength of 6700 psi.

All testing was done using an electro-hydraulic materials testing system (MTS). Using the compliance technique developed by Swartz, Hu and Jones (5), the plain beams were initially notched .40 in. (10.16 mm) to .45 in. (11.43 mm) then precracked to the desired length. This was done by loading the beam in strain control until the slope of the load displacement plot decreased at which point the load was removed. The compliance of the straight part of the curve was used to determine the estimated crack length from the compliance calibration curve. This was repeated until the desired crack length was reached. All precracked specimens were then loaded to failure using load control. The teflon beams were loaded to 0.6 P-max to determine the compliance based on the CMOD trace, then unloaded and reloaded to failure.

A load versus CMOD was obtained for each specimen tested. From these, compliance values were calculated as well as net bending stresses. The average bending stress for each a/w ratio of approx. 0.3, 0.5, 0.7 was plotted versus the a/w ratio. The plots of average stress intensity values versus average a/w ratios indicated that both batches yielded notch-sensitive specimens. It was found that the value of stress intensity decreased with increasing a/w ratios. A relationship between stress intensity values for precracked and prenotched beams for various a/w ratios was found to be:

$$\frac{K_{IP}}{K_{IT}} = .9137 + 1.6118(a/w) \dots \dots \dots (2.4)$$

Fartash concluded that in all cases the naturally cracked beams yield higher failure loads, stress intensity values, and bending stresses than notched beams with the same crack length. True fracture toughness cannot be obtained with notched beams unless a correlation between precracked and notched beams is used.

The presence of the fracture zone in concrete was investigated by Petersson (4). Stable tensile tests were performed on concrete specimens with a maximum aggregate size of 5/16 in. (8 mm.) and a water cement ratio of 0.6. After being cast in steel molds, the specimens were cured in lime saturated water until one day before testing when they were removed and wrapped in plastic foil. Total curing time was seven days. The specimens were allowed to dry slightly while being placed in the testing machine, then all sides but one were rewetted. As the fracture zone developed it became visible as a dark area on the dry side of the specimen. This dark area was a result of the water absorbed by the zone due to capillary forces.

Petersson observed that the fracture zone was about  $9.84 \times 10^{-4}$  in. ( $25 \times 10^{-3}$  mm) to  $19.69 \times 10^{-4}$  in. ( $50 \times 10^{-3}$  mm) wide when the crack became visible. The width of the fracture zone appeared to be of the same magnitude as the size of the maximum aggregate particle.

In addition to investigating the fracture zone Petersson also determined the fracture energy ( $G_F$ ) which he defined to be the amount of energy necessary to create one unit of area of a crack. In order to

measure this accurately, the specimen was loaded to failure under displacement control to obtain a stable and well defined length of crack propagation. Notched beams were loaded in 3-pt-bending and a stable load to failure plot obtained. In half of the beams weights were placed on the beam outside the supports to compensate for the energy due to the weight of the beam alone. These results were compared to those obtained without compensation for the weight of the beam and it was found that the true value obtained by compensation gave values 50% to 250% higher than the uncompensated beams. Two methods of estimating the true  $G_F$  based on the results of uncompensated beams were evaluated. Additional testing was done on prenotched (teflon inset) and notched (sawcut) beams as well as direct tension specimens. The specimens were loaded in displacement control and the plot of load versus displacement obtained. The  $G_F$  values were calculated as the area under the stable curves divided by the uncracked area at the beginning of testing. In determining the energy consumed by the fracture zone, the amount of energy consumed by the material outside the fracture zone before the tensile strength was reached was subtracted. This was done by drawing a straight line, parallel to the major slope of the increasing portion of the graph, to the point of maximum load. The area between this line and the increasing portion of the curve was the area subtracted.

Petersson concluded that although  $G_F$  is slightly affected by beam depth, it seems to be useful as a material parameter. However the  $G_F$  must be calculated using the stable plot obtained using displacement control since dynamic effects are incurred when using load control causing crack growth to become unstable.

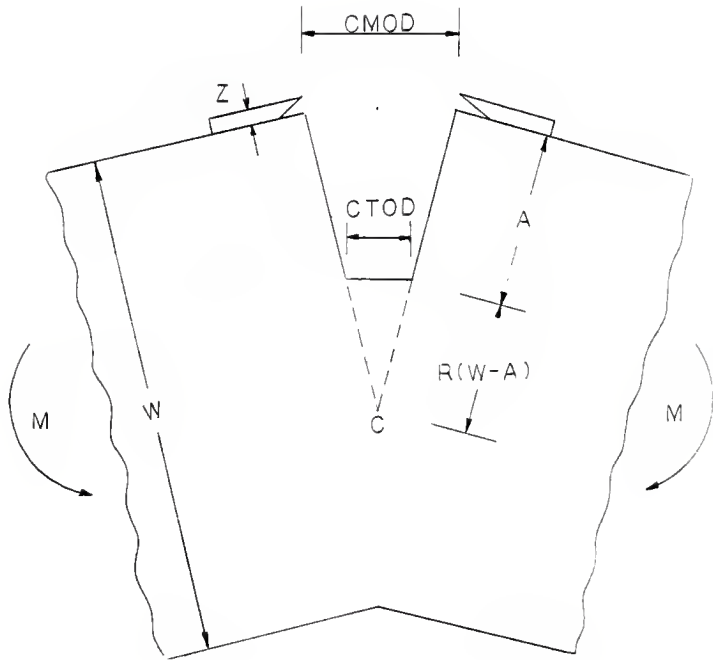


FIG. 2.1 RELATIONSHIP BETWEEN CTOD AND CMOD  
FOR A RIGID ROTATION ABOUT THE CENTER OF ROTATION



## Chapter 3

### EXPERIMENTAL PROGRAM

#### 3.1 Test Specimens

One size of beam was constructed to the following dimensions:

$$\begin{aligned}l &= 16 \text{ in. (406.4 mm)} \\w &= 4 \text{ in. (101.6 mm)} \\b &= 3 \text{ in. (76.2 mm)}\end{aligned}$$

Figure 3.1 shows the beam dimensions. One mix design was used as given in Table 3.1. This gave a nominal cylinder compressive strength of 8100 psi (55.81 MPa), Poisson's Ratio of .195, and a Modulus of Elasticity of  $5.34 \times 10^6$  psi ( $36.79 \times 10^3$  MPa). Figures 3.2 and 3.3 show stress versus transverse strain and stress versus longitudinal strain respectively. Cylinder data are listed in Appendix IV with the raw data. Two sets of twenty beams each were cast for a total of forty beams. Care was taken in construction and curing of the beams to ensure that the two sets would have nearly identical material properties at the time of testing.

Of the forty beams cast, fourteen were used for compliance calibration: two beams for each a/w ratio of .3, .4, .5, .6, .7, .8, and .9. Fifteen beams, five of each a/w ratio of .3, .5, and .7, were precracked and six beams, two of each a/w ratio of .3, .5, and .7, had a teflon insert which simulated the a real crack without the effect of aggregate interlock. The .003 in. (.076 mm) width teflon strips were inserted using the method described in Reference 2. One beam was instrumented with strain gages in an attempt to determine the strain distribution ahead of the crack tip. The remaining beams were used as "spares".

### 3.2 Testing Machine and Set Up

An electro-hydraulic materials testing system (MTS) was used throughout the testing program. Crack mouth opening displacements (CMOD) and load point displacements (LPD) were monitored simultaneously through the use of commercially available displacement transducers (MTS 632.D5 B-60) which have a maximum sensitivity of  $\pm .002$  in. ( $\pm .0508$  mm) per 10 volt full scale output. During loading of the specimens, simultaneous traces of load versus CMOD and load versus LPD were obtained.

The MTS made it possible to load the specimens in three different control modes. Under load control, the span responds to the amount of load as the primary feedback. Operating in this control mode assures a constant load rate regardless of the rate of crack propagation and was used when loading the beams to failure. Under displacement control, the span responds to the displacement of the CMOD transducer as the primary feedback. In this control mode, it is possible to crack the beam to a desired depth without much danger of premature failure since the rate of CMOD is controllable instead of the load rate. Precracking of the beams was done under displacement control. The third control mode is stroke control. It uses the displacement of the loading head as its primary feedback. This mode was used in the dye application process due to its sensitivity and controllability.

Appropriate scale settings on the plotters were important to obtain the best size traces. The plotters used were MTS 431.13A - D2 (Type 2D0 Control Module) and a summary of X (load) and Y (displacement) axis scale settings follows:

X-axis Metric Setting

Ranges using Calib. setting:

0.5% per cm = 0.05 V/cm  
 1.0% per cm = 0.10 V/cm  
 2.5% per cm = 0.25 V/cm  
 5.0% per cm = 0.50 V/cm  
 10.0% per cm = 1.00 V/cm

CM00 - Range 2  $\pm 1 \times 10^{-2}$  in./10V =  $\pm 1 \times 10^{-3}$  in./V

0.5% : 1 cm =  $5.0 \times 10^{-5}$  in.  
 1.0% : 1 cm =  $1.0 \times 10^{-4}$  in.  
 2.5% : 1 cm =  $2.5 \times 10^{-4}$  in.  
 5.0% : 1 cm =  $5.0 \times 10^{-4}$  in.

CM0D - Range 1  $\pm 2 \times 10^{-2}$  in./10V =  $\pm 2 \times 10^{-3}$  in./V

0.5% : 1 cm =  $1 \times 10^{-4}$  in.  
 1.0% : 1 cm =  $2 \times 10^{-4}$  in.  
 2.5% : 1 cm =  $5 \times 10^{-4}$  in.  
 5.0% : 1 cm =  $1 \times 10^{-3}$  in.

LPO - Range 2  $\pm 9.72 \times 10^{-4}$  in./V

0.5% : 1 cm =  $4.86 \times 10^{-5}$  in.  
 1.0% : 1 cm =  $9.72 \times 10^{-5}$  in.  
 2.5% : 1 cm =  $2.43 \times 10^{-4}$  in.  
 5.0% : 1 cm =  $4.86 \times 10^{-4}$  in.

LPO - Range 1  $\pm 19.08 \times 10^{-4}$  in./V

0.5% : 1 cm =  $9.54 \times 10^{-5}$  in.  
 1.0% : 1 cm =  $19.08 \times 10^{-5}$  in.  
 2.5% : 1 cm =  $4.77 \times 10^{-4}$  in.  
 5.0% : 1 cm =  $9.54 \times 10^{-4}$  in.

Y-axis Metric Setting

Ranges using Calib. setting:

0.5% per cm = 0.05 V/cm  
 1.0% per cm = 0.10 V/cm  
 2.5% per cm = 0.25 V/cm  
 5.0% per cm = 0.50 V/cm  
 10.0% per cm = 1.00 V/cm

CM00 and LPO - All Ranges 1.0 V = 1000 lbs.  
 Using load cell with X 10

0.5% : 1 cm = 50 lb.

1.0% : 1 cm = 100 lb.  
 2.5% : 1 cm = 250 lb.  
 5.0% : 1 cm = 500 lb.

The settings used are listed on each trace.

The rate at which the beams are loaded is governed by both the span and the frequency controls on the MTS. The span was generally set on 110 and the frequency at 1.0 with the function generator set at 0.1/1.1 on the MTS model panel 410.21. During loading to failure, this setting gave an average loading rate of 19 lb./sec. (84.55 N/sec.)

A listing of the settings used throughout the testing is as follows:

Model 410.21 Panel

Function: upward ramp function  
 Function Generator: 0.1/1.1  
 Frequency: 1.0

406 Controller

Cal factor = 4.21  
 Excitation = 4.41  
 Gain = 8  
 Rate = 4.6  
 P = 0  
 Fdbk Select = XDCR1 = stroke control  
                   XDCR2 = load control  
                   EXT = strain control

Problems within the MTS caused delays in testing and an erratic testing schedule.

### 3.3 Testing Procedure

#### (a) Compliance Calibration

Each compliance specimen was initially notched at midspan using a concrete saw. The notch was 0.13 in. (3.302 mm) wide and eighty percent

of the desired crack length in depth. The purpose of the starter notch was to ensure cracking at midspan. After the beam had been notched, the yoke shown in Figure 3.4 and the CMOD transducer were mounted on the specimen and placed in the loading set up as shown in Figure 3.1. The beam was then loaded in three point bending using displacement control and a plot of load versus CMOD was obtained. The inverse slope of the major portion of this curve gave the compliance value for the beam's current  $a/w$  ratio. Loading was continued until the slope began to decrease indicating crack growth. Load was removed then reapplied, and the compliance was measured from the new trace. This procedure was repeated until it appeared that the desired crack length had been reached. The CMOD transducer was removed and the specimen was inverted and placed in a reverse three point bending configuration as shown in Figure 3.5. Using stroke control, the beam was loaded to approximately seventy-five percent of the last precracking load applied. This opened the crack for dye insertion. Vanish, a product of The Drackett Products company, was inserted using a pipette and the load then cycled to work the dye into the crack. Once the dye had been worked in, the CMOD transducer was attached again, and the specimen replaced in the loading apparatus as during precracking. The loading head was raised to where it touched the upper head, but no load was being applied. At this point, the LPD transducer was attached to the system shown in Figure 3.6. The beam was then loaded to failure using load control and simultaneous traces of load versus CMOD and load versus LPD were obtained.

The actual average crack depth was determined by finding the area of the beam penetrated by the dye and dividing it by the width of the beam.

Typical failure surfaces are shown in Figure 3.7. The crack depth found corresponds to the compliance of the failure curve. This data provides one point on the compliance curve.

Each of the fourteen compliance specimens were tested in this manner and a compliance versus  $a/w$  ratio curve drawn.

#### (b) Precracked Beams

Each precracked beam was initially notched with a sawcut as the compliance specimens were. A crack was then generated to the desired depth by loading the beam until the corresponding compliance value as found on the compliance curve, was reached. As previously described the dye was applied and the beam loaded to failure. Traces of load versus CMOD and load versus LPO were obtained as well as the areas of the failure surfaces. Typical traces are shown in Figure 3.8 and 3.9. In all traces the vertical axis gives the applied load. The horizontal axis gives LPO or CMOD as appropriate. The scale factors are shown on each trace.

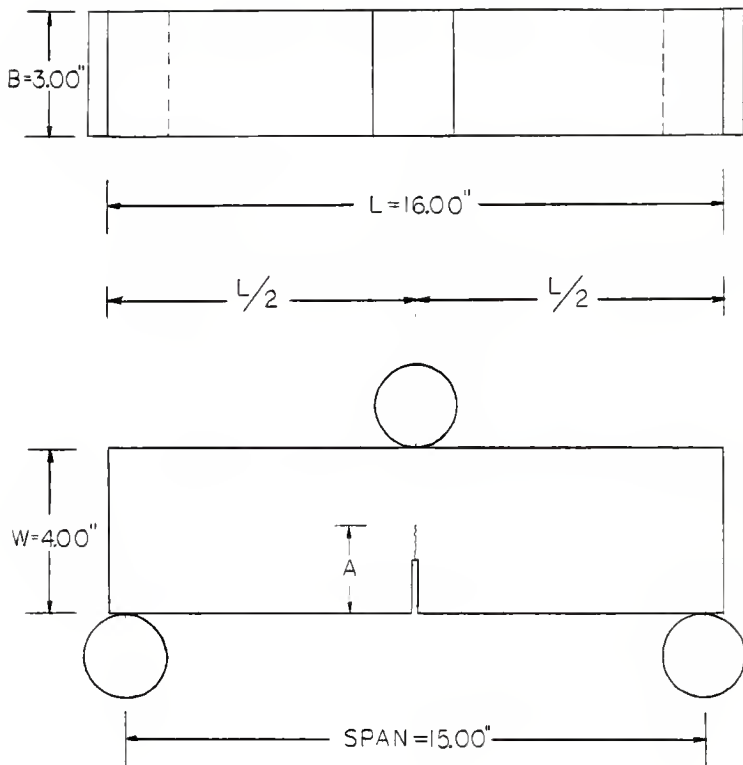
#### (c) Beams With Teflon Insert

Since no precracking and dye insertion were needed, the beams were instrumented with both transducers and loaded to failure under load control. Traces of load versus CMOD and load versus LPO were obtained. The cracked area caused by the teflon was readily visible.

#### (d) Beam With Strain Gages

The beam was initially sawcut 0.96 in. (24.384 mm) to ensure cracking at midspan. Fifteen gages, EA-06-120LZ-120 with a gage length of .375 in. (9.53mm), were affixed to each side of the beam at midspan above the crack tip. Strain data was obtained and recorded through the use of an Optim data acquisition system. The beam was loaded using displacement control until cracking occurred. Strain readings were taken and the compliance at

that point measured. This procedure was repeated for increased crack depths. Figure 3.10 shows the gage placement.



1.0 IN. = 25.4 MM

FIG. 3.1 THREE POINT BENDING CONFIGURATION



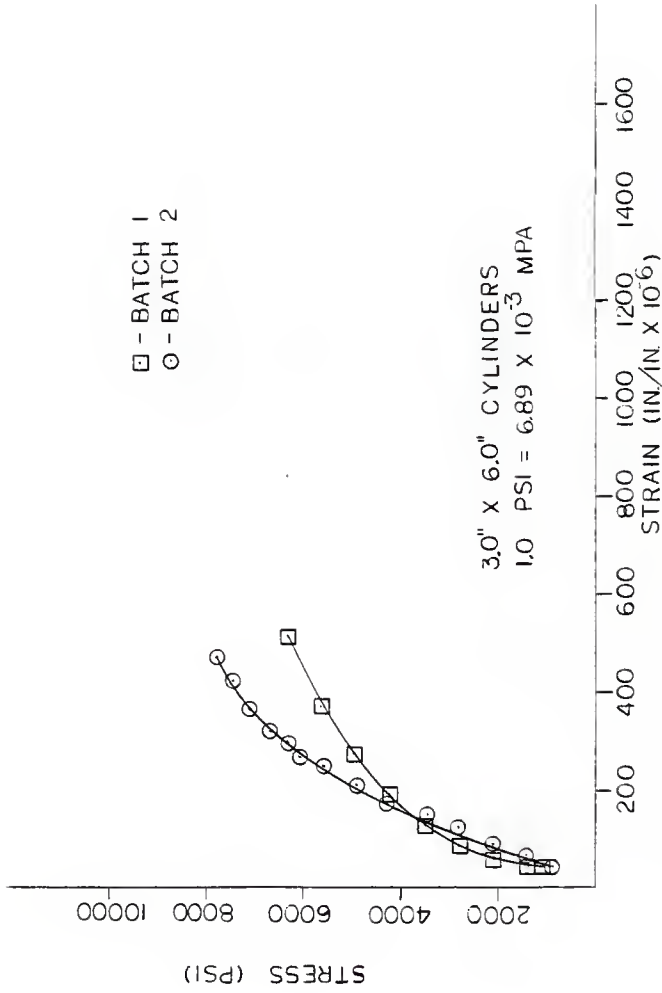


FIG. 3.2 STRESS VERSUS TRANSVERSE STRAIN.

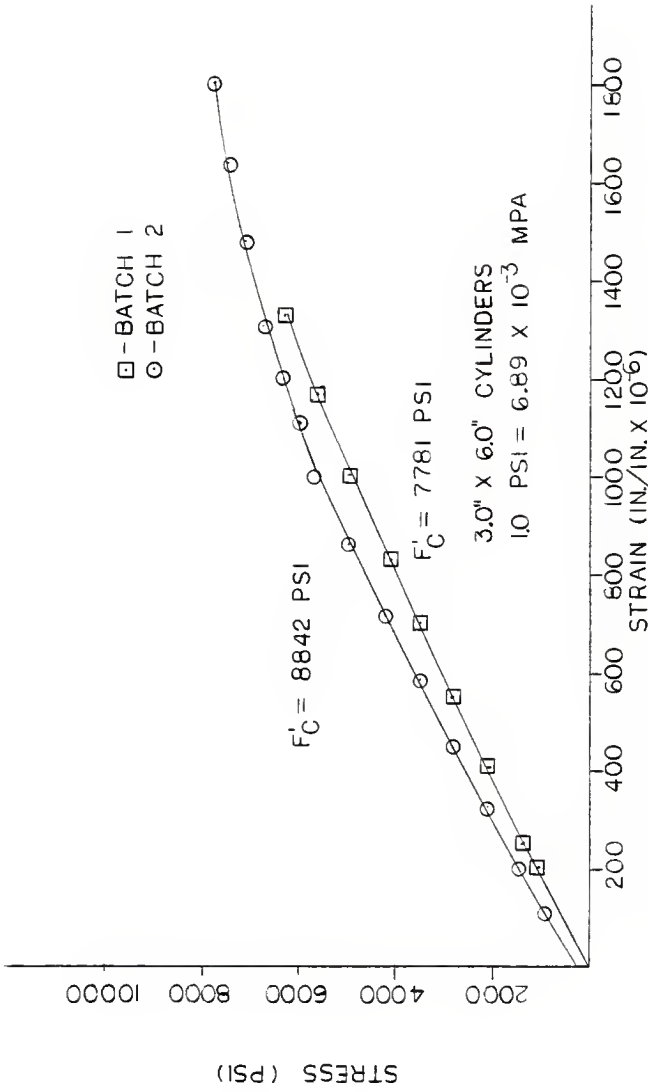
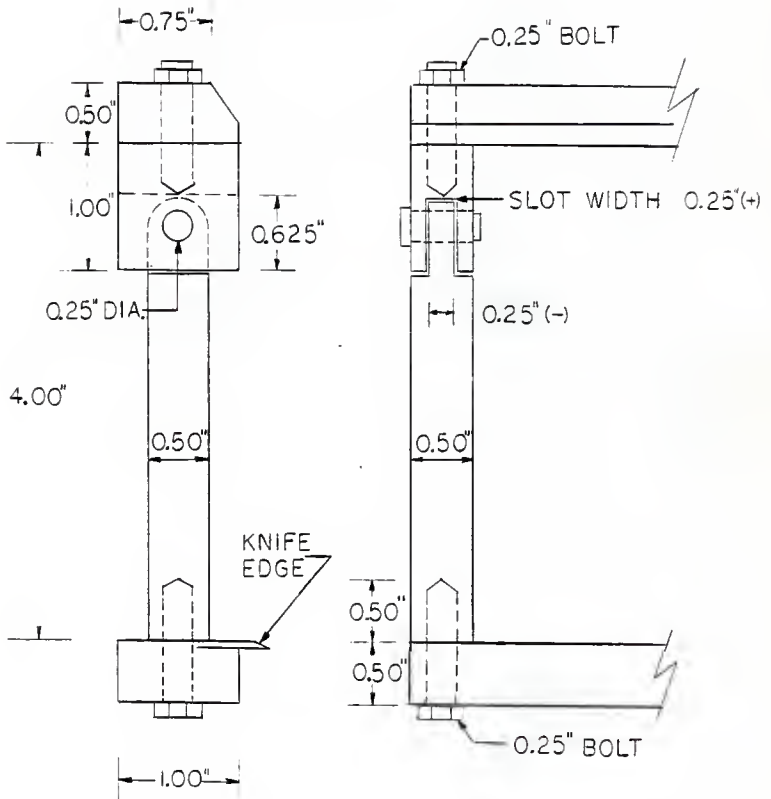
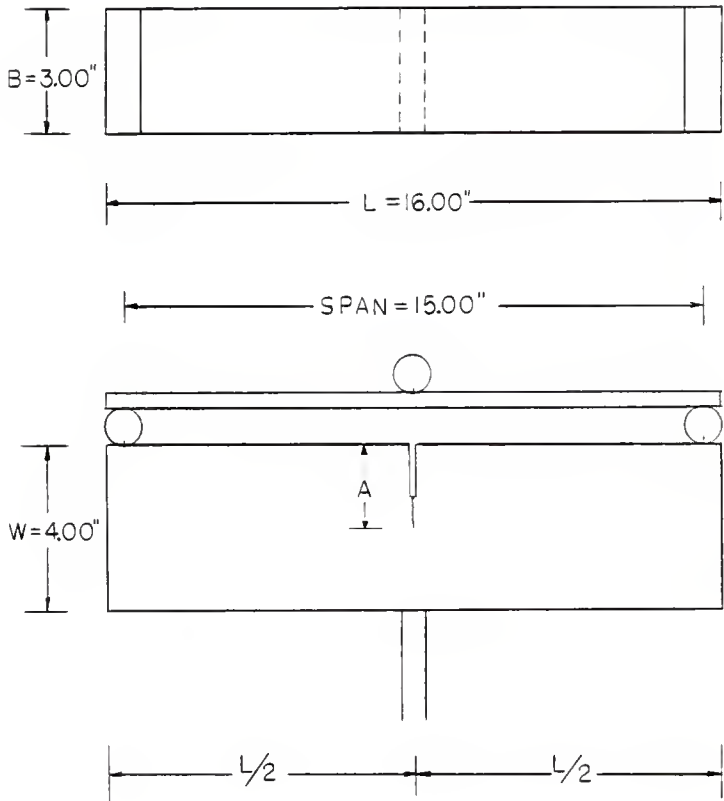


FIG. 3.3 STRESS VERSUS LONGITUDINAL STRAIN.



1.0 IN. = 25.4 MM

FIG. 3.4 CMOD TRANSDUCER YOKES



1.0 IN. = 25.4 MM

FIG. 3.5 REVERSE THREE POINT BENDING CONFIGURATION

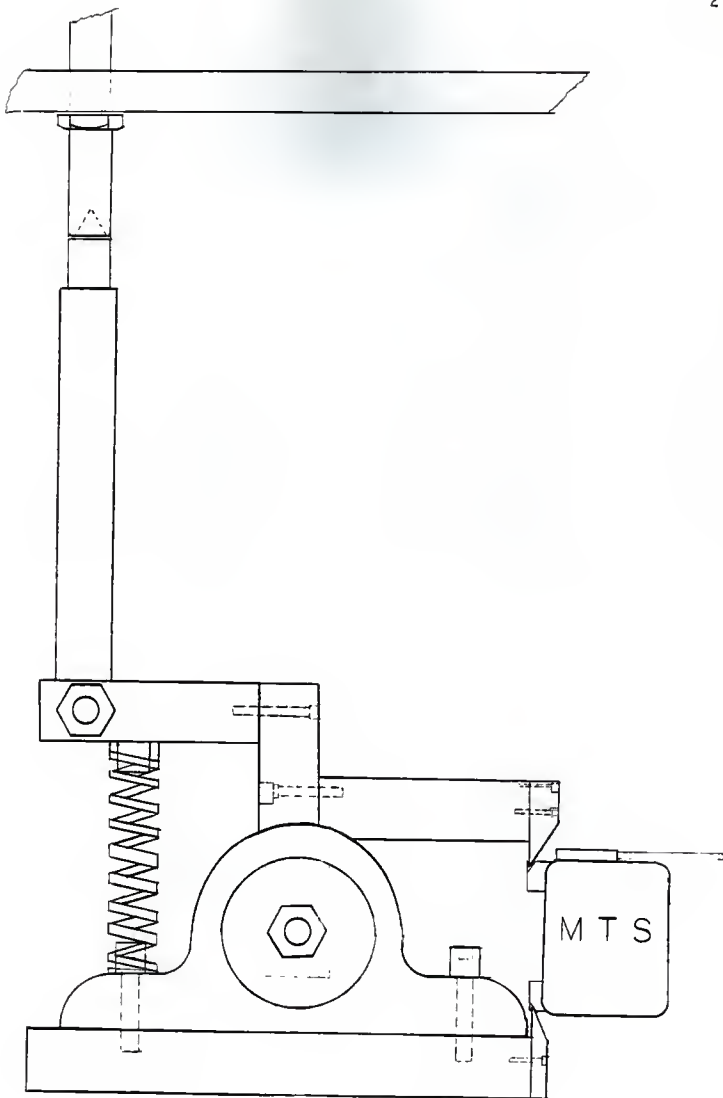
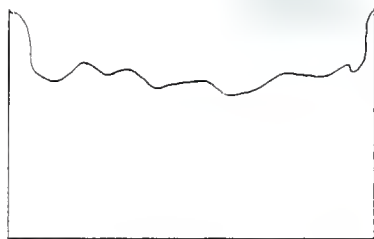
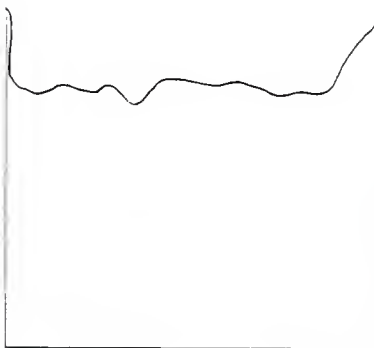


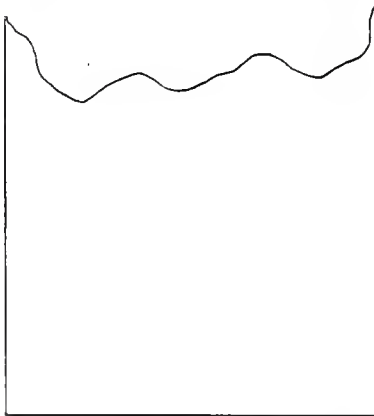
FIG. 3.6 LPD TRANSDUCER SET UP



$A/W = 0.326$   
BEAM NO. C-2



$A/W = 0.525$   
BEAM NO. C-4



$A/W = 0.685$   
BEAM NO. B-19

FIG. 3.7 TYPICAL FAILURE SURFACES

8/17/64  $c_{MOD} - \gamma_{WZ} = 3$   
DATE

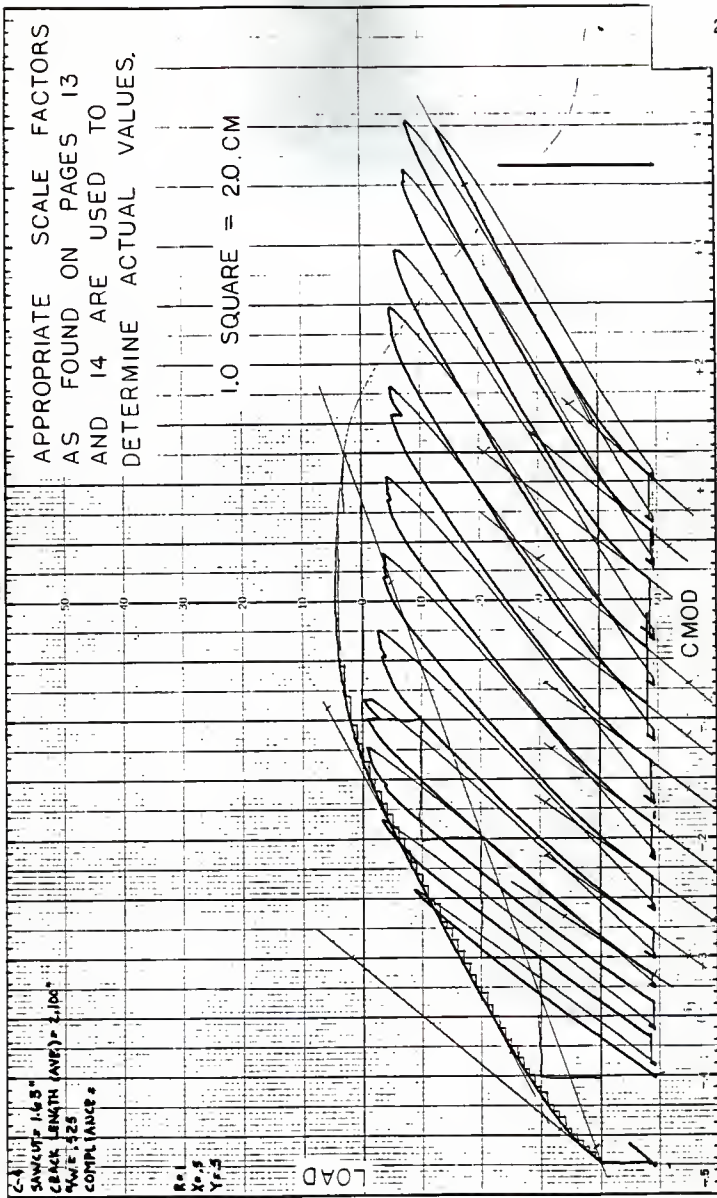


FIG. 3.8 TYPICAL CMOD TRACE.

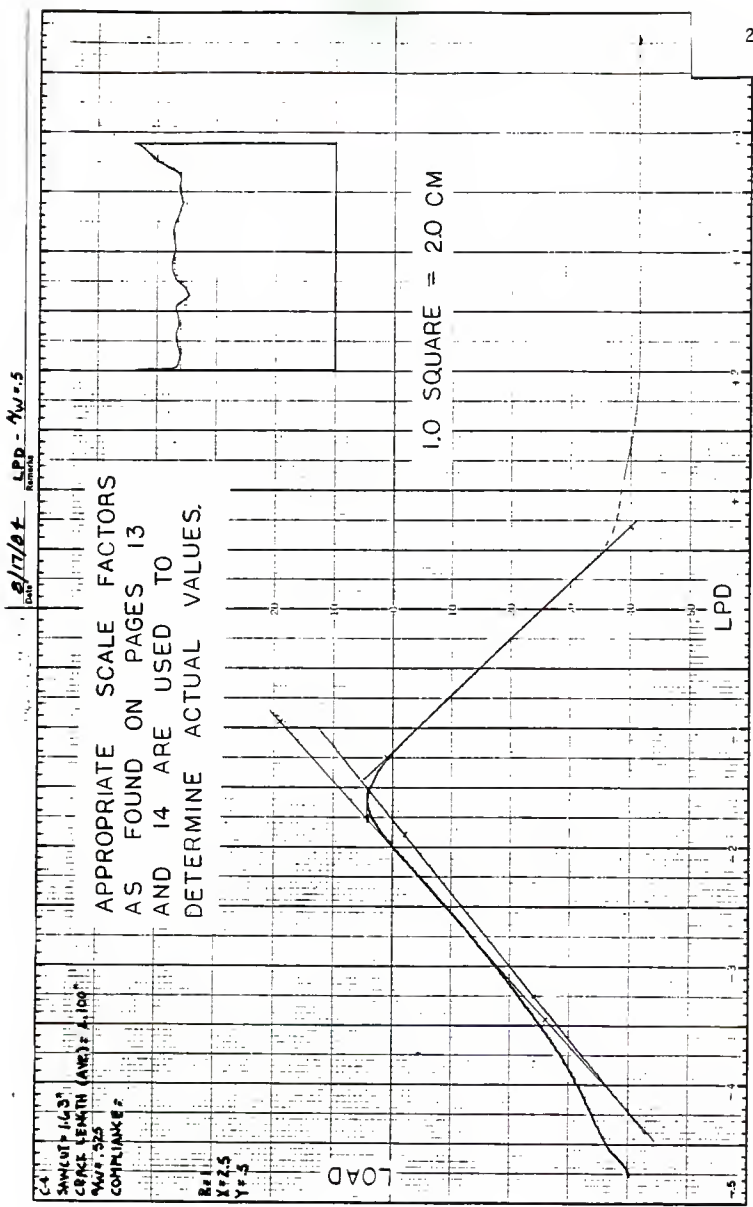
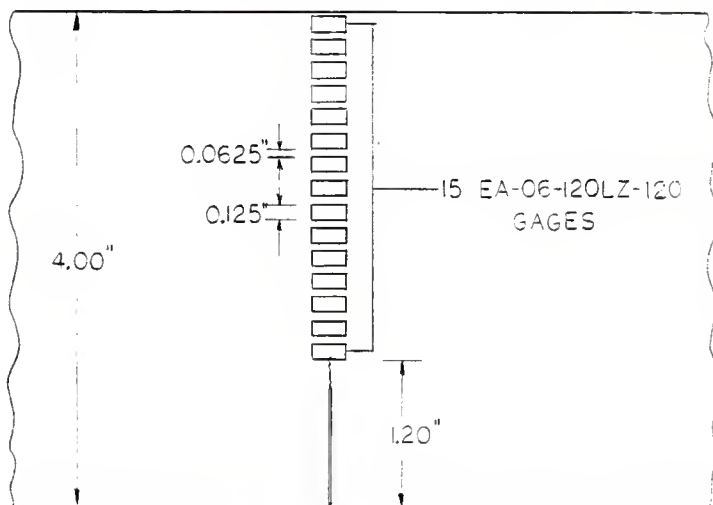


FIG. 3.9 TYPICAL LPD TRACE.





1.0 IN. = 25.4 MM

FIG. 3.10 STRAIN GAGE PLACEMENT ON BEAM

Table 3.1 Mix Design

	<u>Batch 1</u>	<u>Batch 2</u>
Water/Cement	0.50	0.50
Cement Type	I	I
S.G. Sand*	2.65	2.65
S.G. Aggregate*	2.56	2.56
S.G. Cement	3.15	3.15
% Sand by weight	32.68%	32.68%
% Aggregate by weight	47.46%	47.46%
% Cement by weight	13.24%	13.24%
% Water by weight	6.62%	6.62%
Density of concrete	149.7 pcf (23.48 kN/m <sup>3</sup> )	149.7 pcf (23.48 kN/m <sup>3</sup> )
Curing Time	145 days	138 days
Compressive Strength	7950 psi (54.78 MPa)	8130 psi (56.02 MPa)
Tensile Strength**	601 psi (4.14 MPa)	665 psi (4.58 MPa)
Superplasticizer	400 ml	300 ml
Slump	7.25 in. (184.15 mm)	7.00 in. (177.80 mm)
Sand Fineness Modulus	2.91	2.91
Maximum Aggregate Size	0.75 in. (19.05 mm)	0.75 in. (19.05 mm)

\* Sand and aggregate properties and testing procedures in Appendix I.

\*\* Tensile strength determined by split cylinder test as described in ASTM.

## Chapter 4

### EXPERIMENTAL RESULTS

#### 4.1 Compliance Beams

The fourteen compliance beams were tested as described previously. Two compliance curves were drawn by plotting the compliance value versus the  $a/w$  ratio. One was based on compliance values found from the load versus CMOD traces and the other was based on values found from the load versus LPD traces. These compliance values were calculated using the slope of the major portion of the trace rather than the initial slope since the initial slope showed evidence of crack closure and slippage of the testing apparatus. The slippage referred to was primarily in the LPD set up and is noticeable in many of the graphs. A load versus LPD trace without slippage and one with slippage are shown in Figure 4.1. Compliance curves are shown in Figures 4.2 and 4.3.

Some difficulty was had in precracking the compliance specimens with  $a/w$  ratios of .7, .8, and .9.

#### 4.2 Precracked Beams

The fifteen precracked beams were tested as previously described. Stress intensity values and energy release rates were calculated for both the unextended and the extended crack lengths. The value of the crack tip opening displacement (CTOD) was also obtained.

##### (a) Determination of Extended $a/w$

The extended  $a/w$ , corresponding to the point of unstable crack growth, was calculated by drawing a line from the origin of the CMOD trace

to the point at which the load begins to drop off, that is, the point of unstable crack growth. The compliance based on the slope of this line was calculated and the extended  $a/w$  found using the CMOD compliance curve. The CMOD compliance curve was used since it gave more consistent results than the LPO compliance curve, however calculations were made using the LPO values so a comparison could be made.

(b) Stress Intensity Values

The stress intensity values were calculated using the formula developed in Reference 3 by Go and Swartz. A least squares method was used to estimate  $K_I$  with errors less than 3%. The formula is shown below:

$$K_I = \frac{M}{bw^{1.5}} (Az^2 + Bz + C + Dz^{-1} + Ez^{-2}) \dots \dots \dots (2.1)$$

M = Midspan bending moment at failure

b = beam width

w = beam depth

z = 1 - a/w

A = -0.065\*

B = -3.483\*

C = -0.120\*

D = 5.706\*

E = 0.166\*

\* Coefficients for  $L/w = 3.75$  as found in Reference 3.

Stress intensity values were calculated for unextended values of  $a/w$  and for extended values of  $a/w$  ( $K_{IC}$ ). These values are listed in Table 4.1, 4.2, and 4.3.

Average values of  $K_I$  for unextended crack length were  $8.41 \times 10^2$  lb.-in.<sup>-3/2</sup> ( $9.249 \times 10^5$  N-m<sup>-3/2</sup>),  $7.66 \times 10^2$  lb.-in.<sup>-3/2</sup> ( $8.417 \times 10^5$  N-m<sup>-3/2</sup>),  $5.62 \times 10^2$  lb.-in.<sup>-3/2</sup> ( $6.177 \times 10^5$  N-m<sup>-3/2</sup>) for approximate  $a/w$

ratios of 0.3, 0.5, 0.7 respectively. Average values of  $K_{IC}$  for extended crack lengths based on CMOO were  $12.07 \times 10^2 \text{ lb.-in.}^{-3/2}$  ( $13.27 \times 10^5 \text{ N-m}^{-3/2}$ ),  $9.44 \times 10^2 \text{ lb.-in.}^{-3/2}$  ( $10.38 \times 10^5 \text{ N-m}^{-3/2}$ ),  $8.78 \times 10^2 \text{ lb.-in.}^{-3/2}$  ( $9.65 \times 10^5 \text{ N-m}^{-3/2}$ ), for the same respective  $a/w$  ratios. Average values of  $K_{IC}$  for extended crack lengths based on LPO were  $10.30 \times 10^2 \text{ lb.-in.}^{-3/2}$  ( $11.43 \times 10^5 \text{ N-m}^{-3/2}$ ),  $7.92 \times 10^2 \text{ lb.-in.}^{-3/2}$  ( $8.71 \times 10^5 \text{ N-m}^{-3/2}$ ),  $6.81 \times 10^2 \text{ lb.-in.}^{-3/2}$  ( $7.49 \times 10^5 \text{ N-m}^{-3/2}$ ) for the same respective  $a/w$  ratios. Figures 4.4, 4.5, and 4.6, show graphs of  $K_{IC}$  vs.  $a/w$ .

### c) Energy Release Rates

Energy release rates were calculated three ways, each of which is described below.

1. The first method calculated the energy release rate using the corresponding stress intensity value. The equations used are as follows:

$$G_I = \frac{1 - \nu^2}{E_C} K_I^2 \text{ For unextended } a/w \dots \dots \dots (4.1)$$

$$G_{IC} = \frac{1 - \nu^2}{E} K_{IC}^2 \text{ For extended } a/w \dots \dots \dots (4.2)$$

These values are listed in Tables 4.1, 4.2, and 4.3.

2. The second method calculated the energy release rate by dividing the total energy to failure by the remaining uncracked area. The total energy to failure was found by calculating the area under the load versus LPO trace up to the point of unstable crack growth. This point was chosen because the beam was failed under load control. The uncracked area was calculated as follows:

$$A = bw(1 - a/w)(1.15) \dots \dots \dots (4.3)$$

The factor 1.15 was used to compensate for the rough surface (3). The energy release rates were calculated for unextended and extended a/w. Average values of these energy release rates based on unextended crack length are .248 lb./in. (43.45 N/m), .196 lb./in. (34.34 N/m), and .155 lb./in. (27.16 N/m) for approximate initial a/w ratios of 0.3, 0.5, D.7. Values based on extended crack length by CMDD are .308 lb./in. (53.96 N/m), .232 lb./in. (40.65 N/m), .232 lb./in. (40.65 N/m) for the same respective a/w ratios. Values based on extended crack lengths by LPD are .280 lb./in. (49.06 N/m), .207 lb./in. (36.27 N/m), .183 lb./in. (32.06 N/m) for the same respective a/w ratios. Graphs of  $G_{IC}$  calculated this way versus a/w are shown in figures 4.7, 4.8, and 4.9. All values are listed in Table 4.4.

3. The third method calculated the energy release rate using the J-integral approach in which the slope of a graph of the energy up to the point of instability, U, versus a/w is used. The slope of this line divided by the effective total area, that is,  $1.15 \times b \times w$ , gives the energy release rate. Plots were made using both the unextended value and the extended values of a/w. These are shown in Figure 4.10, 4.11, and 4.12. The energy release rate was calculated as follows:

$$G_I = \frac{\text{slope}}{bw(1.15)} \text{ For unextended a/w . . . . . (4.4)}$$

$$G_{IC} = \frac{\text{slope}}{bw(1.15)} \text{ For extended a/w . . . . . (4.5)}$$

Using beam with a/w of D.5 and D.7, the  $G_I$  values were found to be .251 lb./in. (66.96 N/m) for unextended a/w values, .207 lb./in. (55.22 N/m) for extended a/w values based on CMDD, and .222 lb./in. (59.22 N/m) for extended a/w values based on LPD. Average values of .229 (for CMDD) and

.251 (for LPO) are used in comparing to the other methods. It is seen that these values are fairly constant for nominal a/w values of 0.5 and 0.7.

A summary of the average  $K_{IC}$  and  $G_{IC}$  values is shown in Table 4.5.

(d) CTOD

The CTOD was calculated using an equation, based on William's Stress Function, which was developed by Go and Swartz in Reference 3, which relates the CMOD to the CTOD. The equation is as follows:

$$CTOD = \frac{R(w-a)}{R(w-a) + a + z} CMOD \dots \dots \dots (2.3)$$

- R = Rotation factor taken as 0.45 for three point bending
- w = beam depth
- a = crack depth
- z = .125 in. (3.1 mm) = knife edge thickness.
- CMOD = Crack mouth opening displacement at unstable crack growth

The CTOD was calculated for both the unextended and the extended crack lengths, and these values are listed in Table 4.6.

The average CTOD values based on unextended crack length a/w ratios of 0.3, 0.5, 0.7 are  $8.92 \times 10^{-4}$  in. ( $2.27 \times 10^{-2}$ mm),  $7.65 \times 10^{-4}$  in. ( $1.94 \times 10^{-2}$ mm),  $6.75 \times 10^{-4}$  in. ( $1.72 \times 10^{-2}$ mm) respectively. For extended crack length a/w ratios based on CMOD, the average CTOD values are  $6.41 \times 10^{-4}$  in. ( $1.63 \times 10^{-2}$ mm),  $6.18 \times 10^{-4}$  in. ( $1.57 \times 10^{-2}$ mm),  $4.73 \times 10^{-4}$  in. ( $1.20 \times 10^{-2}$ mm). For extended crack length a/w ratios based on LPD, the average CTOD values are  $7.49 \times 10^{-4}$  in. ( $1.90 \times 10^{-2}$ mm),  $7.47 \times 10^{-4}$  in. ( $1.90 \times 10^{-2}$ mm),  $5.63 \times 10^{-4}$  in. ( $1.43 \times 10^{-2}$ mm) for the respective approximate a/w ratios of 0.3, 0.5, and 0.7. The CTOD values based on extended crack length give consistent results regardless of the initial

which may be significant in determining a suitable fracture toughness parameter.

#### 4.3 Teflon Beams

The six teflon beams were tested as previously described. The extended  $a/w$  was found and the stress intensity, energy release rate, and CTOD values were calculated in the same manner as in the precracked beam. These results are listed in Tables 4.7 and 4.8. Average values are listed in Table 4.9.

#### 4.4 Strain Beam

The beam with strain gages was tested as previously described. The data were used to obtain profiles which are shown in Appendix II. From these profiles the strain reversal point was located, and the rotation factor,  $R$ , was calculated for these profiles and is noted on each profile in Appendix III. The values found proved inconsistent, so the value of  $R=0.45$  as found by Go and Swartz in Reference 3 was used in the calculation of all CTOD values.



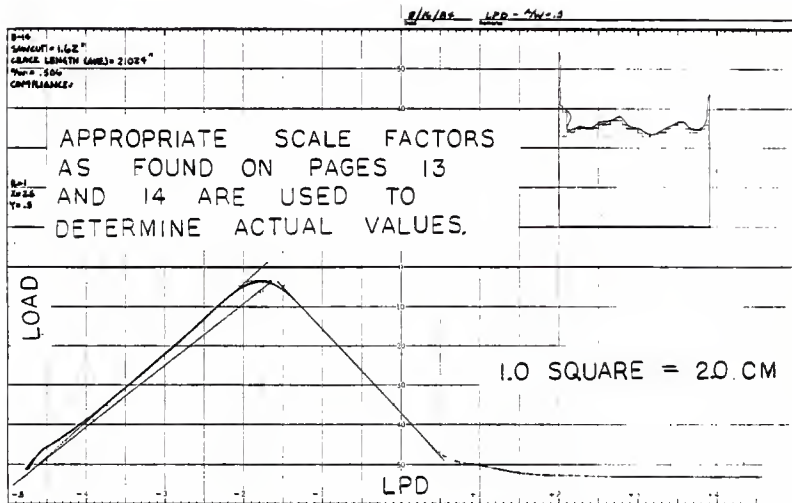


FIG. 4.1A LPD TRACE WITHOUT SLIPPAGE.

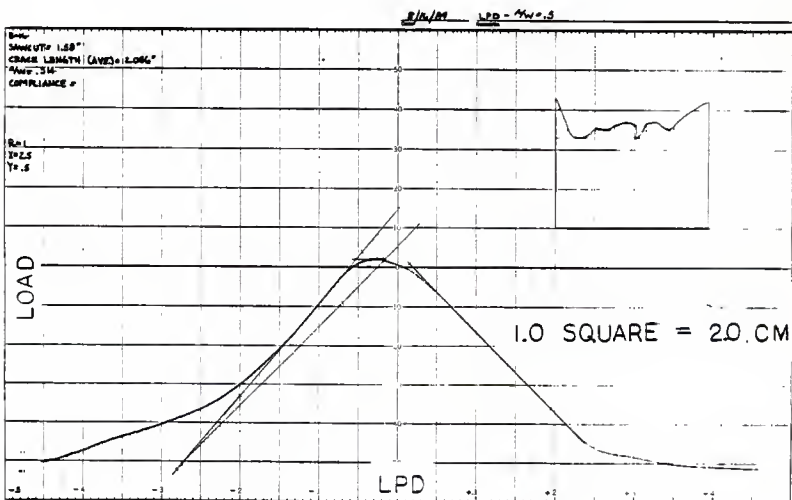


FIG. 4.1B LPD TRACE WITH SLIPPAGE.

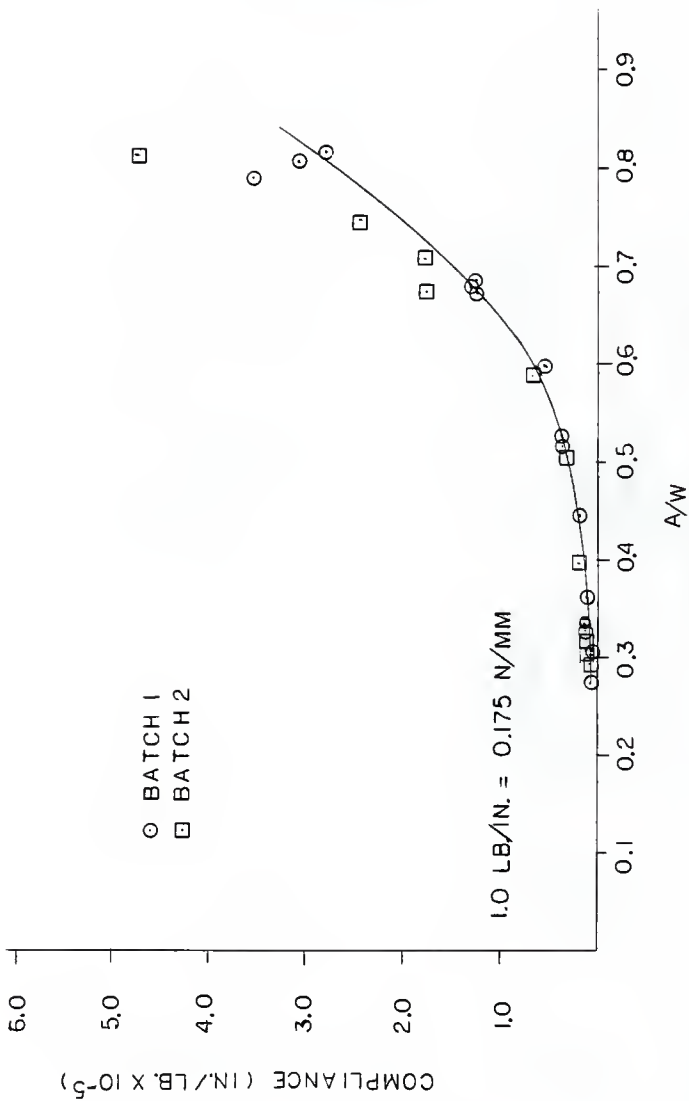


FIG 4.2 CMOD COMPLIANCE CALIBRATION CURVE

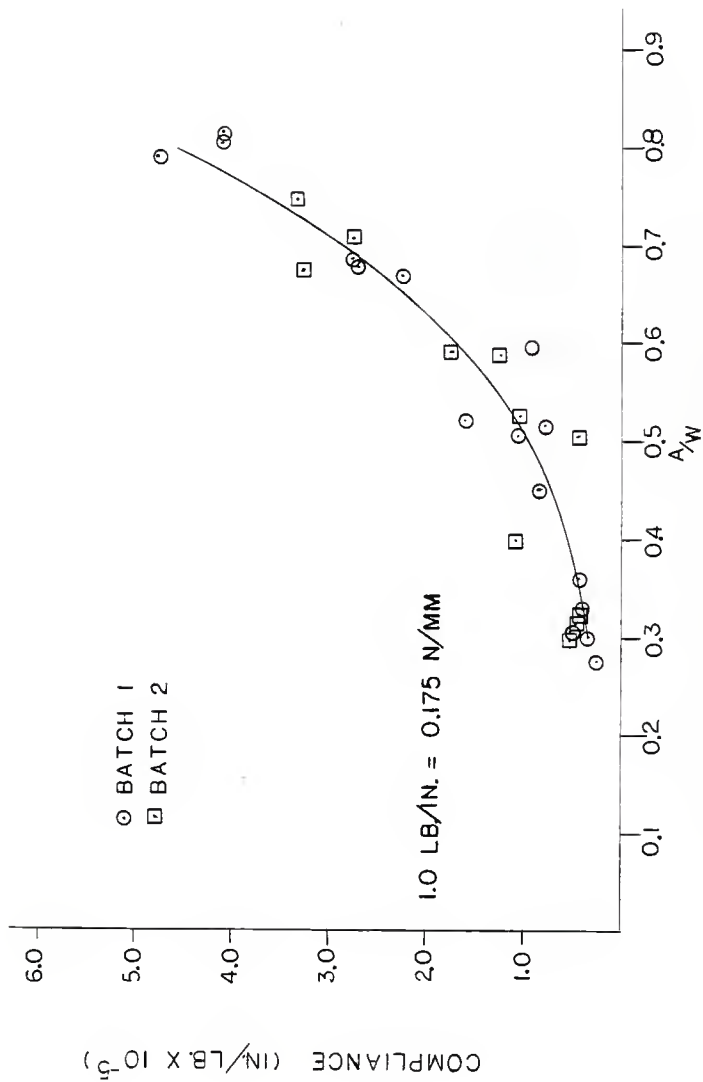


FIG. 4.3 LPD COMPLIANCE CALIBRATION CURVE

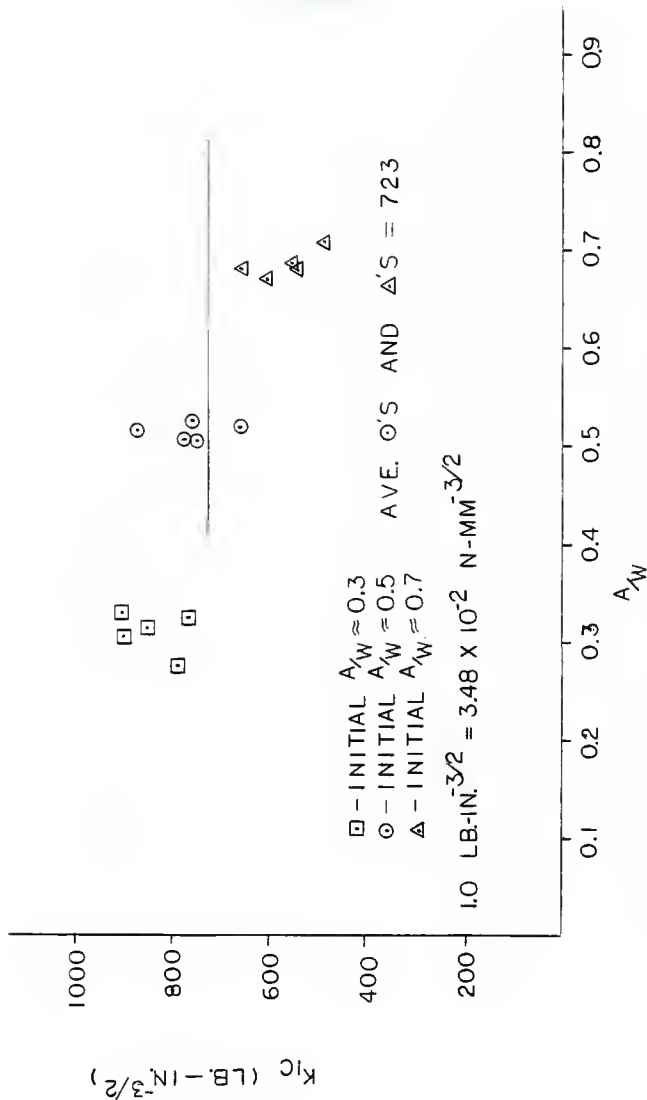


FIG. 4.4  $K_{IC}$  VERSUS  $A_{1W}$  FOR UNEXTENDED CRACK LENGTH.

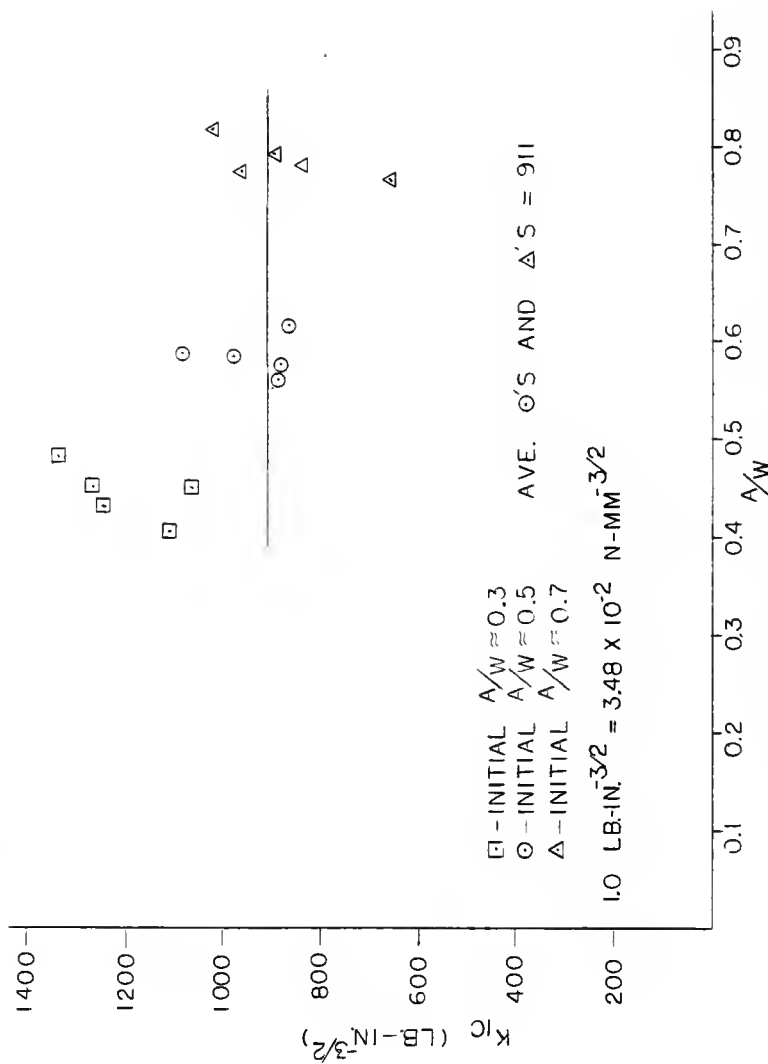


FIG. 4.5  $K_{IC}$  VERSUS  $A/W$  FOR EXTENDED CRACK LENGTH BASED ON CMOD.

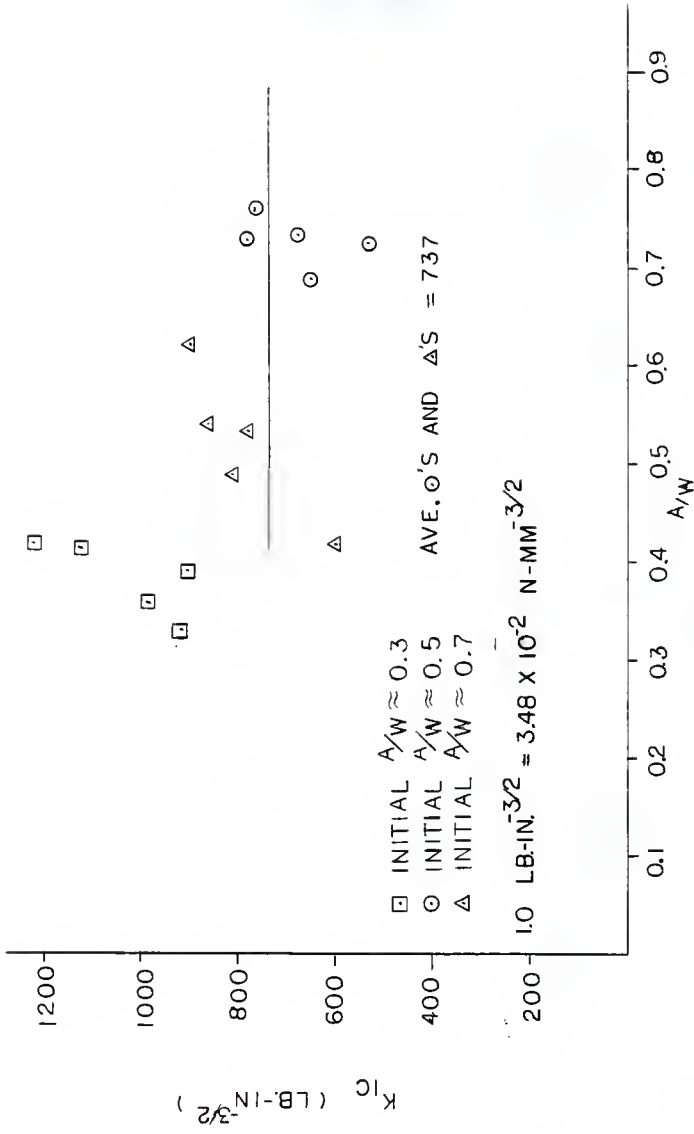


FIG 4.6  $K_{IC}$  VERSUS  $A/W$  FOR EXTENDED CRACK LENGTH BASED ON LPD

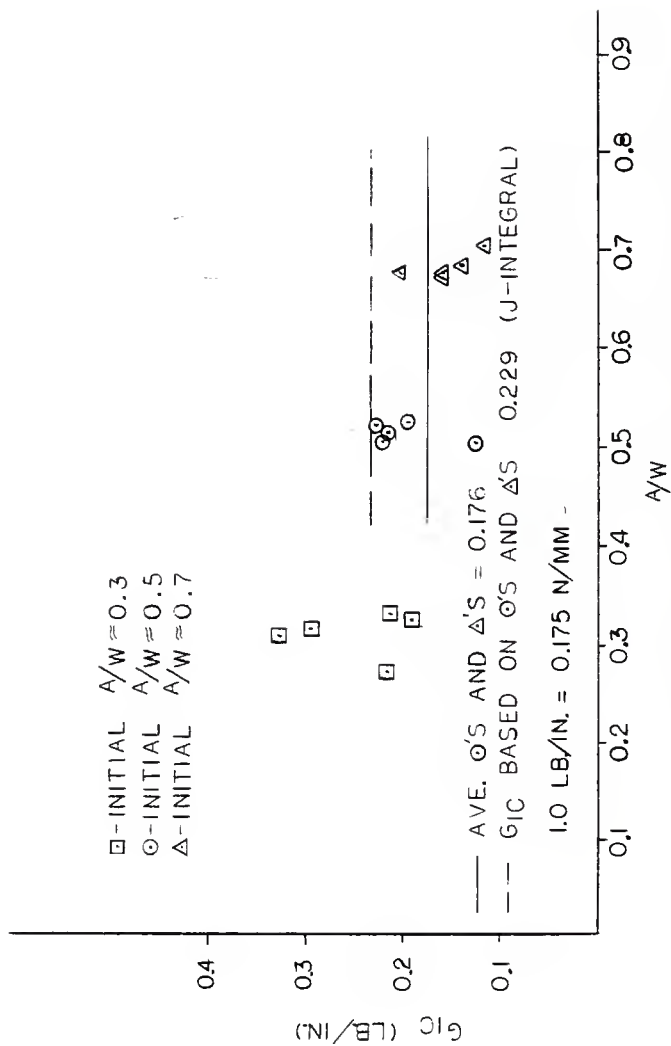


FIG. 4.7 GIC VERSUS  $A/W$  FOR UNEXTENDED CRACK LENGTH.

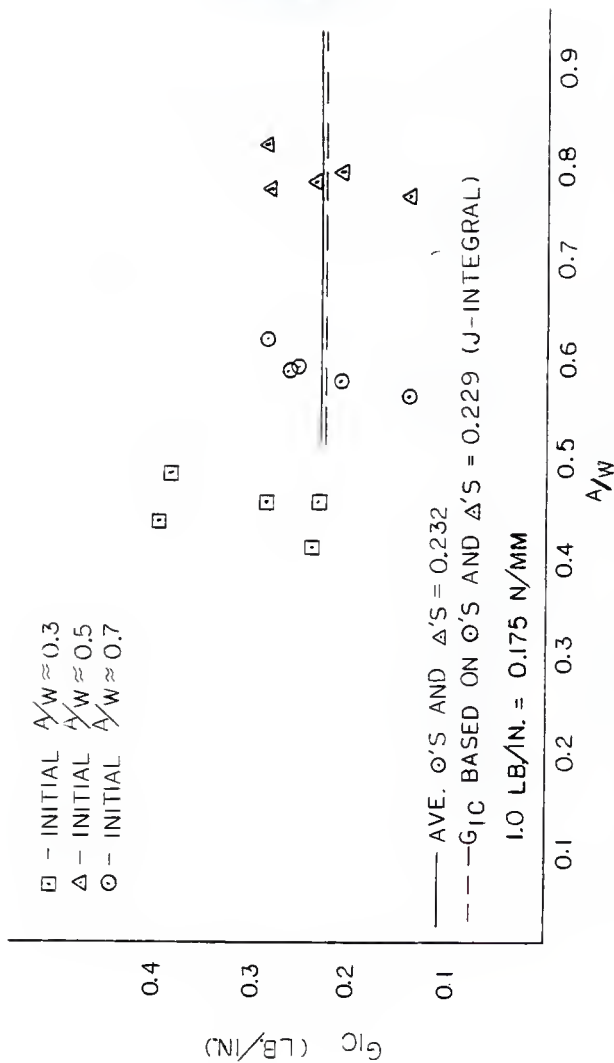


FIG. 4.8  $G_{IC}$  VERSUS  $A/W$  FOR EXTENDED CRACK LENGTH BASED ON CMOD.



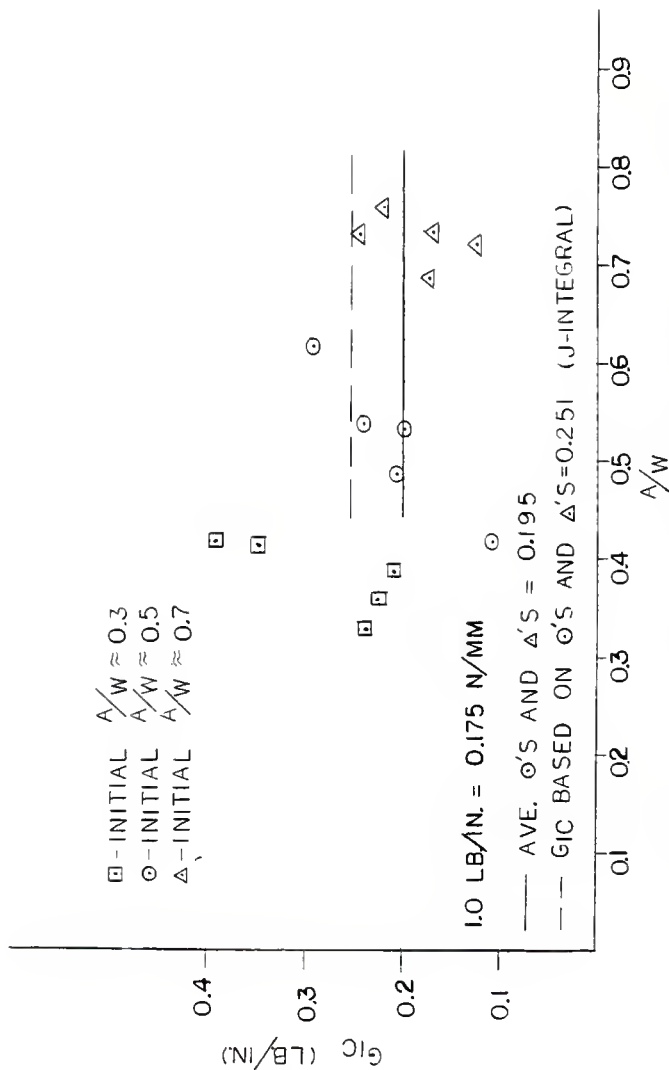


FIG. 4.9  $G_{IC}$  VERSUS  $A/W$  FOR EXTENDED CRACK LENGTH BASED ON LPD.

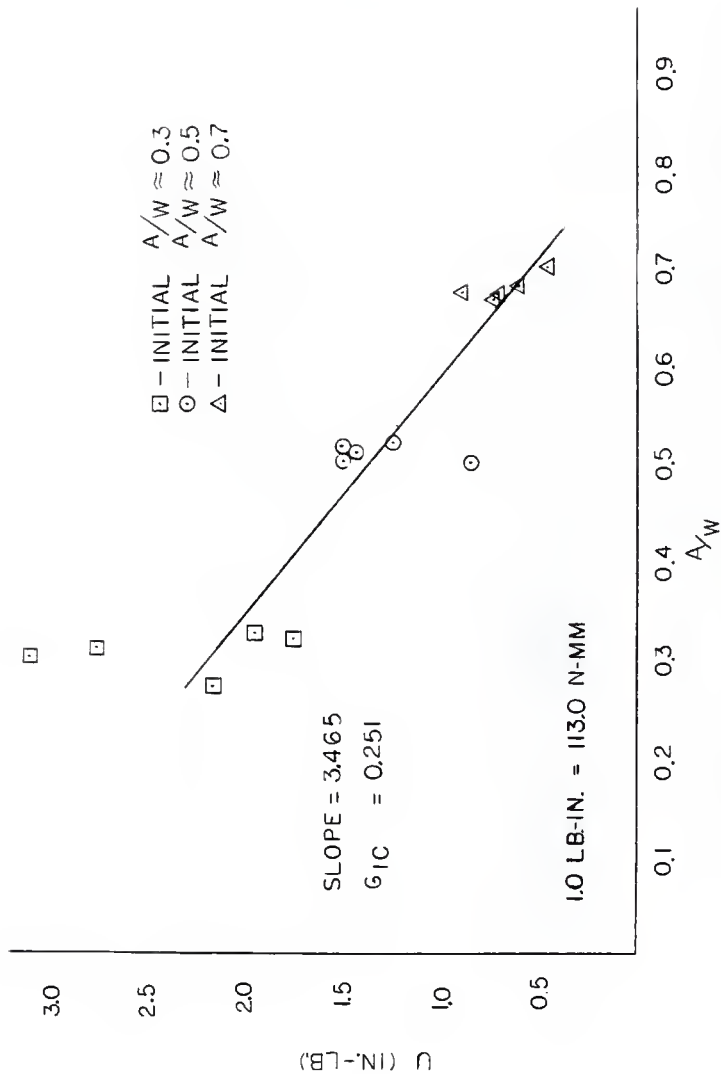


FIG. 4.10 U VERSUS  $A/W$  FOR UNEXTENDED CRACK LENGTH

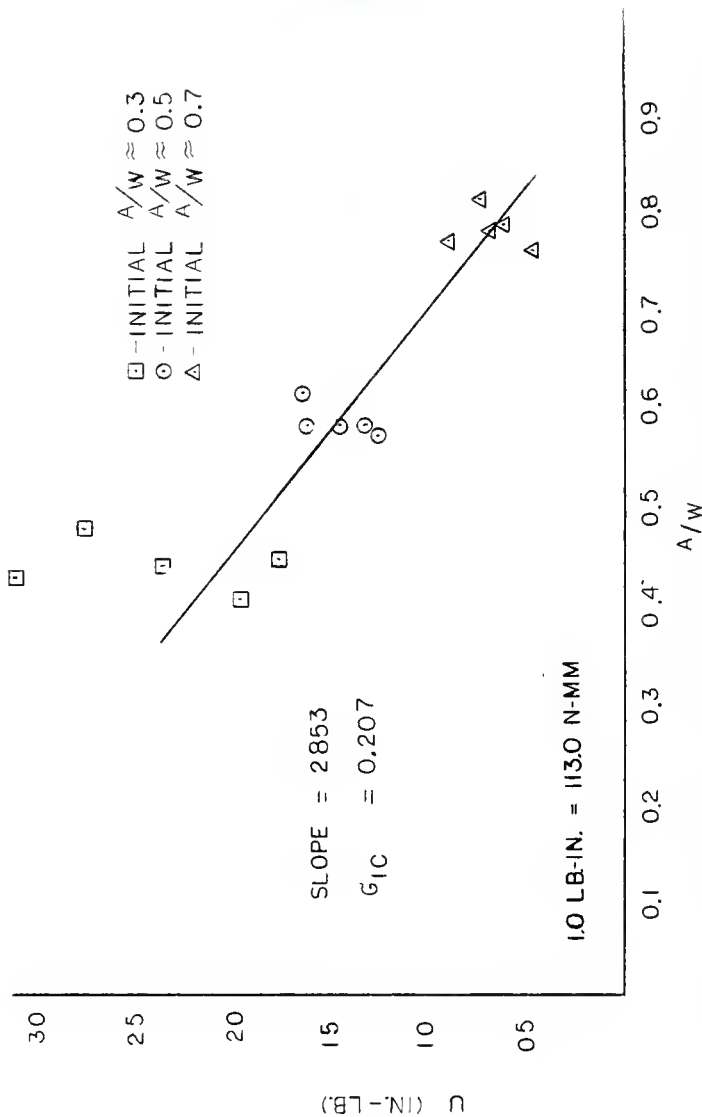


FIG. 4.11 U VERSUS  $A/W$  FOR EXTENDED CRACK LENGTH BASED ON CMOD. 45

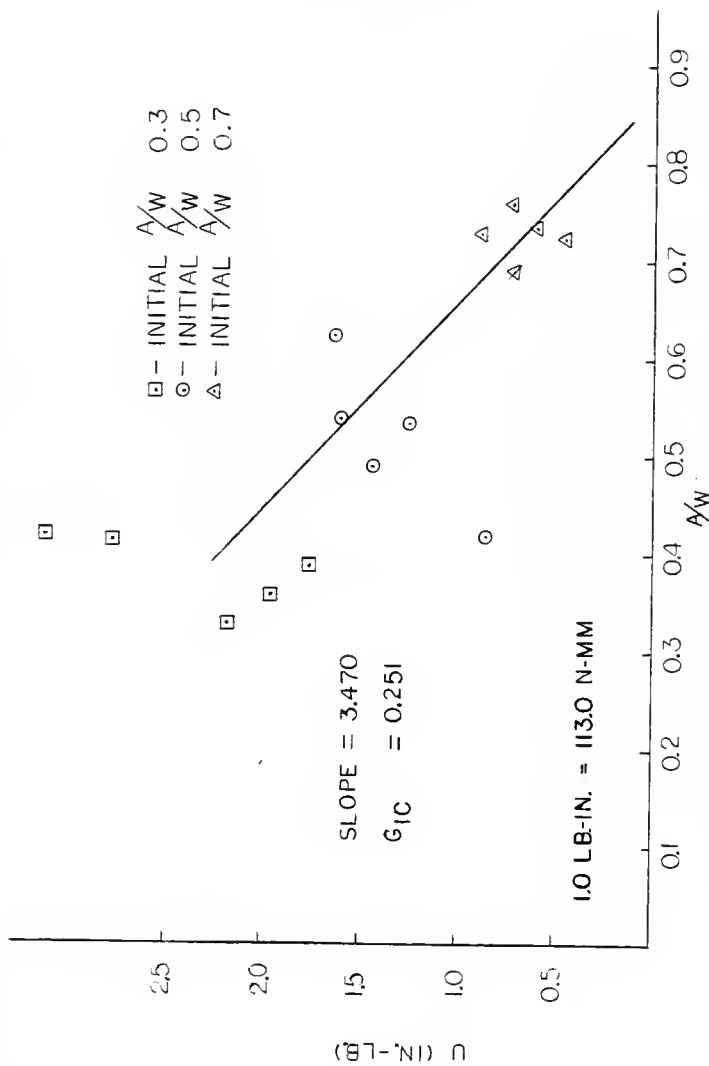

 FIG. 4.12 U VERSUS  $A/W$  FOR EXTENDED CRACK LENGTH BASED ON LPD.

Table 4.1  $K_I$  and  $G_I$  Values for Unextended a/w in Precracked Beams

Beam No.	P-max (lb.)	a/w unextended	$K_I$ (lb.-in. $^{-3/2}$ )	$G_I$ (lb./in.)
B-9*	915	.276	$7.90 \times 10^2$	.112
B-10*	905	.330	$9.06 \times 10^2$	.148
B-11	955	.307	$8.98 \times 10^2$	.145
C-1	890	.314	$8.53 \times 10^2$	.131
C-2**	770	.326	$7.62 \times 10^2$	.105
B-14	480	.506	$7.78 \times 10^2$	.109
B-16	525	.514	$8.71 \times 10^2$	.137
B-17**	390	.521	$6.60 \times 10^2$	.079
C-3	470	.504	$7.58 \times 10^2$	.103
C-4	445	.525	$7.62 \times 10^2$	.105
B-18	225	.679	$6.38 \times 10^2$	.073
B-19**	190	.685	$5.51 \times 10^2$	.055
B-20	220	.671	$6.05 \times 10^2$	.066
C-5	155	.706	$4.89 \times 10^2$	.043
C-6	190	.673	$5.27 \times 10^2$	.050

\* Beams loaded at a faster rate.

\*\* Beams precracked one day, and failed the next.

1 lb. = 4.45 N

1 lb.-in.  $^{-3/2}$  =  $3.48 \times 10^{-2}$  N-mm  $^{-3/2}$

1 lb./in. = 0.175 N/mm

Table 4.2  $K_{IC}$  and  $G_{IC}$  Values for Extended a/w in  
Precracked Beams Based on CMOO

<u>Beam No.</u>	<u>P-max (lb.)</u>	<u>a/w extended</u>	<u><math>K_{IC}</math> (lb.-in. <math>^{-3/2}</math>)</u>	<u><math>G_{IC}</math> (lb./in.)</u>
B-9*	915	.450	$12.68 \times 10^2$	.290
B-10*	905	.405	$11.09 \times 10^2$	.222
B-11	955	.430	$12.53 \times 10^2$	.283
C-1	890	.480	$13.25 \times 10^2$	.324
C-2**	770	.450	$10.67 \times 10^2$	.205
B-14	480	.585	$9.85 \times 10^2$	.175
B-16	525	.588	$10.88 \times 10^2$	.213
B-17**	390	.618	$8.68 \times 10^2$	.136
C-3	470	.560	$8.93 \times 10^2$	.144
C-4	445	.575	$8.85 \times 10^2$	.141
B-18	225	.773	$9.65 \times 10^2$	.168
B-19*	190	.790	$8.93 \times 10^2$	.144
B-20	220	.817	$10.23 \times 10^2$	.189
C-5	155	.766	$6.62 \times 10^2$	.079
C-6	190	.780	$8.45 \times 10^2$	.129

\* Beams loaded at a faster rate.

\*\* Beams precracked one day, and failed the next.

1 lb. = 4.45 N

1 lb.-in.  $^{-3/2}$  =  $3.48 \times 10^{-2}$  N-mm  $^{-3/2}$

1 lb./in. = 0.175 N/mm

Table 4.3  $K_{IC}$  and  $G_{IC}$  Values for Extended a/w in  
 Precracked Beams Based on LPD

Beam No.	P-Max (lb.)	a/w Extended	$K_{IC}$ (lb.-in. <sup>-3/2</sup> )	$G_{IC}$ (lb./in.)
B-9*	915	.330	$9.16 \times 10^2$	.151
B-10*	905	.360	$9.82 \times 10^2$	.174
B-11	955	.420	$12.19 \times 10^2$	.268
C-1	890	.415	$11.21 \times 10^2$	.226
C-2**	770	.390	$9.06 \times 10^2$	.148
B-14	480	.540	$8.59 \times 10^2$	.133
B-16	525	.490	$8.13 \times 10^2$	.119
B-17**	390	.622	$9.03 \times 10^2$	.148
C-3	470	.420	$6.00 \times 10^2$	.065
C-4	445	.535	$7.85 \times 10^2$	.111
B-18	225	.730	$7.86 \times 10^2$	.111
B-19*	190	.735	$6.78 \times 10^2$	.083
B-20	220	.690	$6.51 \times 10^2$	.076
C-5	155	.725	$5.30 \times 10^2$	.050
C-6	190	.760	$7.63 \times 10^2$	.105

\*Beams loaded at a faster rate.

\*\*Beams precracked one day, and failed the next.

1 lb. = 4.45 N

1 lb.-in.<sup>-3/2</sup> =  $3.48 \times 10^{-2}$  N-mm<sup>-3/2</sup>

1 lb./in. = 0.175 N/mm

Table 4.4 U and  $G_{IC}$  Values in Precracked Beams

Beam No.	U (lb.-in.)	$G_{IC}$ (lb/in.) (unextended a/w)	$G_{IC}$ (lb/in.) (extended CM00 a/w)	$G_{IC}$ (lb/in.) (extended LPO a/w)
B-9*	2.18	.218	.287	.236
B-10*	1.96	.212	.239	.222
B-11	3.12	.326	.397	.390
C-1	2.77	.293	.386	.343
C-2**	1.76	.189	.232	.209
B-14	1.51	.222	.264	.238
B-16	1.44	.215	.253	.205
B-17**	1.51	.229	.286	.289
C-3	0.86	.126	.142	.107
C-4	1.25	.191	.213	.195
B-18	0.89	.201	.284	.239
B-19**	0.61	.140	.210	.167
B-20	0.73	.160	.289	.171
C-5	0.46	.114	.142	.121
C-6	0.72	.160	.237	.217

\* Beams loaded at a faster rate.

\*\* Beams precracked one day, and failed the next.

1 lb.-in. = 113.03 N-mm

1 lb./in. = 0.175 N/mm



Table 4.5 Summary of Average Values

	Nominal a/w	Average Initial a/w	Average Final a/w (CMOD)	a/w % Change	Average Final a/w (LPO)	a/w % Change
Group 1	0.3	0.311	0.433	42%	0.383	23%
Group 2	0.5	0.514	0.585	14%	0.521	1%
Group 3	0.7	0.683	0.785	15%	0.728	7%

CMOD

Average Final a/w	$K_{IC}$ (lb.-in. <sup>-3/2</sup> )	$G_{IC}$ (lb./in.) From $K_{IC}$	$G_{IC}$ (lb./in.) From U	$G_{IC}$ (lb./in.) <sup>*</sup> From $J_{IC}$
0.433	1207	0.265	0.308	
0.585	944	0.162	0.232	.207
0.785	878	0.142	0.232	.207

LPO

Average Final a/w	$K_{IC}$ (lb.-in. <sup>-3/2</sup> )	$G_{IC}$ (lb./in.) From $K_{IC}$	$G_{IC}$ (lb./in.) From U	$G_{IC}$ (lb./in.) <sup>*</sup> From $J_{IC}$
0.383	1040	0.193	0.280	--
0.521	792	0.115	0.207	0.251
0.728	681	0.085	0.183	0.251

Unextended a/w

Average Initial a/w	$K_{IC}$ (lb.-in. <sup>-3/2</sup> )	$G_{IC}$ (lb./in.) From $K_{IC}$	$G_{IC}$ (lb./in.) From U	$G_{IC}$ (lb./in.) <sup>*</sup> From $J_{IC}$
0.311	841	.128	.248	--
0.514	766	.106	.196	.251
0.683	562	.057	.155	.251

\* Based on initial a/w of 0.5 and 0.7.

1 lb.-in.<sup>-3/2</sup> =  $3.48 \times 10^{-2}$  N-mm<sup>-3/2</sup>

1 lb./in. = 0.175 N/mm

Table 4.6 CMOO and CT00 Values for Precracked Beams

<u>Beam No.</u>	<u>CMOO (in.) at instability</u>	<u>CT00 (in.) for a/w unextended</u>	<u>CT00 (in.) for a/w extended (CMOO)</u>	<u>CT00 (in.) for a/w extended (LPO)</u>
B-9*	$1.99 \times 10^{-3}$	$10.24 \times 10^{-4}$	$6.76 \times 10^{-4}$	$9.05 \times 10^{-4}$
B-10*	$1.47 \times 10^{-3}$	$6.69 \times 10^{-4}$	$5.59 \times 10^{-4}$	$6.23 \times 10^{-4}$
B-11	$1.80 \times 10^{-3}$	$8.64 \times 10^{-4}$	$6.43 \times 10^{-4}$	$6.60 \times 10^{-4}$
C-1	$2.30 \times 10^{-3}$	$10.86 \times 10^{-4}$	$7.22 \times 10^{-4}$	$8.53 \times 10^{-4}$
C-2**	$1.78 \times 10^{-3}$	$8.17 \times 10^{-4}$	$6.05 \times 10^{-4}$	$7.02 \times 10^{-4}$
B-14	$2.70 \times 10^{-3}$	$7.90 \times 10^{-4}$	$6.28 \times 10^{-4}$	$7.18 \times 10^{-4}$
B-16	$2.92 \times 10^{-3}$	$8.36 \times 10^{-4}$	$6.73 \times 10^{-4}$	$8.93 \times 10^{-4}$
B-17**	$3.02 \times 10^{-3}$	$8.48 \times 10^{-4}$	$6.32 \times 10^{-4}$	$6.24 \times 10^{-4}$
C-3	$2.33 \times 10^{-3}$	$6.86 \times 10^{-4}$	$5.85 \times 10^{-4}$	$8.54 \times 10^{-4}$
C-4	$2.39 \times 10^{-3}$	$6.64 \times 10^{-4}$	$5.73 \times 10^{-4}$	$6.45 \times 10^{-4}$
B-18	$4.34 \times 10^{-3}$	$7.34 \times 10^{-4}$	$5.52 \times 10^{-4}$	$5.97 \times 10^{-4}$
B-19**	$3.80 \times 10^{-3}$	$6.28 \times 10^{-4}$	$4.54 \times 10^{-4}$	$5.12 \times 10^{-4}$
B-20	$4.38 \times 10^{-3}$	$7.63 \times 10^{-4}$	$4.96 \times 10^{-4}$	$7.10 \times 10^{-4}$
C-5	$3.60 \times 10^{-3}$	$5.48 \times 10^{-4}$	$4.20 \times 10^{-4}$	$5.06 \times 10^{-4}$
C-6	$4.08 \times 10^{-3}$	$7.05 \times 10^{-4}$	$4.44 \times 10^{-4}$	$4.90 \times 10^{-4}$
	AVERAGE	$7.77 \times 10^{-4}$	$5.77 \times 10^{-4}$	$6.86 \times 10^{-4}$

\* Beams loaded at a faster rate.

\*\* Beams precracked one day, and failed the next.

1 in. = 25.40 mm

Table 4.7  $K_I$  and  $G_I$  Values in Teflon Beams

Beam No.	P-Max (lb.)	a/w Unextended	$K_I$ (lb.-in. $^{-3/2}$ )	$G_I$ (lb./in.)
C-15	570	.293	$5.16 \times 10^2$	.048
C-16	570	.325	$5.63 \times 10^2$	.057
C-17	385	.455	$5.41 \times 10^2$	.053
C-18	290	.514	$4.81 \times 10^2$	.042
C-19	160	.625	$3.74 \times 10^2$	.025
C-20 Beam No.	95 P-Max (lb.)	.670 a/w Extended CMOD	$2.60 \times 10^2$	.012
Beam No.	P-Max (lb.)	a/w Extended (LPD)	$K_{IC}$ (lb.-in. $^{-3/2}$ )	$G_{IC}$ (lb./in.)
C-15	570	.510	$9.35 \times 10^2$	.157
C-16	570	.513	$9.43 \times 10^2$	.160
C-17	385	.617	$8.76 \times 10^2$	.138
C-18	290	.670	$7.95 \times 10^2$	.114
C-19	160	.825	$9.32 \times 10^2$	.157
C-20 Beam No.	95 P-Max (lb.)	.910 a/w Extended (LPD)	$12.39 \times 10^2$	.276
C-15	570	.625	$13.32 \times 10^2$	.320
C-16	570	.693	$17.06 \times 10^2$	.524
C-17	385	.717	$12.71 \times 10^2$	.291
C-18	290	.732	$10.22 \times 10^2$	.188
C-19	160	.805	$8.21 \times 10^2$	.121
C-20	95	--	--	--

1 lb. = 4.45 N

1 lb.-in.  $^{-3/2}$  =  $3.48 \times 10^{-2}$  N-mm  $^{-3/2}$ 

1 lb./in. = 0.175 N/mm

Table 4.8 U,  $G_{IC}$ , CMOD and CTOD Values for Teflon Beams

Beam No.	U (lb.-in.)	$G_{IC}$ (lb/in) Unextended a/w	$G_{IC}$ (lb/in) Extended CMOD a/w	$G_{IC}$ (lb/in) (Extended LPO a/w)
C-15	2.40	.246	.355	.464
C-16	3.30	.354	.491	.778
C-17	1.75	.232	.331	.448
C-18	1.18	.176	.259	.319
C-19	.86	.167	.358	.321
C-20	.39	.084	.309	--

Beam No.	CMOD (in.) at instability	CTOD (in.) for a/w unextended	CTOD (in.) for a/w extended (CMOD)	CTOD (in.) for a/w extended (LPO)
C-15	$1.86 \times 10^{-3}$	$9.21 \times 10^{-4}$	$5.38 \times 10^{-4}$	$3.81 \times 10^{-4}$
C-16	$1.92 \times 10^{-3}$	$8.84 \times 10^{-4}$	$5.51 \times 10^{-4}$	$3.08 \times 10^{-4}$
C-17	$2.84 \times 10^{-3}$	$9.52 \times 10^{-4}$	$5.96 \times 10^{-4}$	$4.13 \times 10^{-4}$
C-18	$3.24 \times 10^{-3}$	$9.28 \times 10^{-4}$	$5.66 \times 10^{-4}$	$4.42 \times 10^{-4}$
C-19	$4.40 \times 10^{-3}$	$9.00 \times 10^{-4}$	$3.71 \times 10^{-4}$	$4.18 \times 10^{-4}$
C-20	$4.38 \times 10^{-3}$	$7.65 \times 10^{-4}$	$1.81 \times 10^{-4}$	---
	AVERAGE	$5.11 \times 10^{-4}$	$4.67 \times 10^{-4}$	$3.92 \times 10^{-4}$

1 lb.-in. = 113.03 N-m

1 lb./in. = 0.175 N/mm

1 in. = 25.40mm

Table 4.9 Summary of Average Values of  $K_{IC}$  and  $G_{IC}$  for Teflon Beams

Nominal a/w	Average Initial a/w	Average Final a/w (CMOD)	a/w % Change	Average Final a/w (LPD)	a/w % Change
0.3	0.309	0.512	66%	0.659	113%
0.5	0.485	0.644	33%	0.725	49%
0.7	0.648	0.868	59%	0.805	24%

<u>CMOD</u>			
Average Final a/w	$K_{IC}$ (lb.-in. <sup>-3/2</sup> )	$G_{IC}$ (lb./in.) From $K_{IC}$	$G_{IC}$ (lb./in.) From U
0.512	$9.39 \times 10^2$	0.159	0.423
0.644	$8.36 \times 10^2$	0.126	0.295
0.868	$10.86 \times 10^2$	0.217	0.334

<u>LPD</u>			
Average Final a/w	$K_{IC}$ (lb.-in. <sup>-3/2</sup> )	$G_{IC}$ (lb./in.) From $K_{IC}$	$G_{IC}$ (lb./in.) From U
0.659	$15.19 \times 10^2$	0.422	0.621
0.725	$11.47 \times 10^2$	0.240	0.384
0.805	$8.21 \times 10^2$	0.121	0.321

<u>Unextended a/w</u>			
Average Initial a/w	$K_{IC}$ (lb.-in. <sup>-3/2</sup> )	$G_{IC}$ (lb./in. <sup>-3/2</sup> ) From $K_{IC}$	$G_{IC}$ (lb./in.) From U
0.309	$5.39 \times 10^2$	0.053	0.300
0.485	$5.11 \times 10^2$	0.047	0.204
0.648	$3.17 \times 10^2$	0.019	0.126

$$1 \text{ lb.-in.}^{-3/2} = 3.48 \times 10^{-2} \text{ N-mm}^{-3/2}$$

$$1 \text{ lb./in.} = 0.175 \text{ N/mm}$$

## Chapter 5

## SUMMARY AND CONCLUSIONS

The experimental results are interpreted and summarized as follows:

1. The extended crack lengths in precracked beams based on the CMOD compliance calibration curve were found to be 39%, 14% and 15% higher for nominal a/w ratios of 0.3, 0.5, and 0.7 respectively than the unextended crack lengths. For those based on the LPD curve, the extended crack lengths were found to be 23%, 1% and 7% higher for the same nominal a/w ratios. The teflon beams exhibited larger variations of 66%, 33%, and 34% based on the CMOD curve and 113%, 49%, and 24% based on the LPD curve for nominal a/w ratios of 0.3, 0.5, and 0.7 respectively.
2. The  $K_I$  values for precracked beams were consistently higher than for teflon beams, supporting earlier reports. The  $K_I$  values for extended crack lengths based on CMOD were 44%, 23%, and 56% higher than the unextended crack lengths for nominal a/w ratios of 0.3, 0.5, and 0.7. Based on LPD, the crack lengths were 22%, 3%, and 21% higher. Although the  $K_I$  value is higher for smaller a/w ratios, it is fairly constant for a/w ratios of approximately 0.5 and 0.7.
3. The energy release rates showed the following trends:
  - (a) Those found using stress intensity values were much lower than those found by the energy method for both the unextended crack

length and the extended crack length based on CMOO. The values found based on LPO were only slightly lower.

(b) Based on the data from nominal a/w ratios of 0.5 and 0.7 there is good agreement between the energy release rates based on the energy approach and the J-integral approach for unextended a/w values and extended a/w values based on CMOO as well as LPD.

(c) Energy release rates found using extended a/w ratios based on CMOO tended to be higher than those based on LPD except those found by the J-integral approach which only differed slightly.

4. The CTOD values found using the extended crack lengths based on CMOO and LPO gave very consistent results of  $5.77 \times 10^{-4}$  in. ( $1.47 \times 10^{-2}$ mm) and  $6.86 \times 10^{-4}$  in. ( $1.74 \times 10^{-2}$ mm) respectively with less than 10% average deviation. The CTOD based on the unextended a/w values gave an average value of  $7.77 \times 10^{-4}$  with less than 15% average deviation. The CTOD values found for teflon beams were only slightly less. The consistency of the CTOD demonstrates that it may be an excellent indicator of fracture toughness.

Recommendations for future work include the investigation of size variation of the specimen and continued statistical evaluation of the methods presented here.

## Appendix I

## REFERENCES

1. American Society for Testing and Materials, 1981, "Concrete and Mineral Aggregates", Annual Book of ASTM Standards, Part 14.
2. Fartash, M., "Stress Intensity Values For Prenotched And Precracked, Plain Concrete Beams," A Masters Thesis Presented at Kansas State University, 1981.
3. Go, C.G. and Swartz, S.E., "Fracture Toughness Techniques To Predict Crack Growth And Tensile Failure In Concrete," Report No. 154, Engineering Experiment Station, Kansas State University, Manhattan Kansas, July 1983.
4. Petersson, P.E., "Crack Growth And Development Of Fracture Zones In Plain Concrete And Similar Materials", Report TVBM-1006, Lund Institute of Technology, Lund, Sweden 1981.
5. Swartz, S.E., Hu, K.K., Jones, G.L., "Compliance Monitoring of Crack Growth in Concrete," Journal of the Engineering Mechanics Division, ASCE, Vol. 104, No. EM4, August, 1978.



## APPENDIX II

## Sand and Aggregate Properties

A specific gravity test was performed on the sand as per ASTM C128-79.

Briefly, the following procedure was used:

Weigh approximately 500 grams of oven dry sand and place into a pycnometer. Add distilled water to fill the pycnometer to about 75% to 90% capacity. Using a vacuum and a burner, boil the air out of the sample and water, shaking the bottle continuously. (This takes about 20 minutes.) Cool to room temperature and add de-aired, distilled water to the calibrated mark on the pycnometer. Weigh the bottle, water and sand, and measure the temperature of the sample. Empty the contents of the pycnometer into an evaporating dish using distilled water to remove all of the grains from the bottle. Fill the pycnometer with distilled water to the calibrated mark and weigh (Make sure the temperature is the same as recorded before). Place the sand and water in a drying oven until all the moisture has been removed, about 24 hours. Weigh the dried sand. Calculate the specific gravity using the following equation:

$$\text{S.G. (at temp. measured)} = \frac{\text{wt. dry sand}}{(\text{wt. flask+water})+(\text{wt. dry sand})-(\text{wt. flask, sand, water})}$$

The test was performed on two samples. Sample 1 had a S.G. of 2.658 and sample 2 had a S.G. of 2.651. The average of these two was used (S.G.=2.655)

A specific gravity test was performed on the aggregate as per ASTM C127-81. Briefly, the following procedure was used:

For 3/4" aggregate, soak 6.6 pounds of aggregate in water for 24 hours prior to testing. After soaking, remove the sample from the water and dry the surface of the particles. Weigh the saturated surface-dry sample. Put the sample in a wire bucket with a small enough mesh that none of the aggregate will fall through. Weigh the sample submerged. Remove the sample and place in an evaporating dish and oven dry for 24 hours. When

sample is completely dry, weigh again. Use the following formula to calculate the specific gravity:

$$S.G. = \frac{(\text{wt. oven dry})}{(\text{wt. sat., surface dry}) - (\text{wt. sat., submerged})}$$

This test was performed on two samples. Sample 1 had a S.G. of 2.54 and sample 2 had a S.G. of 2.57. The average of these two was used. (S.G.=2.56) A sieve analysis was done on both the sand and the aggregate as per ASTM C136-82.

For the sand, 500 gram samples were used for each test. The oven-dry sample was placed into a standard sieve set consisting of the following sieve sizes: .150mm, .300mm, .600mm, 1.18mm, 2.38mm. The sieves were shaken for 10 minutes in the mechanical shaker, and the amount retained on each sieve was recorded. The fineness modulus was calculated to be 2.91, and the gradation curve was plotted.

The aggregate sample was 11 pounds as recommended and was broken into five parts. Each of the five partial samples was put through the sieve test using the following sieve sizes: #10(2.00mm), #8(2.38mm), #4(4.76mm), 3/8"(9.52mm), 1/2"(12.70mm), 3/4"(19.10mm). As with the sand, they were shaken with the mechanical shaker for 10 minutes and the gradation curve was plotted.

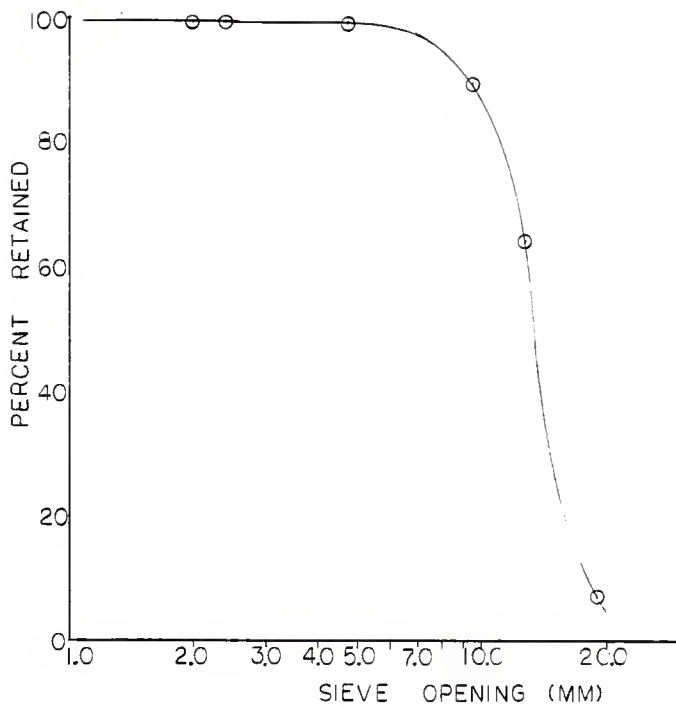
In both the sand and aggregate sieve analysis, an analysis of any material finer than the 75X10<sup>-6</sup>m sieve, that is the dust, was neglected.

A dry rodded unit weight was performed on the aggregate as per ASTM C29-78.

Find the volume of a bucket by weighing the bucket empty, then weighing it full of water at room temperature, and then dividing the weight of the water by the density of water at room temperature. Fill the bucket 1/3 full and rod 25 times. Add another 1/3 and rod 25 times penetrating the first layer by 1-2 inches. Repeat with the third layer. Level off the bucket and weigh the bucket and aggregate. Divide the weight of the

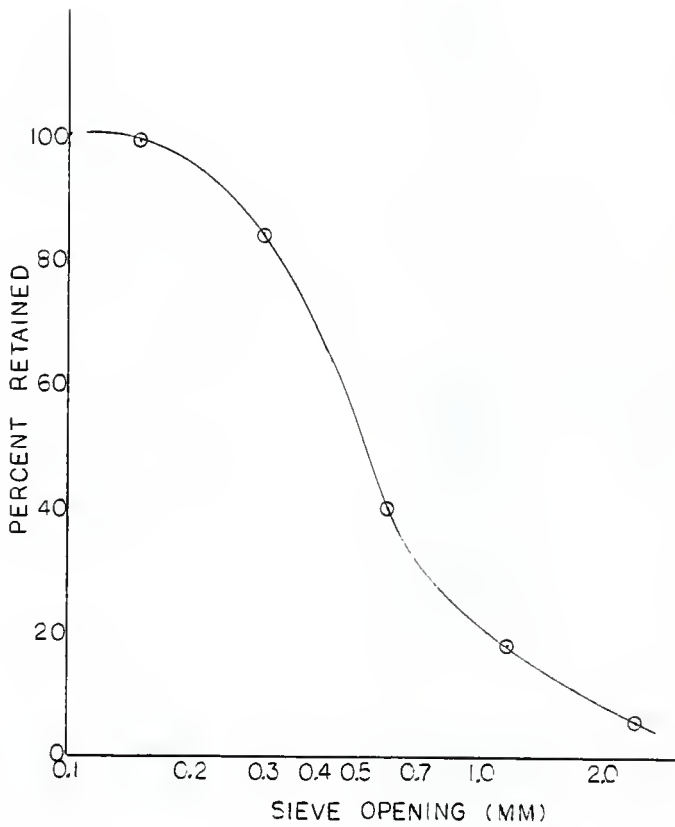
aggregate by the volume of the bucket to get the dry rodded unit weight.

This test was performed two times and the average dry rodded unit weight was 94 lbs./ft.<sup>3</sup>



1.0 IN. = 25.4 MM

GRADATION OF LARGE AGGREGATE



1.0 IN. = 25.4 MM

GRADATION OF SAND

## Appendix III

## STRAIN PROFILES

STRAID PROFILE. #2

LOAD= 560

AW = .28

R = .5139



1.12"

65

81

7000

6000

5000

4000

3000

2000

1000

0

-1000

-2000

-3000

-4000

-5000

-6000

-7000

-8000

-9000

-5

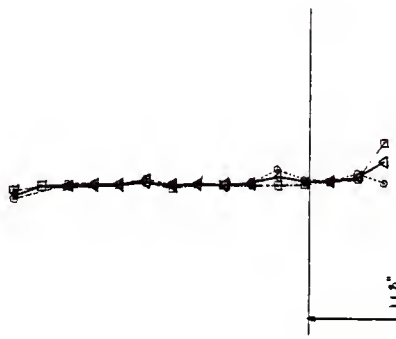
STRAIIN PROFILE #3

LOAD = 780

$\Delta W = .42$

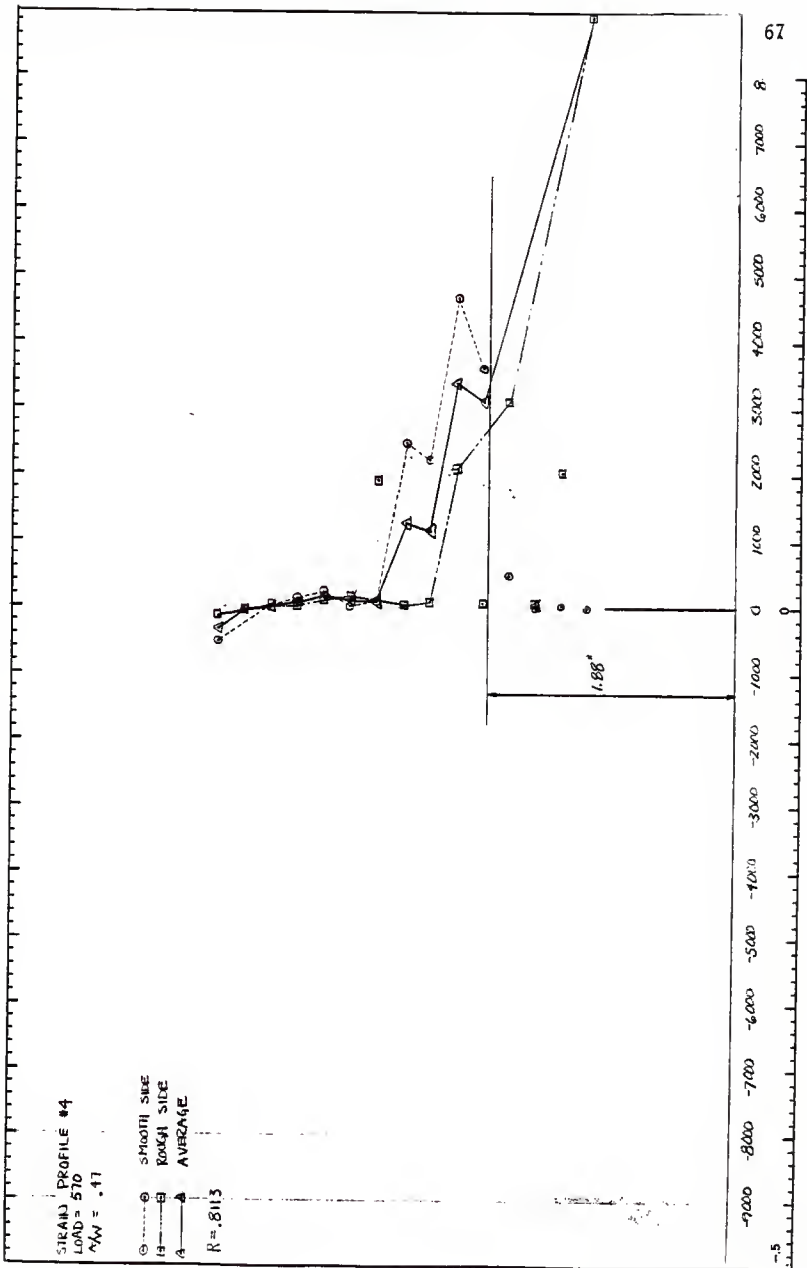
○ ..... ○ SMOOTH SIDE  
□ ..... □ RAUGH SIDE  
▲ ..... ▲ AVERAGE

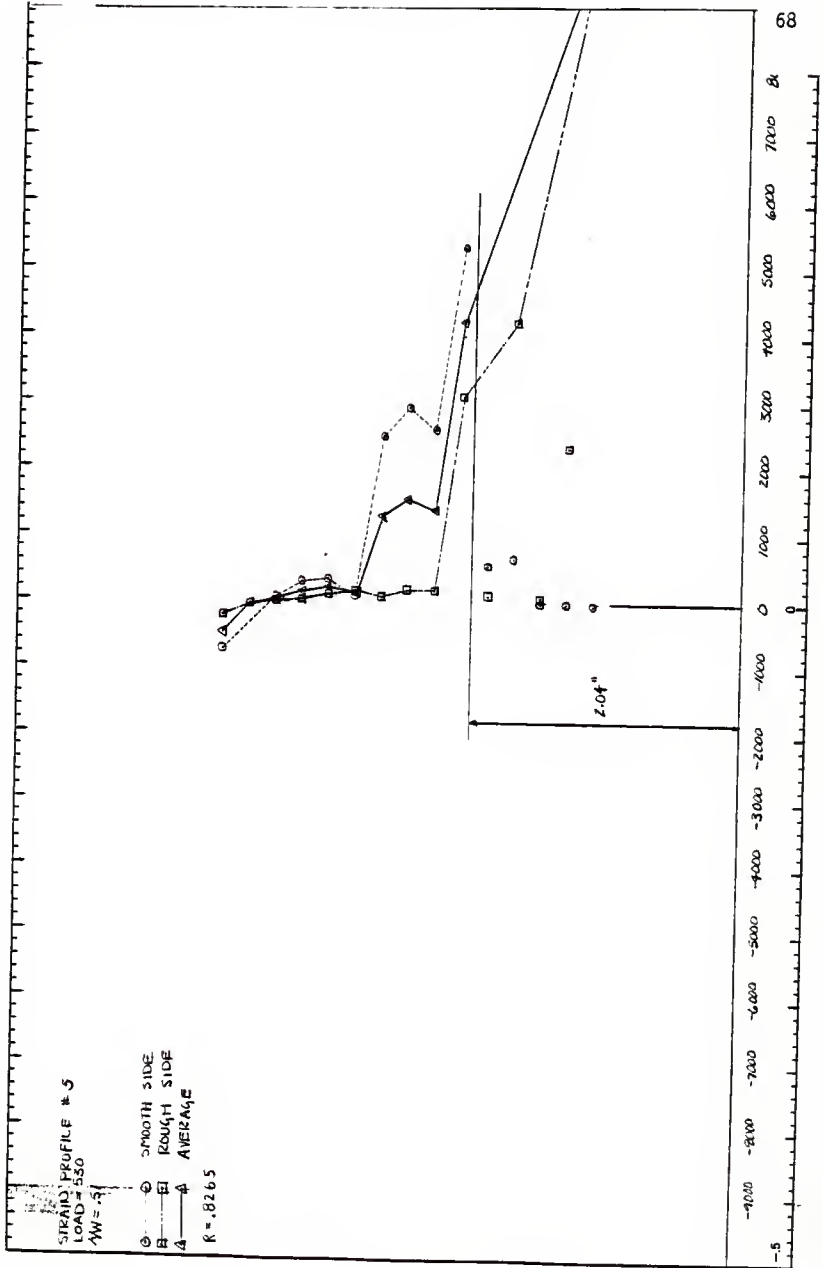
R = .4377

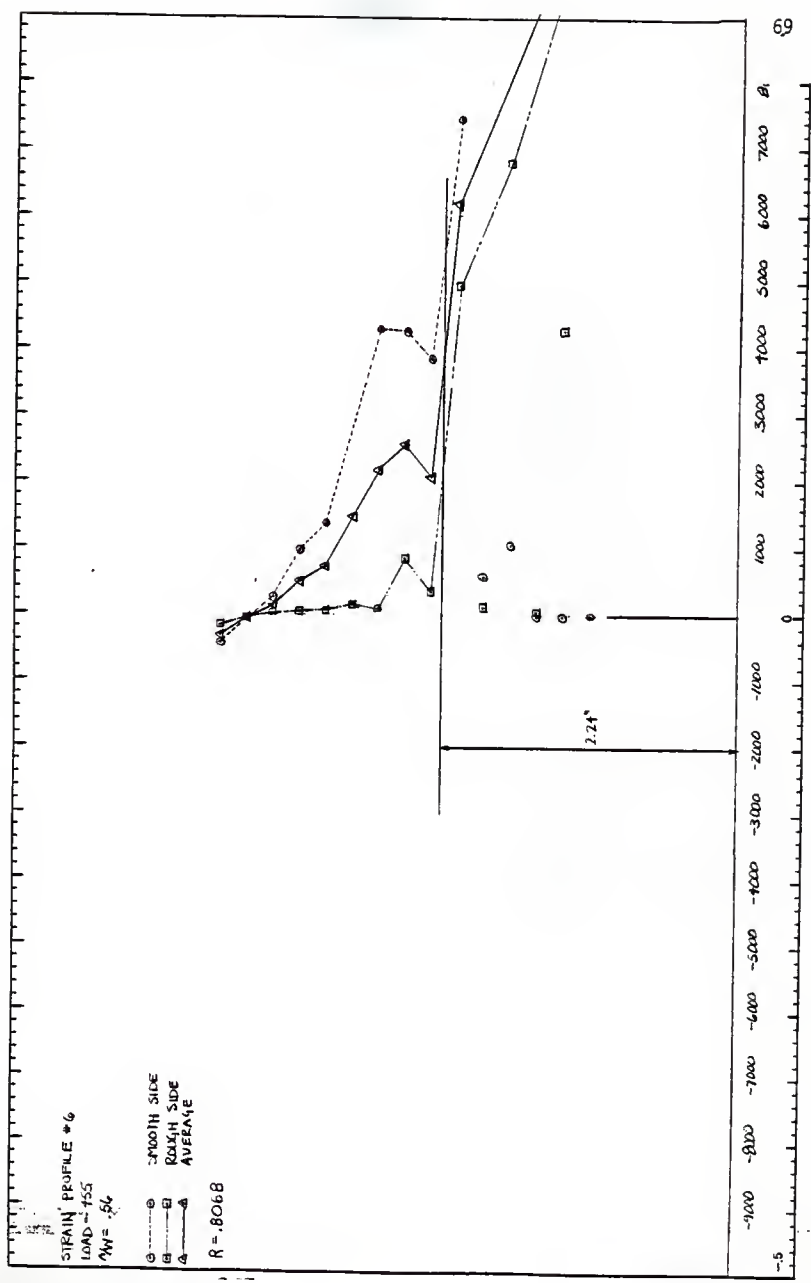


-9000 -8000 -7000 -6000 -5000 -4000 -3000 -2000 -1000 0 1000 2000 3000 4000 5000 6000 7000 8000 9000









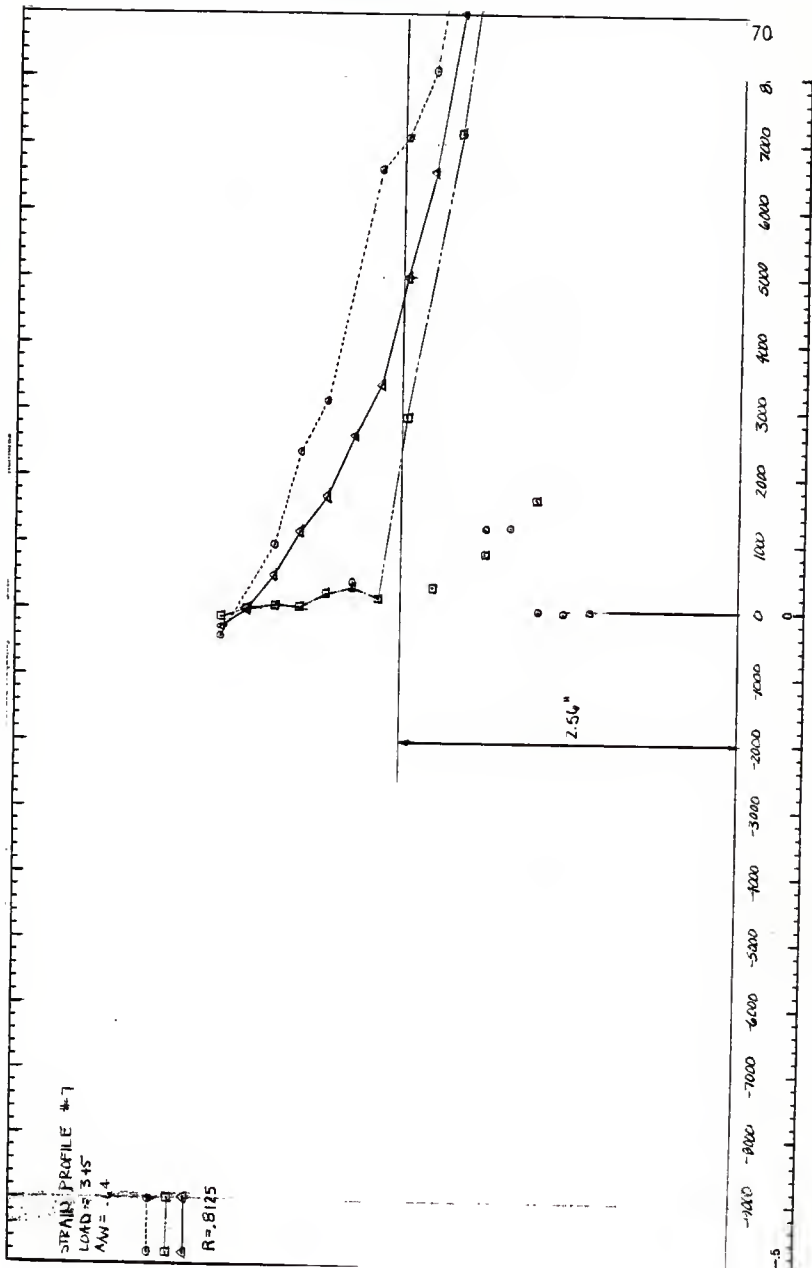
STRAIN PROFILE #7

LOAD = 345

$\Delta W = 1.4$



$R = 0.125$



STRAIN PROFILE # 9

LOAD # 110

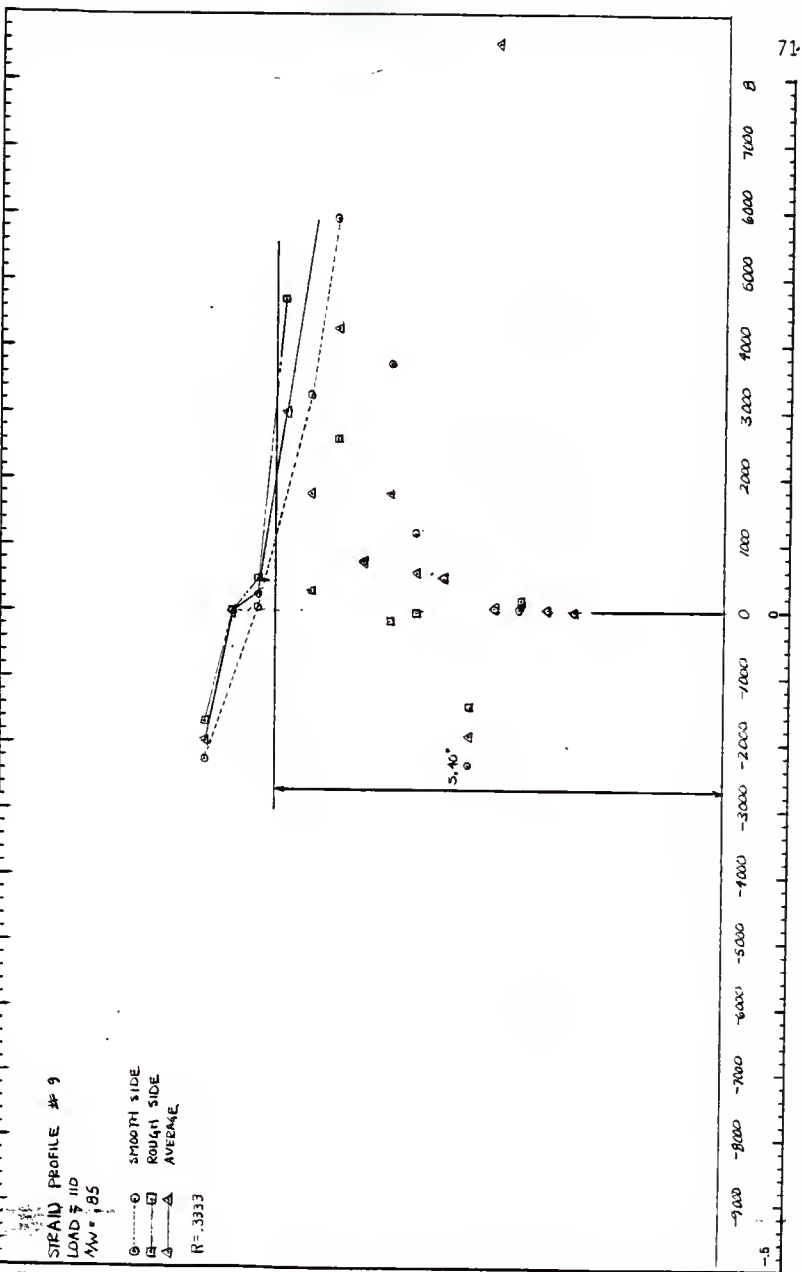
$\gamma/W = 1.95$

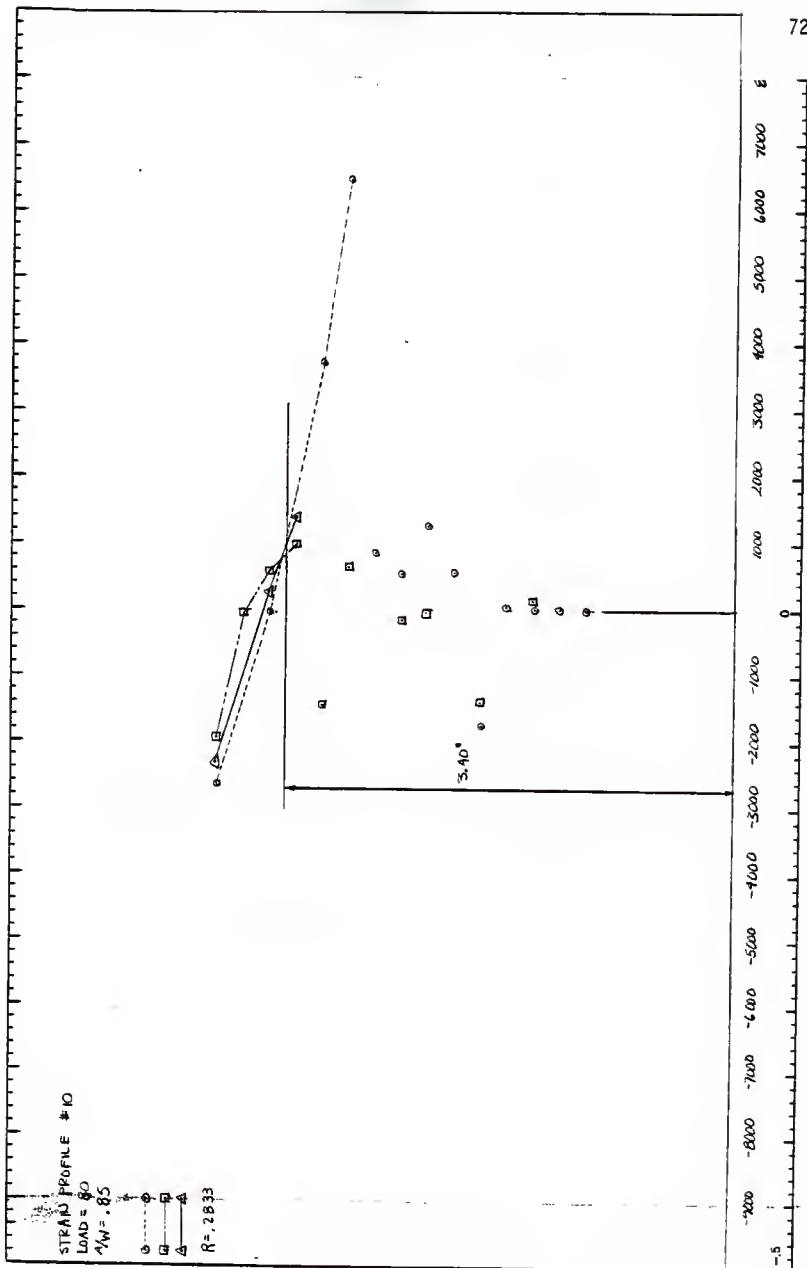
○ ..... ○ SMOOTH SIDE

□ ..... □ ROUGH SIDE

△ ..... △ AVERAGE

R = .3333





## Appendix IV

## RAW DATA

Scale for all raw data graphs is as follows:

X-axis     1 square (as noted on p.75) = 2 cm

Y-axis     1 square = 2 cm

Scale factors to determine actual values of load (Y-axis) and displacement (X-axis) are found on pages 13 and 14. Each graph is labeled CMOD or LPD to identify what kind of displacement is represented.

## Cylinder Test Data

---

Compressive Strength in PSI

---

Batch A:	4074*	Batch B:	8078
	4711*		7993
	7569		8050
	7512		9181
	7172		7116
	8715		7937
	8573		9153
	8191		7908
			8446
			8361
			6805
			8474

---

Tensile Strength in PSI

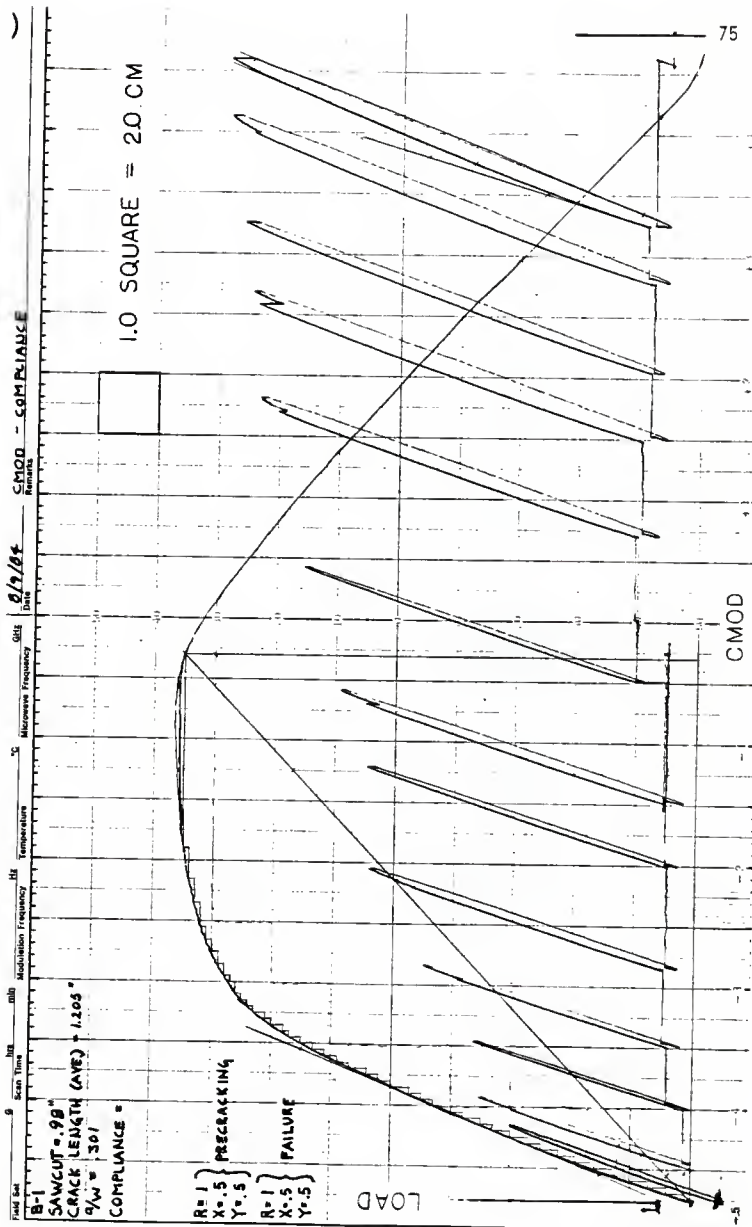
---

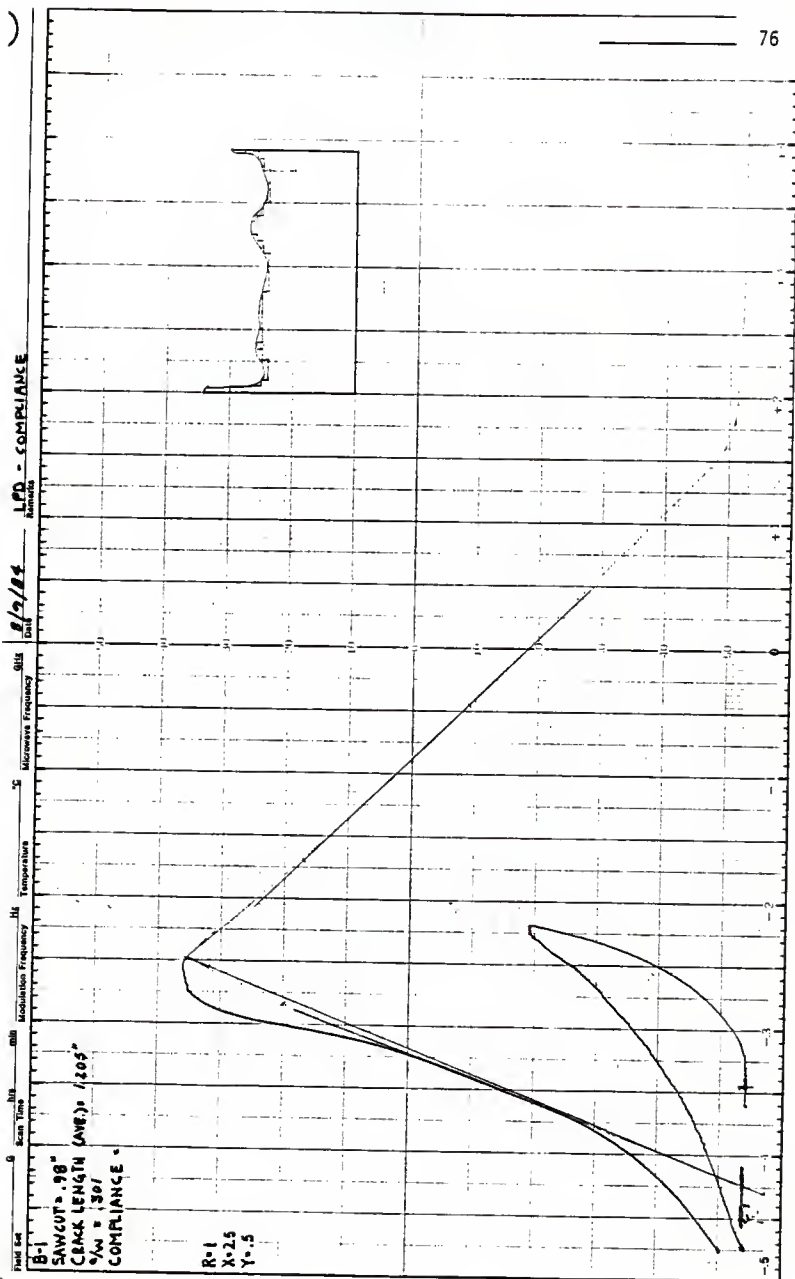
Batch A:	601	Batch B:	665
----------	-----	----------	-----

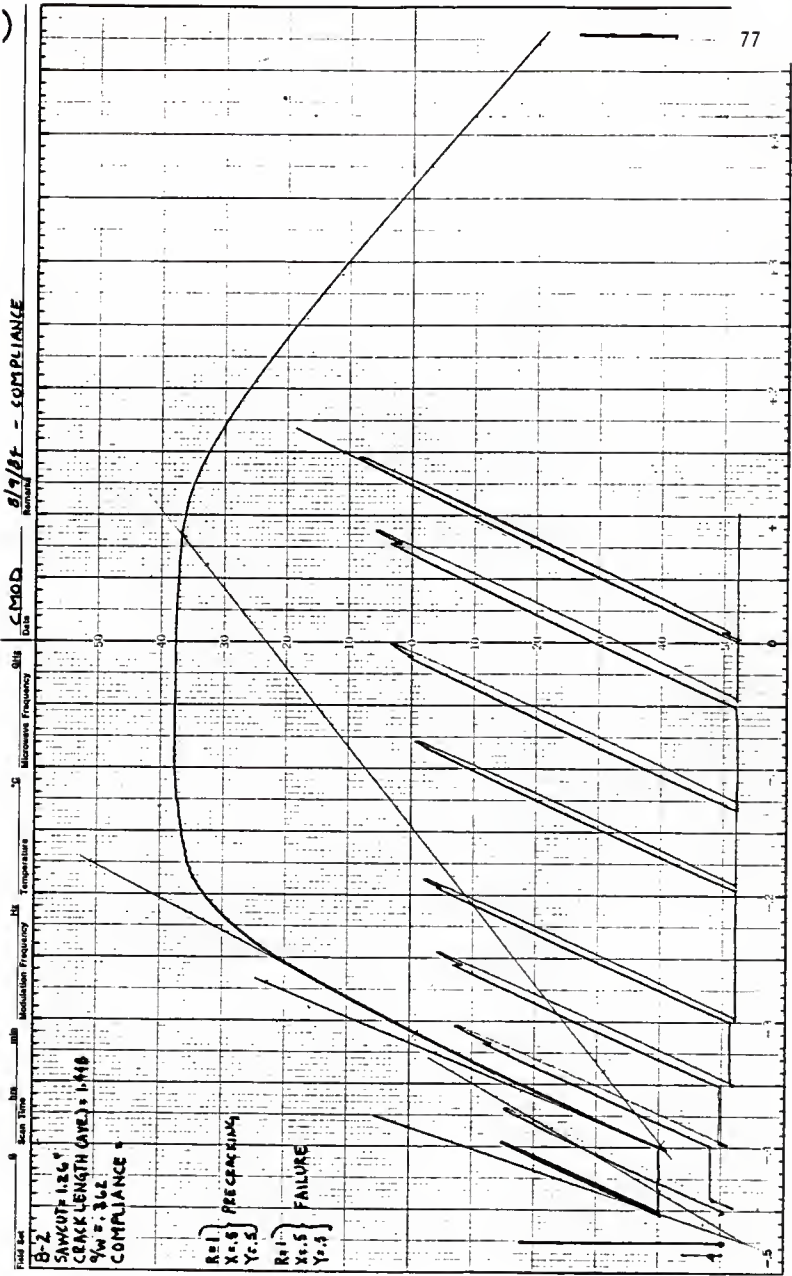
\*Testing machine not working properly so these values are disregarded.

$$1.0 \text{ PSI} = 6.89 \times 10^{-2} \text{ MPa}$$









8/9/84 - COMPLIANCE

CMOD

Modulation Frequency MHz

Temperature

Modulation Frequency MHz

Scale Time

Scale Time

SAWCUT = 1.86"  
 CRACK LENGTH (AVE.) = 1.418  
 W = 3.62  
 COMPLIANCE =

R=1 } PRE CRACKING  
 X=5  
 Y=3

R=1 } FAILURE  
 X=5  
 Y=3

L.P.O. - COMPLIANCE

8/7/81

Gills

Temperature

Modulation Frequency

MHz

Scan Time

Full Set

B-2

SANGUET 1.26"

CRACK LENGTH (AVE) = 1.418"

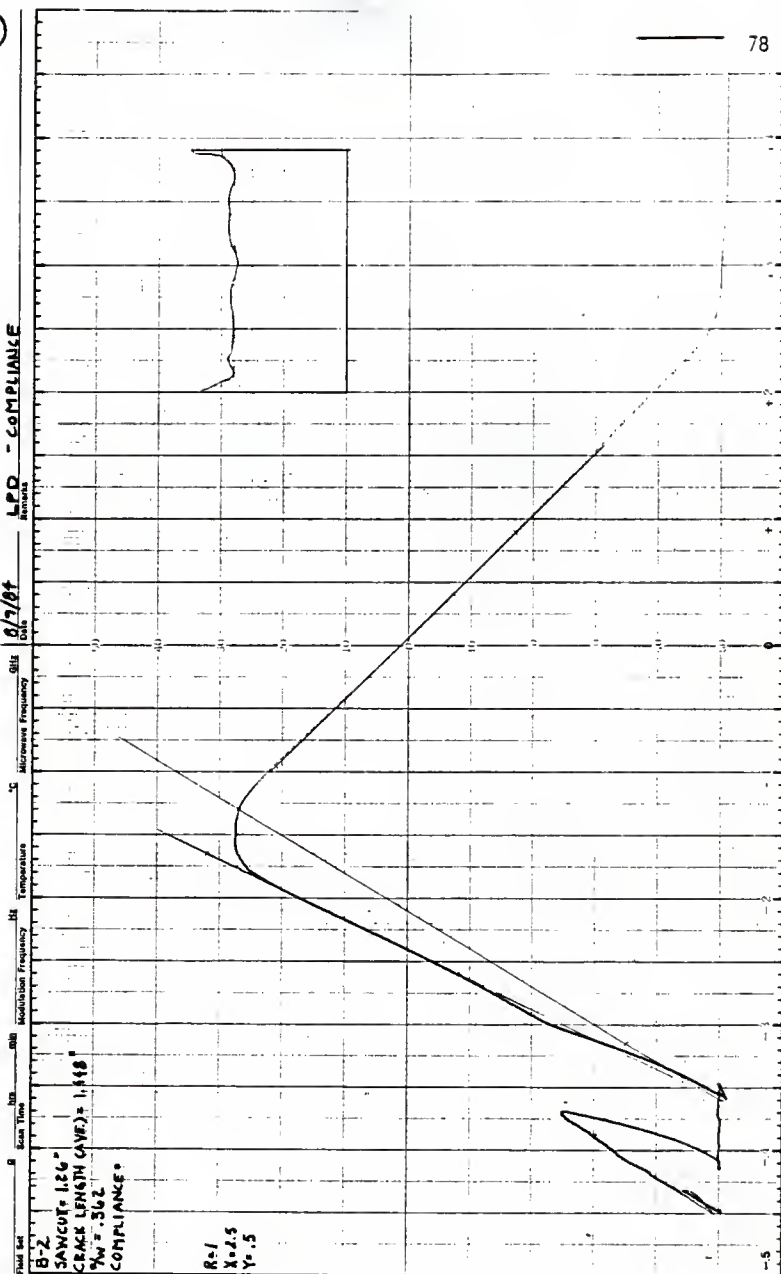
W = .362

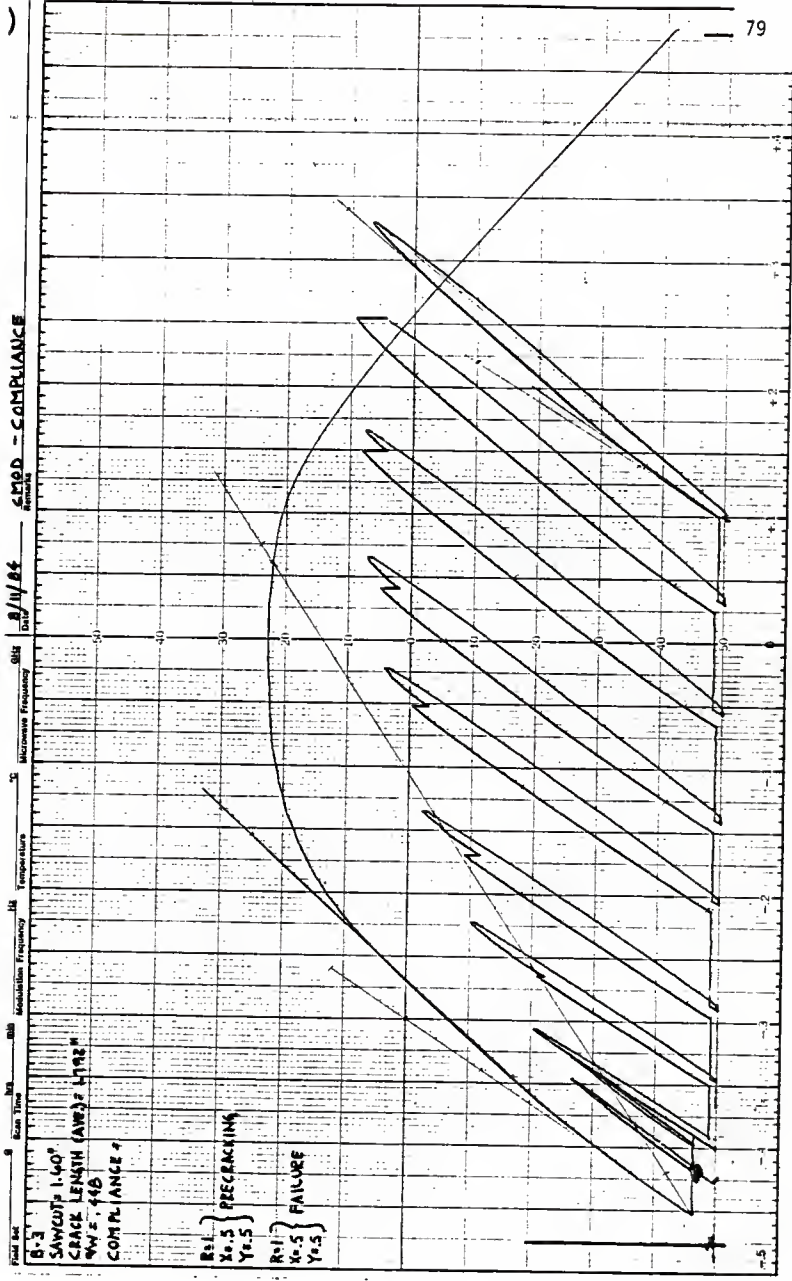
COMPLIANCE =

R = 1

X = 1.5

Y = .5



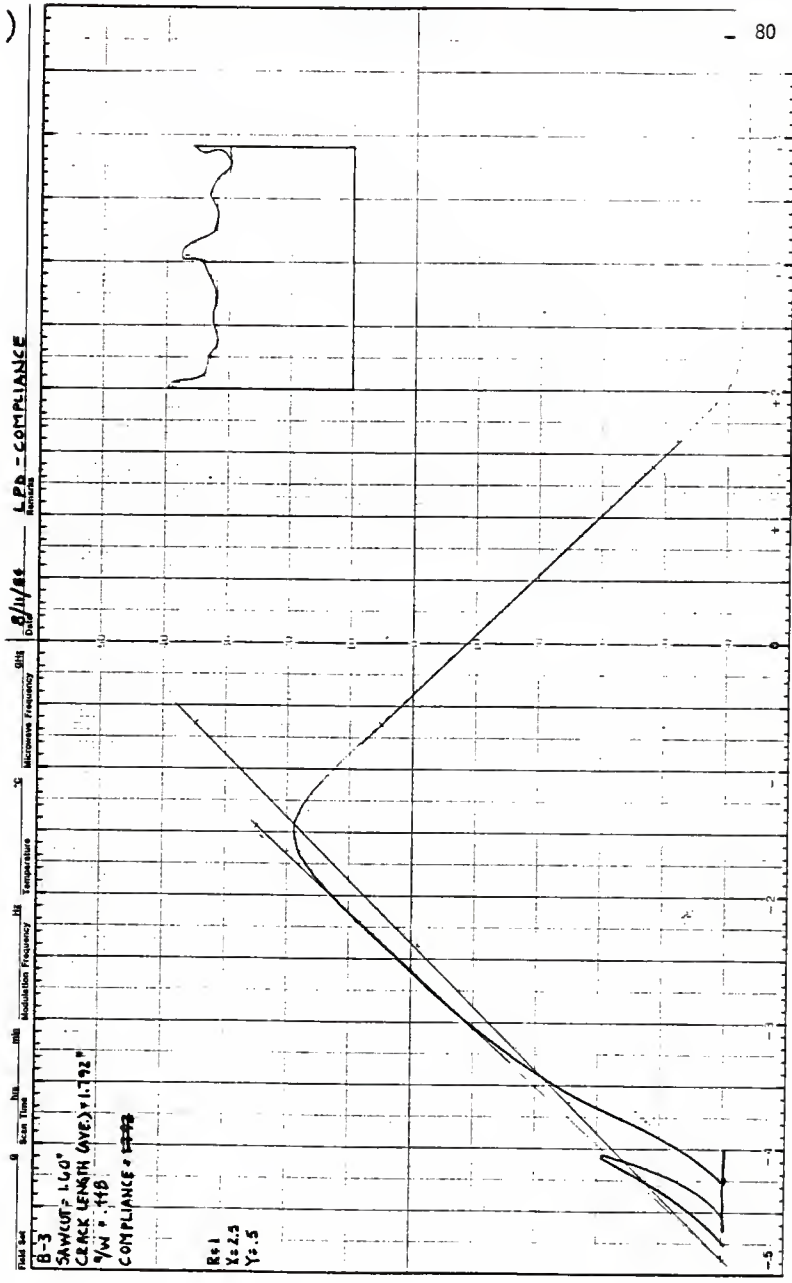


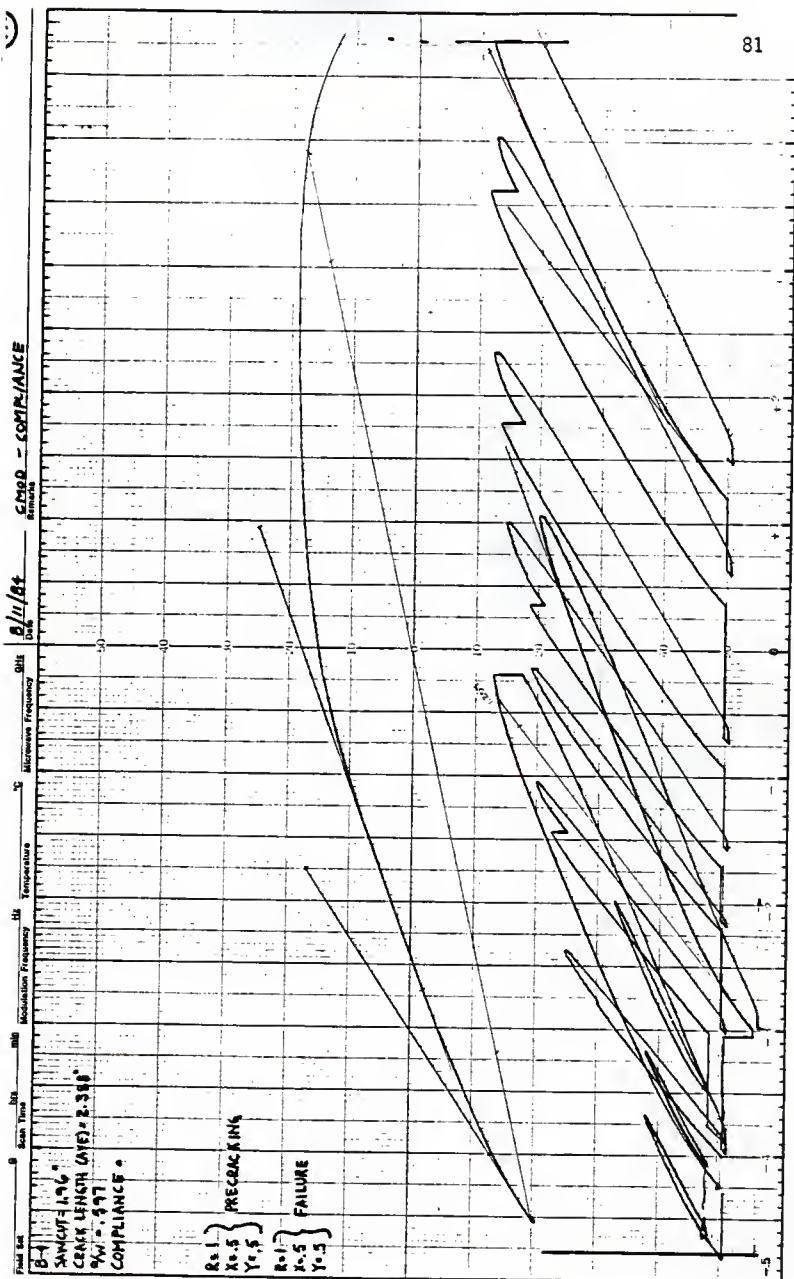
8/11/84 SMD - COMPLIANCE

79

B-3  
 SAWTOOTH 1.40"  
 CRACK LENGTH (AWD) 1.78"  
 W x E 4 x 8  
 COMPLIANCE 4

R:1 } RECRACKING  
 Y:5 }  
 R:1 } FAILURE  
 Y:5 }





8/11/84 LPD - COMPLIANCE

08H

Temperature

Modulation Frequency

Scan Time

Field Set

SAWG/CF 1.96"

SPACE LENGTH (AVE.) = 2.888"

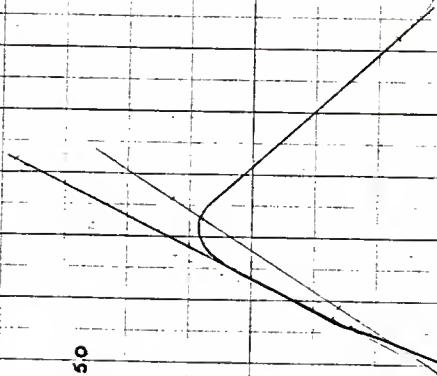
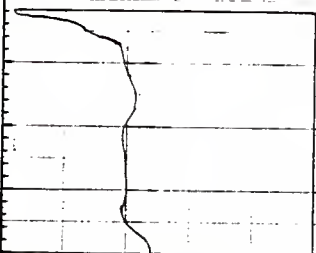
%W = 597

COMPLIANCE = "

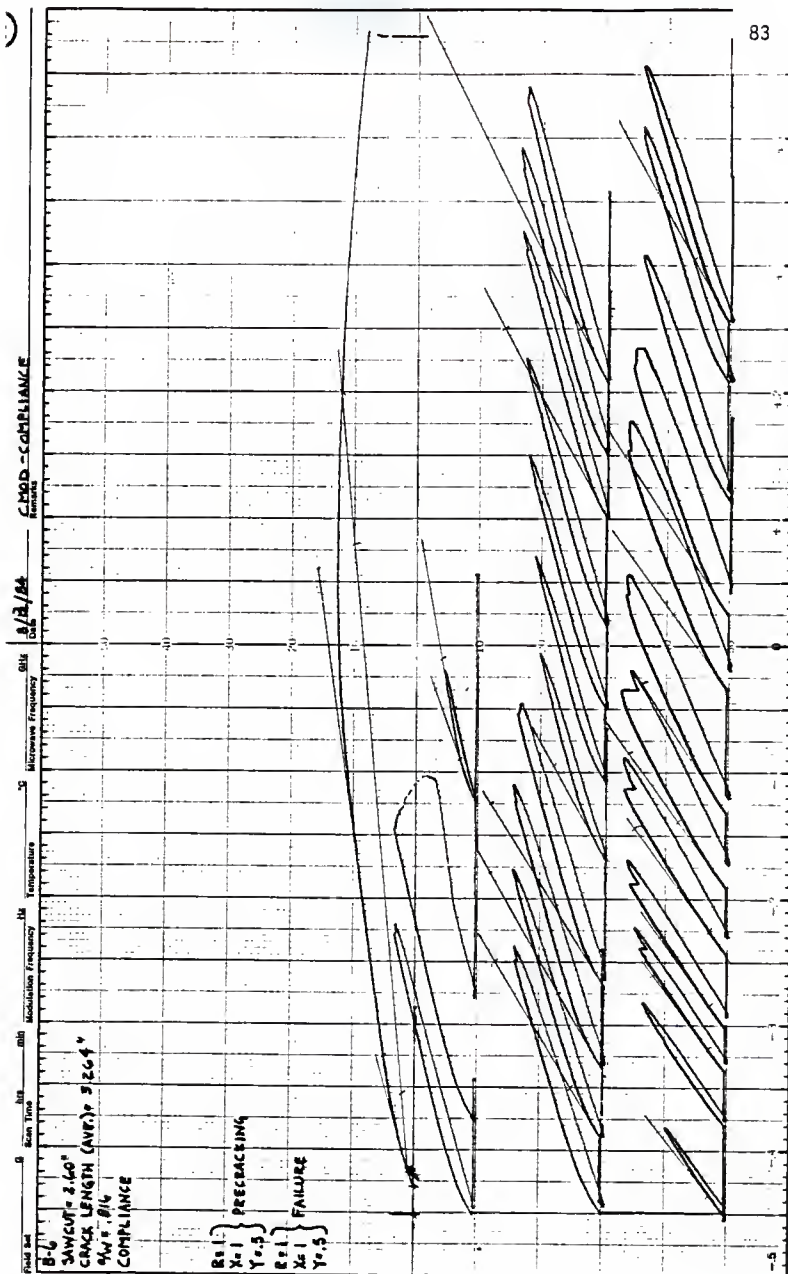
R=1

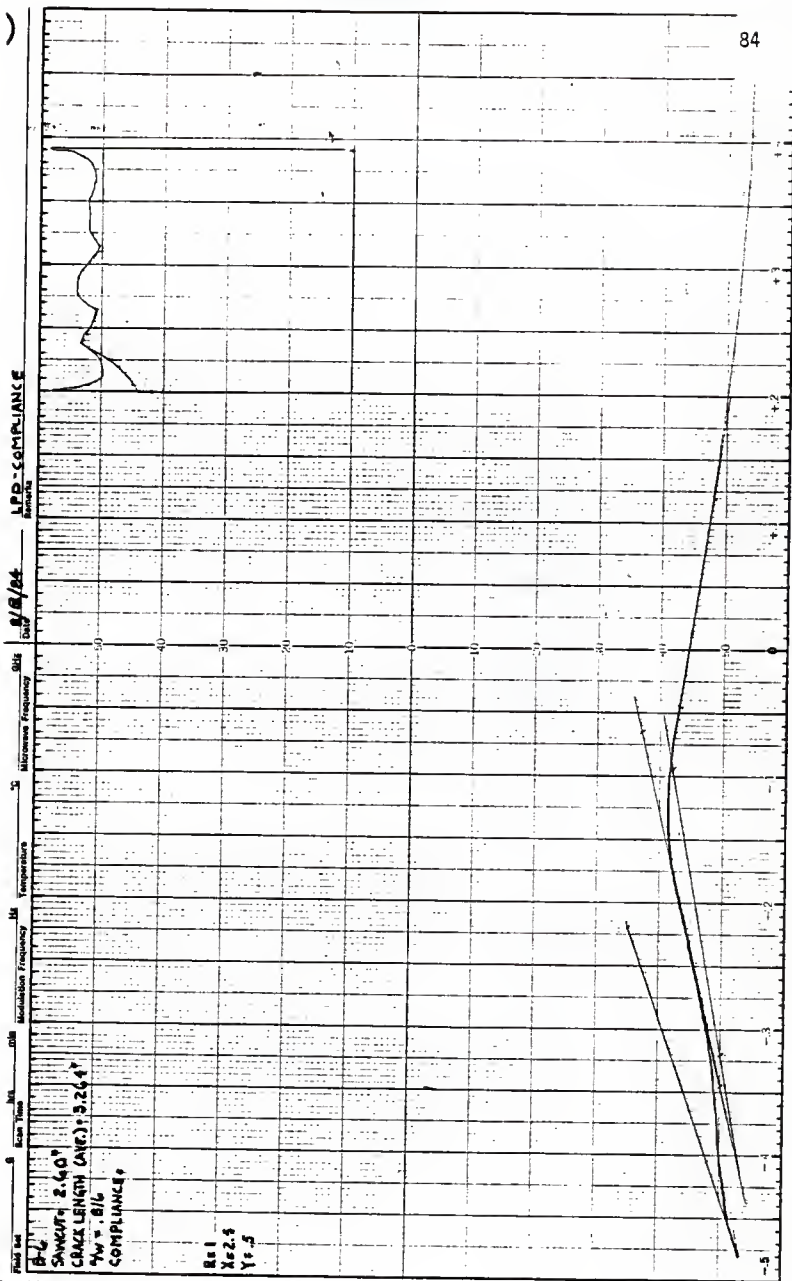
X=2650

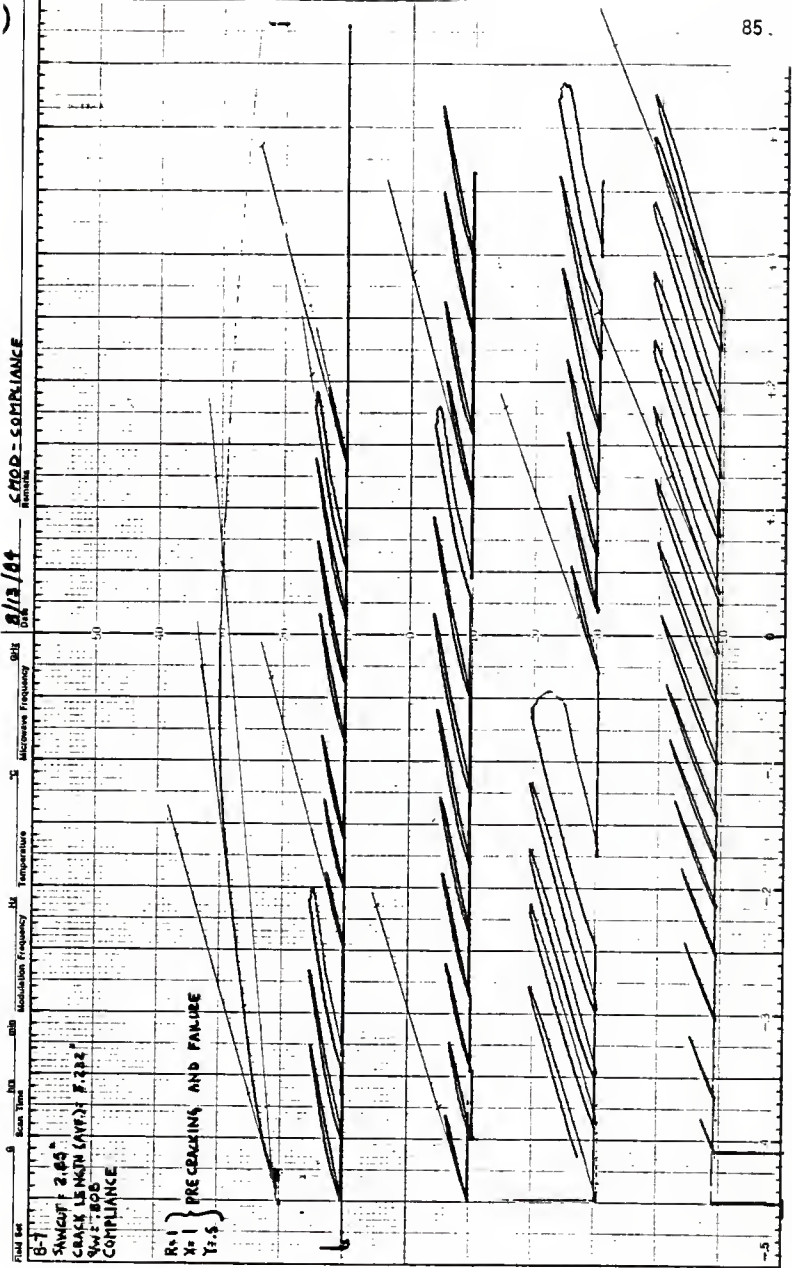
Y=5











C-MOD - COMPLIANCE

8/13/64

Modulation Frequency

Temperature

Modulation Frequency

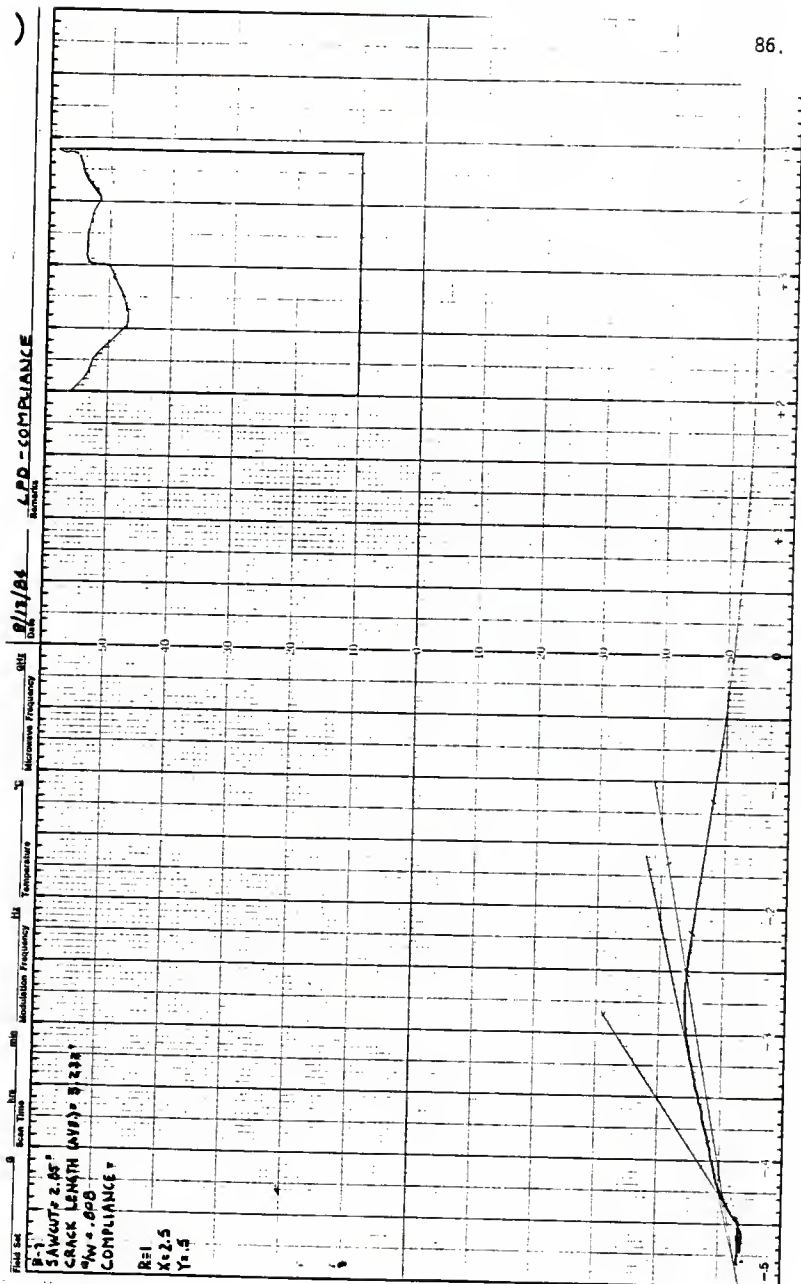
Scan Time

0 1 2 3 4 5 6 7 8 9 10

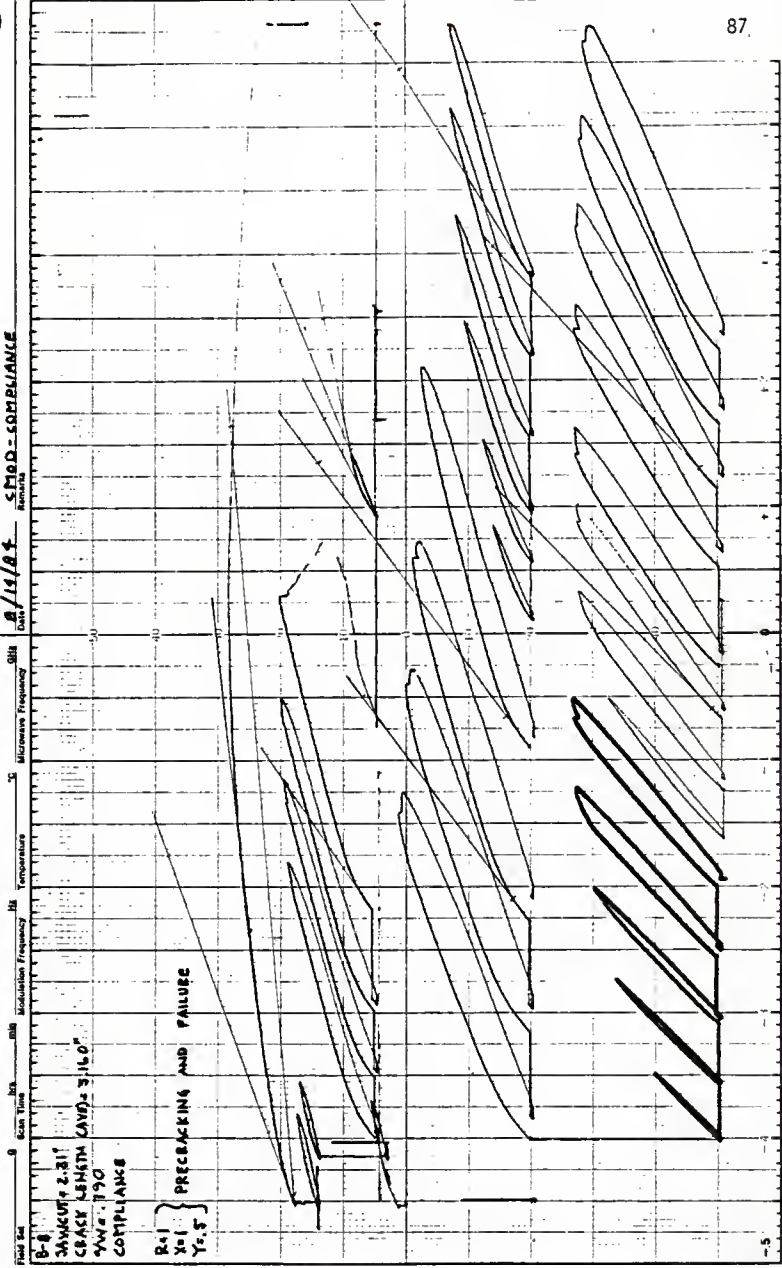
Field Set

SINGUP: 2.65"  
 CRACK LENGTH (AVG): 0.282"  
 SWS: 800  
 COMPLIANCE

R-1 } PRE-CRACKING, AND FAILURE  
 R-2 }  
 T-1, 5 }

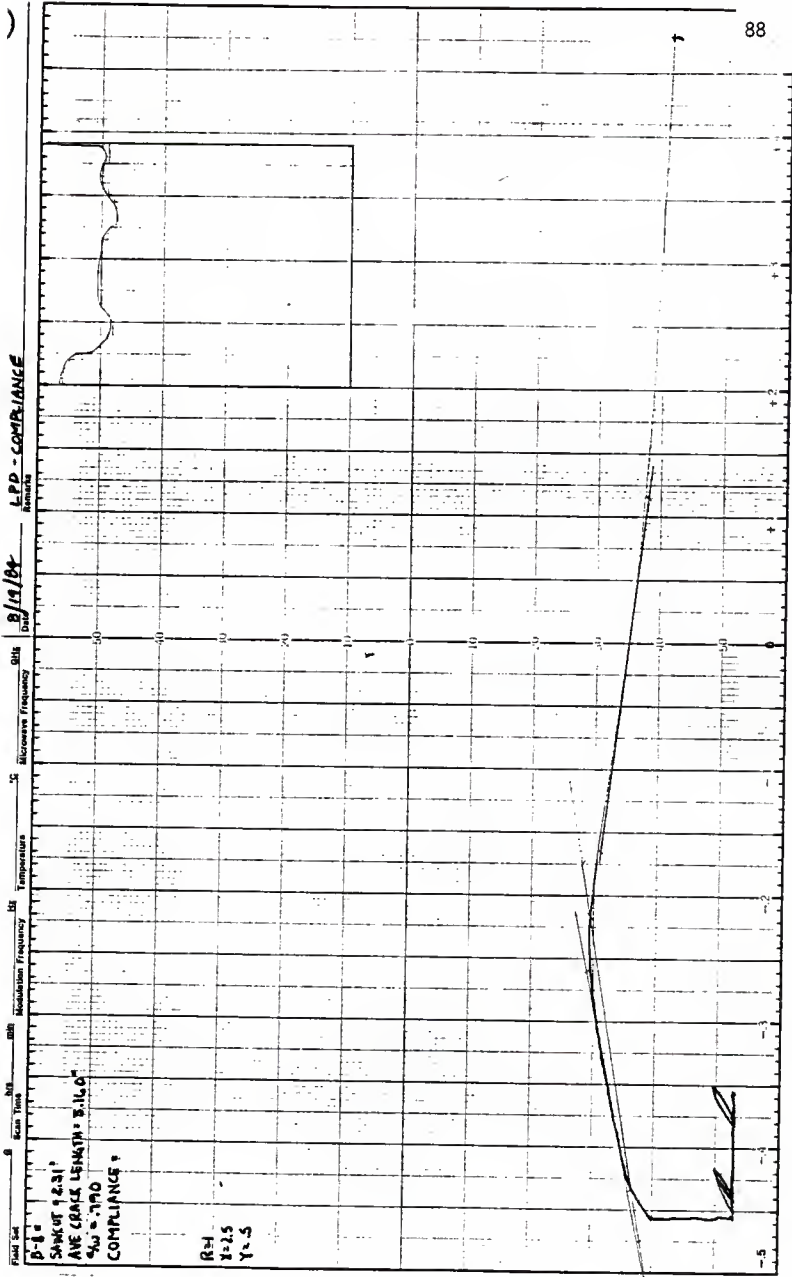


8/19/84 SMOG-COMPLIANCE  
 Date Remarks



B-6  
 SAMPLE 2.31"  
 CRACK LAMINA (AYD) 3.160"  
 WAVE 190  
 COMPLIANCE

R-1 } PREBACKING AND FAILURE  
 R-2 }  
 R-3 } Yr. 5



L.P.D. - COMPLIANCE

8/19/84

Microwave Frequency GHz

Temperature

Modulation Frequency

dB

Scan Time

Plot Set  
P-1

SHAKOR 9231  
AVE CRANE LEMAY BILCO  
400 0.110  
COMPLIANCE

RH  
X=2.5  
Y=5

-5

CMOP - COMPLIANCE

8/19/86  
Date

GHz  
Microwave Frequency

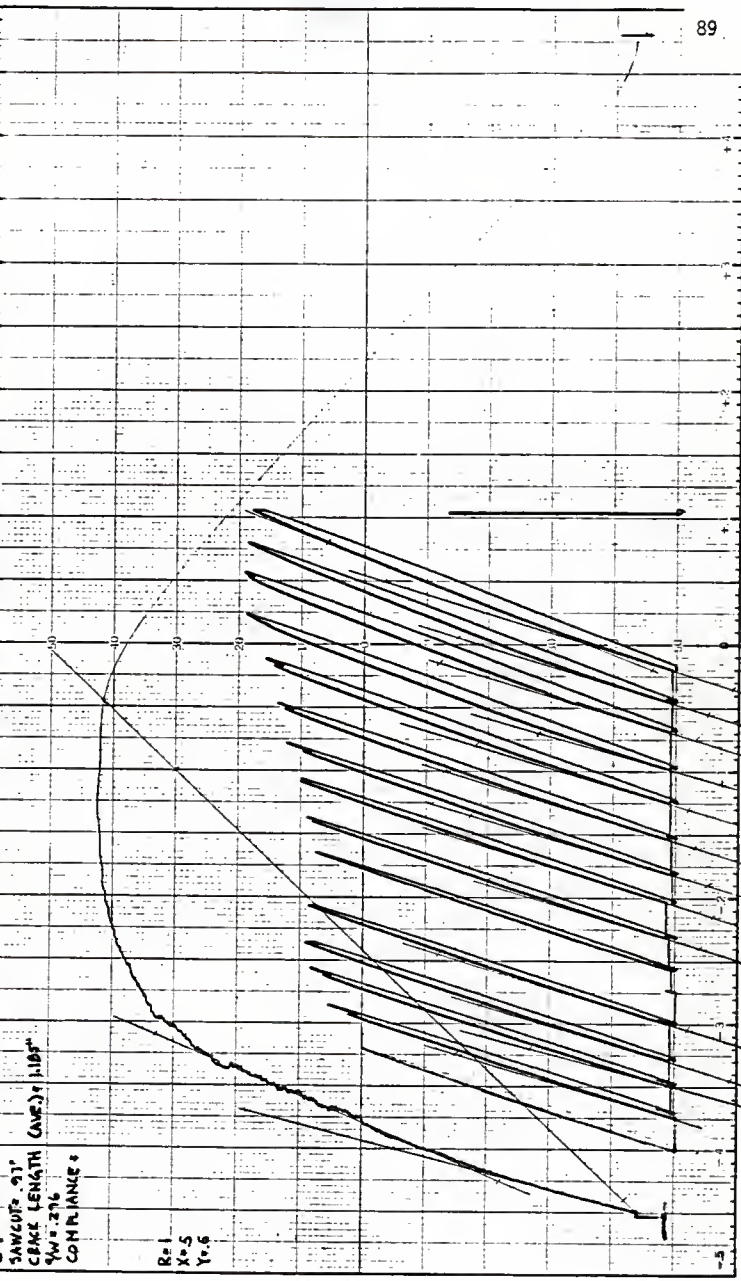
Temperature

Modulation Frequency

dB

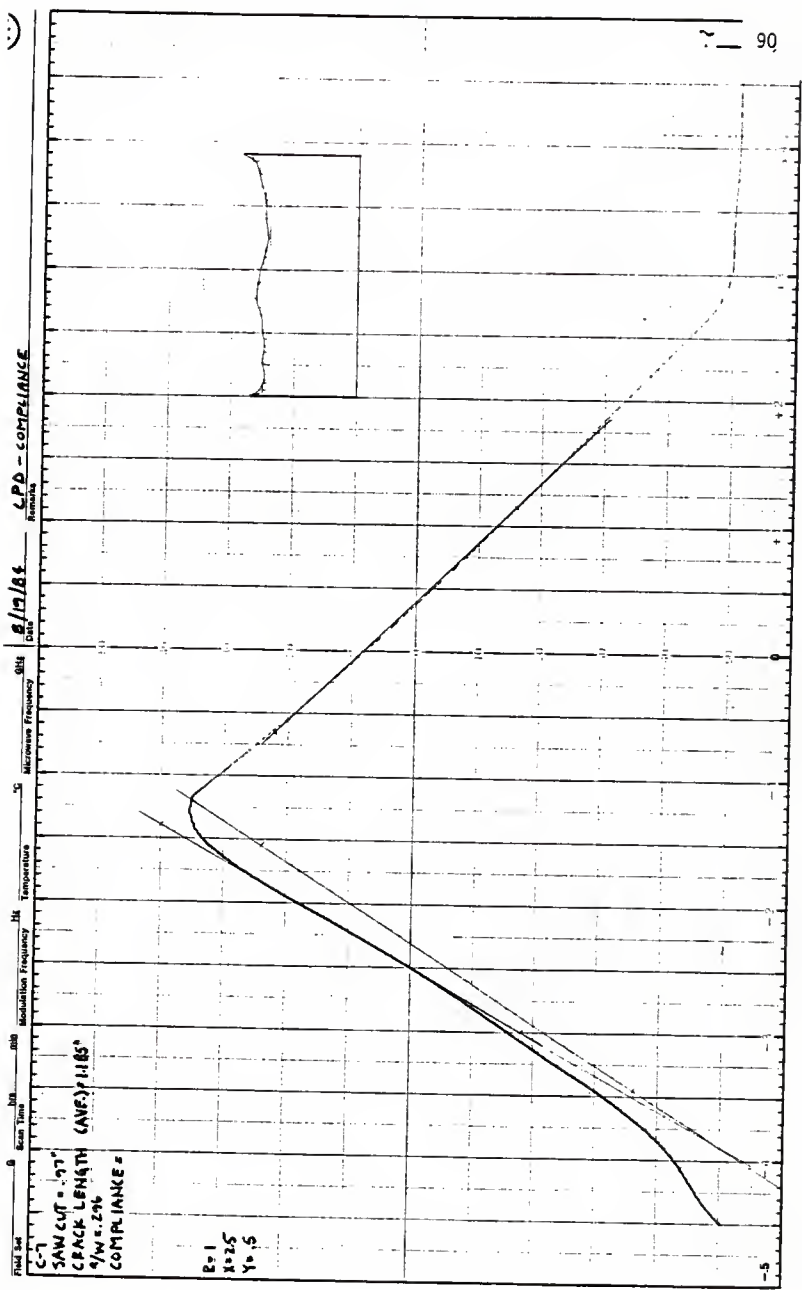
Scan Time

8

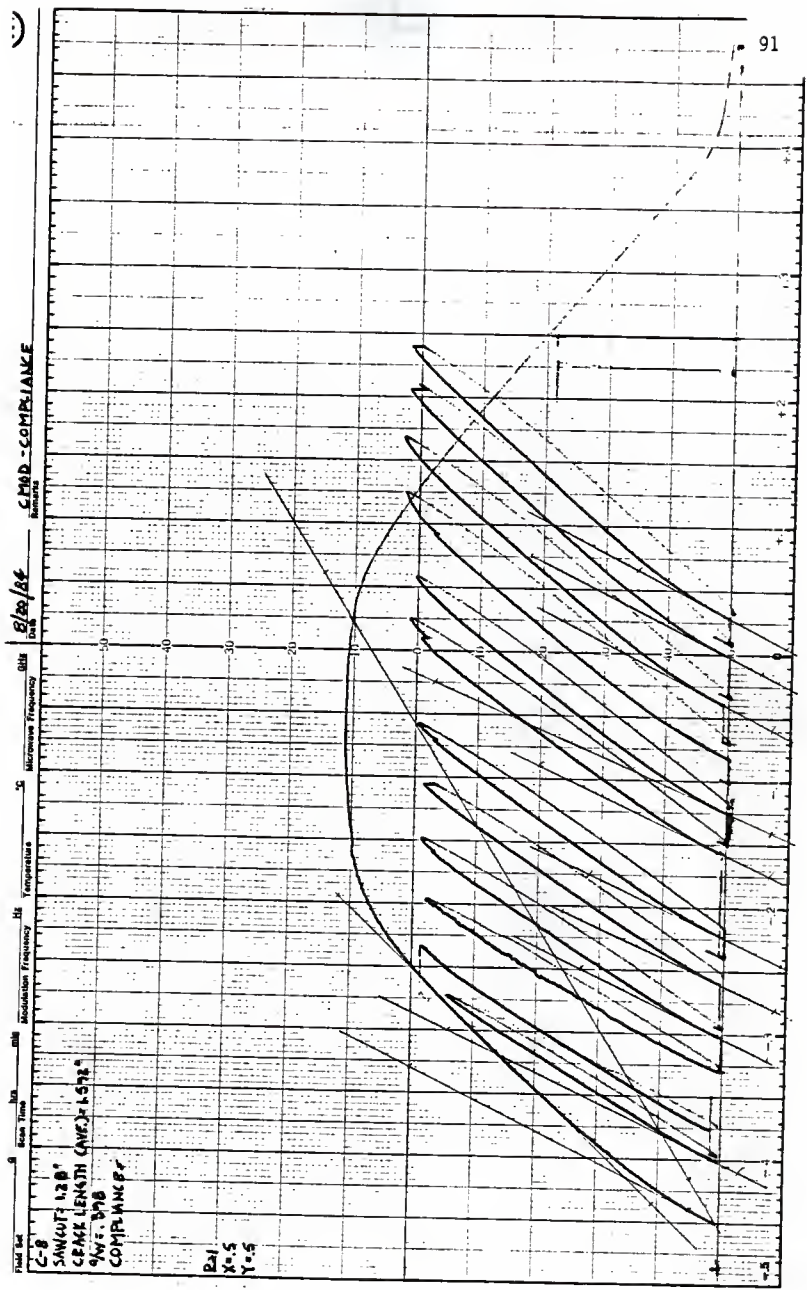


SAWCOP = 91  
 CABLE LENGTH (AVE) = 1.10"  
 $\gamma_W = 276$   
 COMPLIANCE =

R = 1  
 X = 5  
 Y = 6

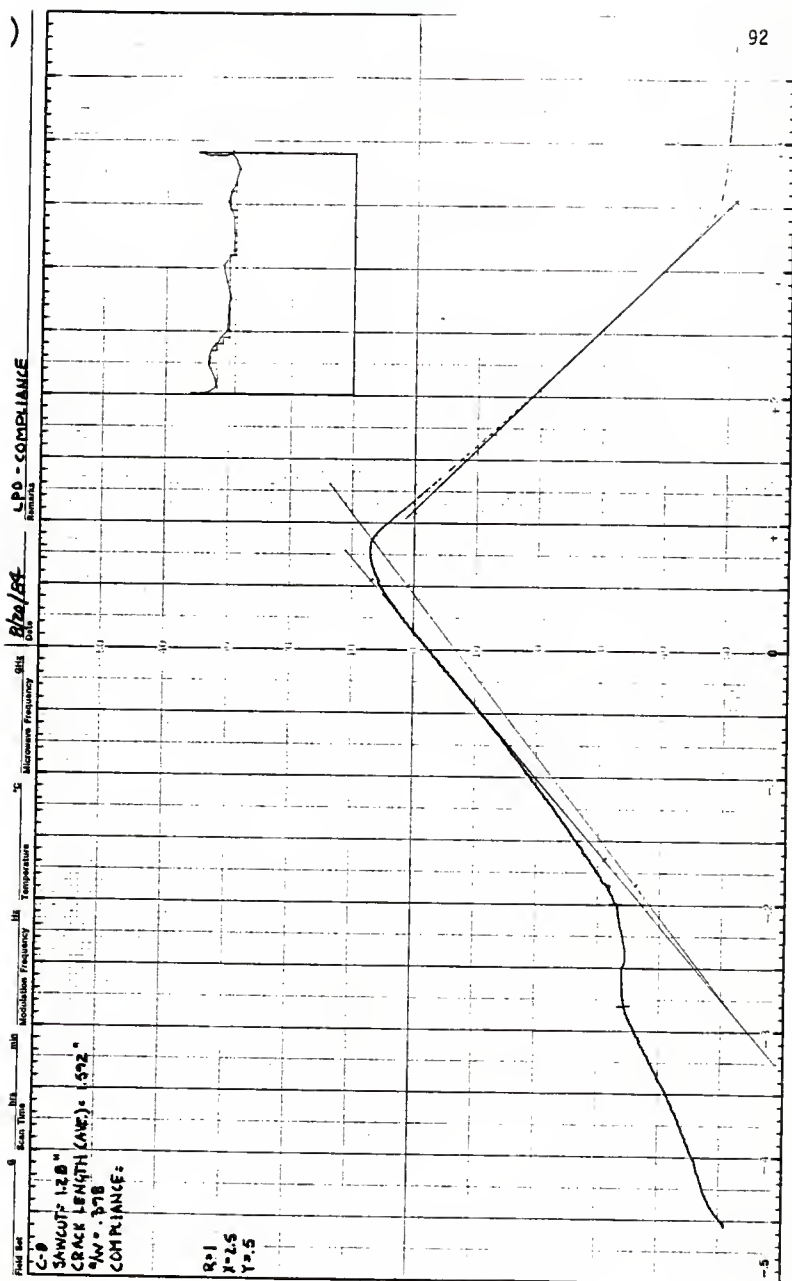






C-8  
 SAW CUT 1.20"  
 CRACK LENGTH 0.0578"  
 94% 0.08  
 COMPLIANCE

B-1  
 N-5  
 T-5



8/20/84 CHRD - COMPLIANCE  
DATE RENEW

8/20/84  
DATE

800  
MHz  
Frequency

800  
MHz  
Frequency

TEMPERATURE

800  
MHz  
Frequency

800  
MHz  
Frequency

800  
MHz  
Frequency

800  
MHz  
Frequency

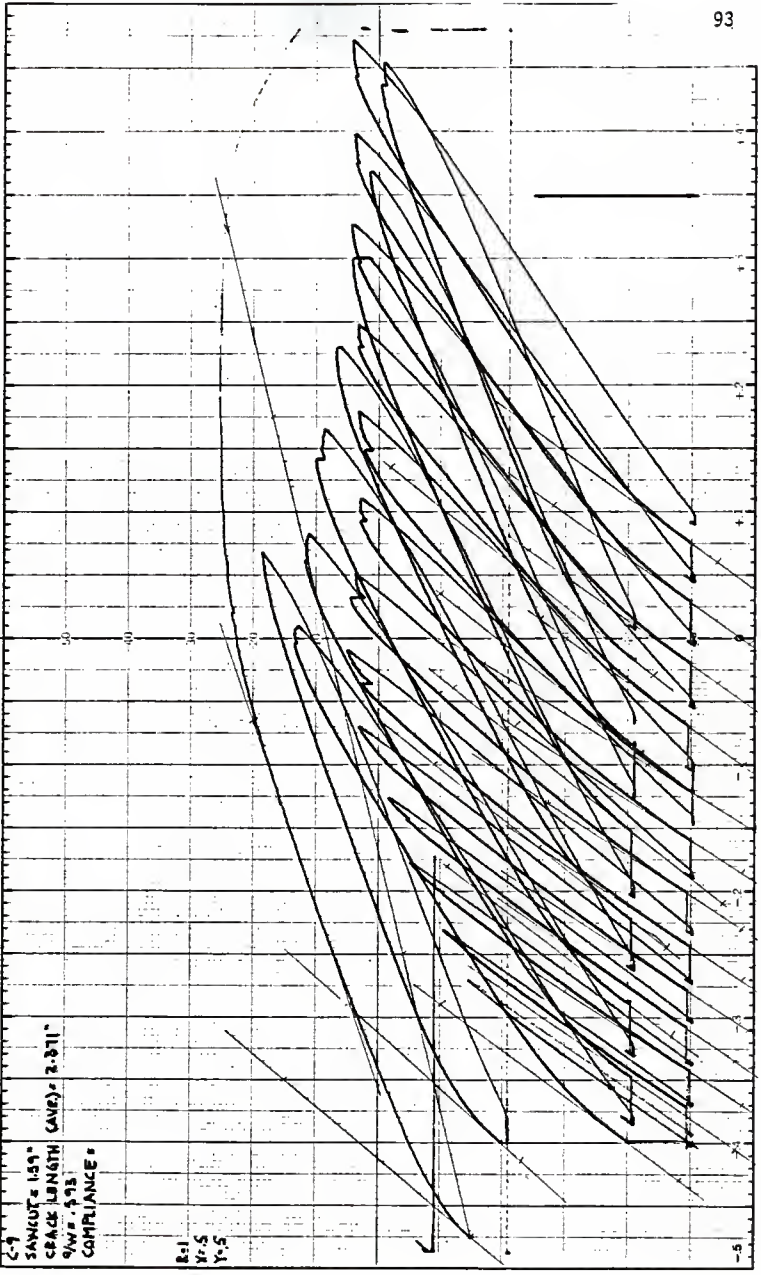
800  
MHz  
Frequency

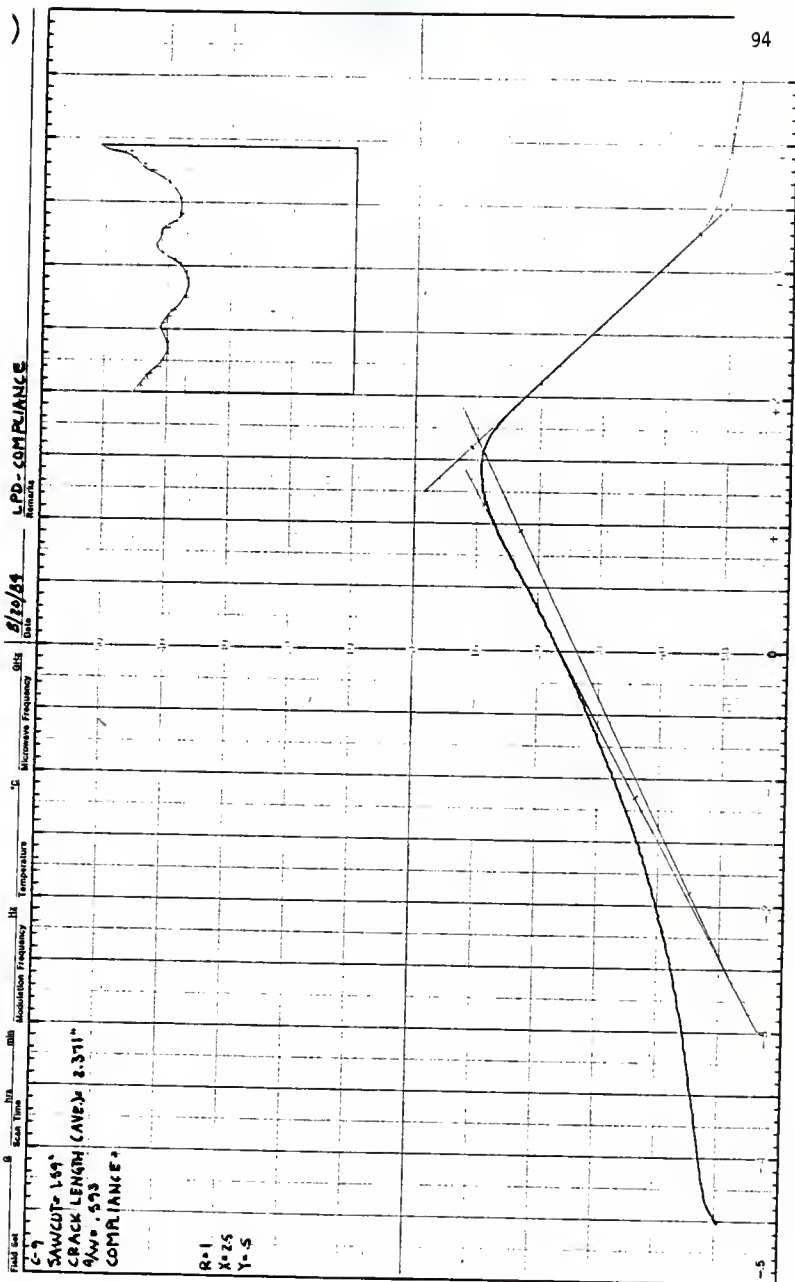
800  
MHz  
Frequency

800  
MHz  
Frequency

SPANOUT = 159"  
CRACK LENGTH (AVE) = 3.311"  
Q/W = 93  
COMPLIANCE =

R=1  
V=5  
V=5





CMOD - COMPLIANCE

8/20/84

0115  
Microseis Frequency

°C  
Temperature

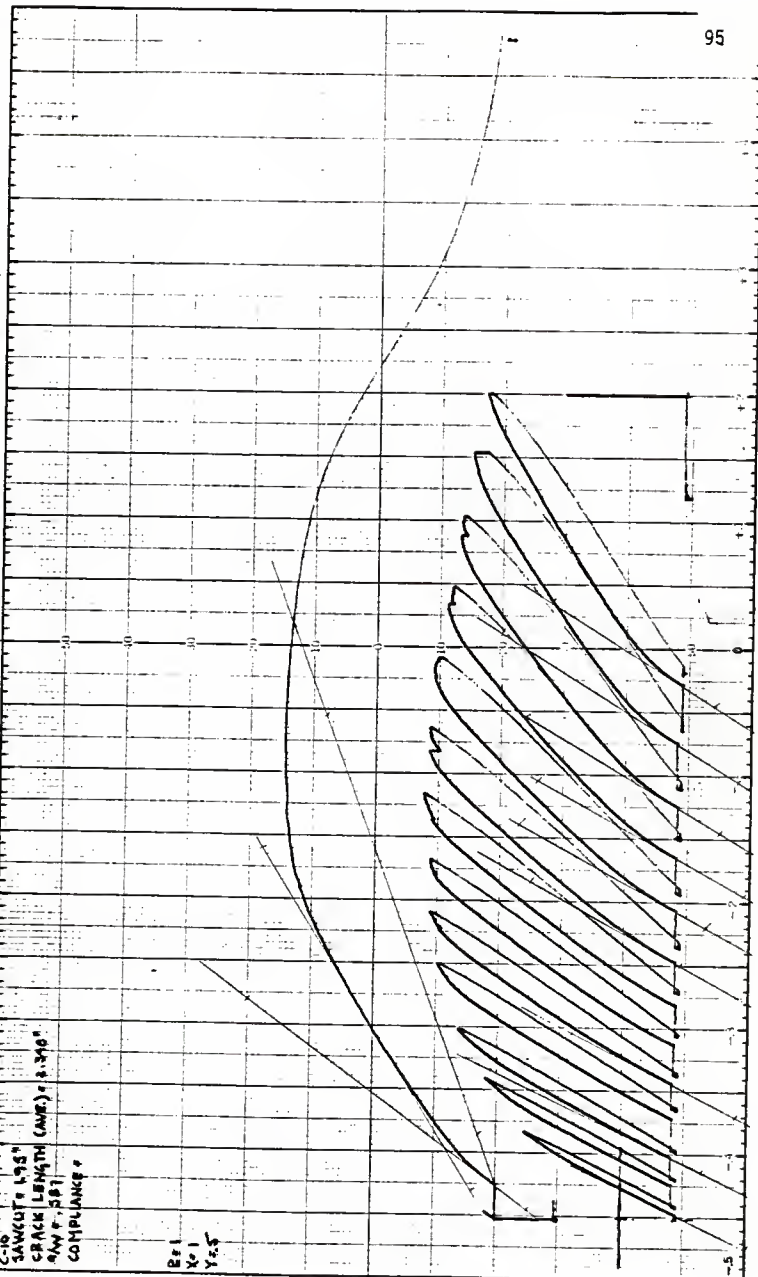
Hz  
Resonance Frequency

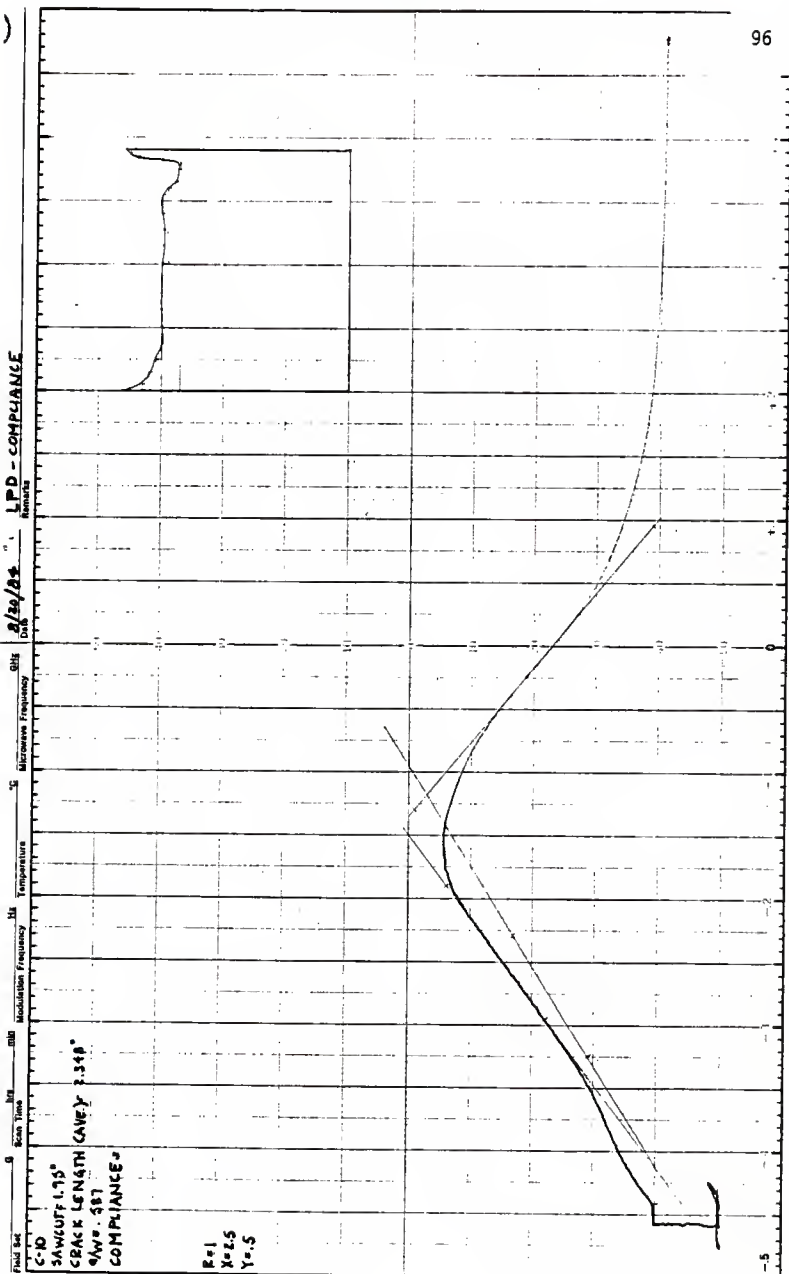
0.020  
Scan Time

0  
PLOT END

C-10  
SANGUET 198"  
CRACK LENGTH (AVE) = 3.340"  
AWP = .581  
COMPLIANCE =

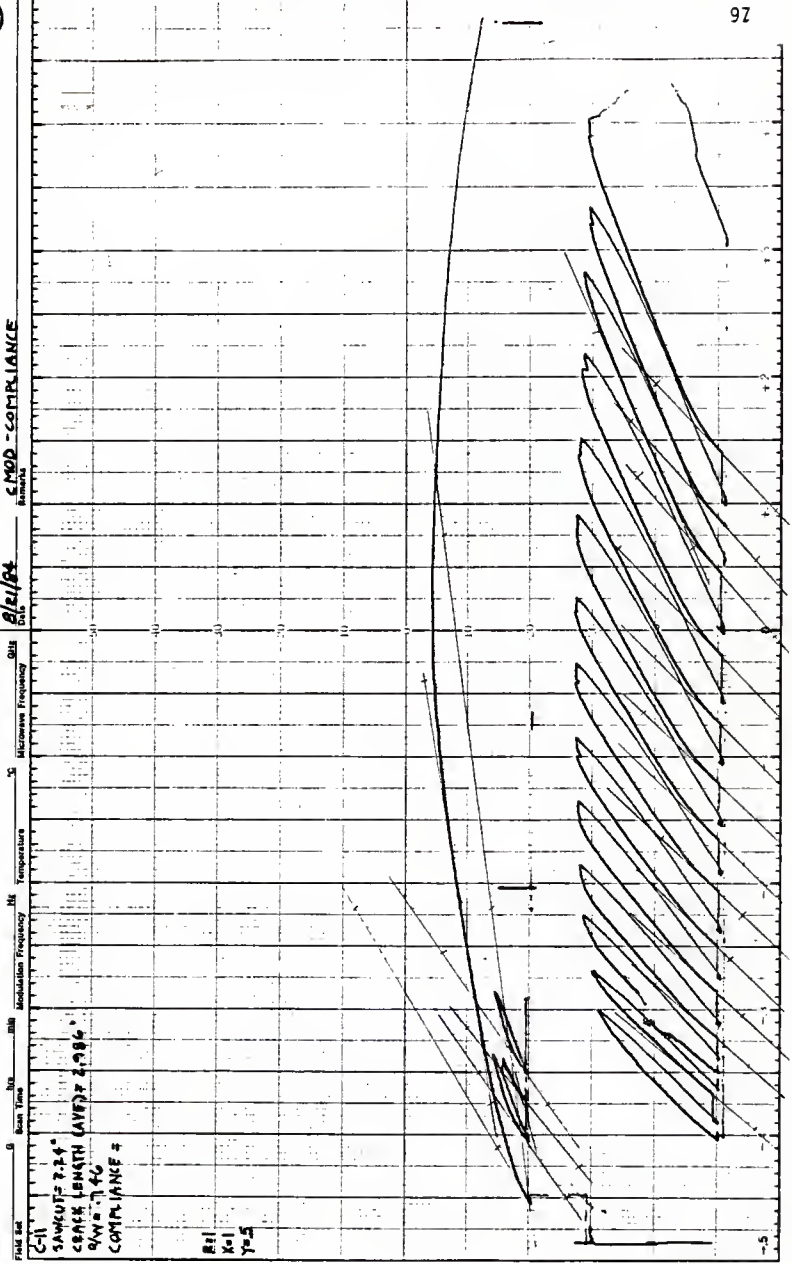
B#1  
N#1  
Y#5





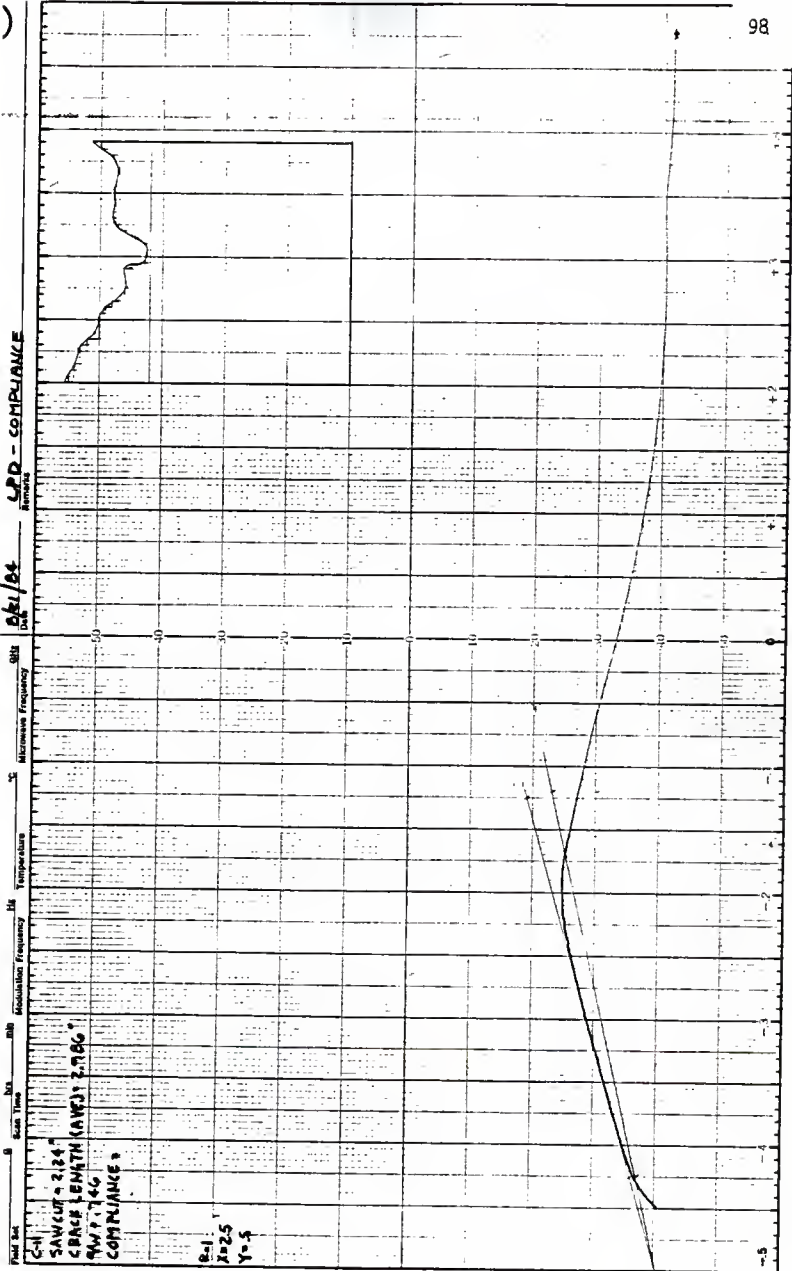
**C-MOD - COMPLIANCE**

**0121/84**  
DATE



FILE # C-11  
 SAMPLER # 7.24  
 CRACK LENGTH (AVE) 2.986  
 R/W = 7.6  
 COMPLIANCE #

R=1  
 K=1  
 Y=5



LPD - COMPLIANCE

8/21/64

Microwave Frequency MHz

°C

Temperature

Resolution Frequency MHz

dB

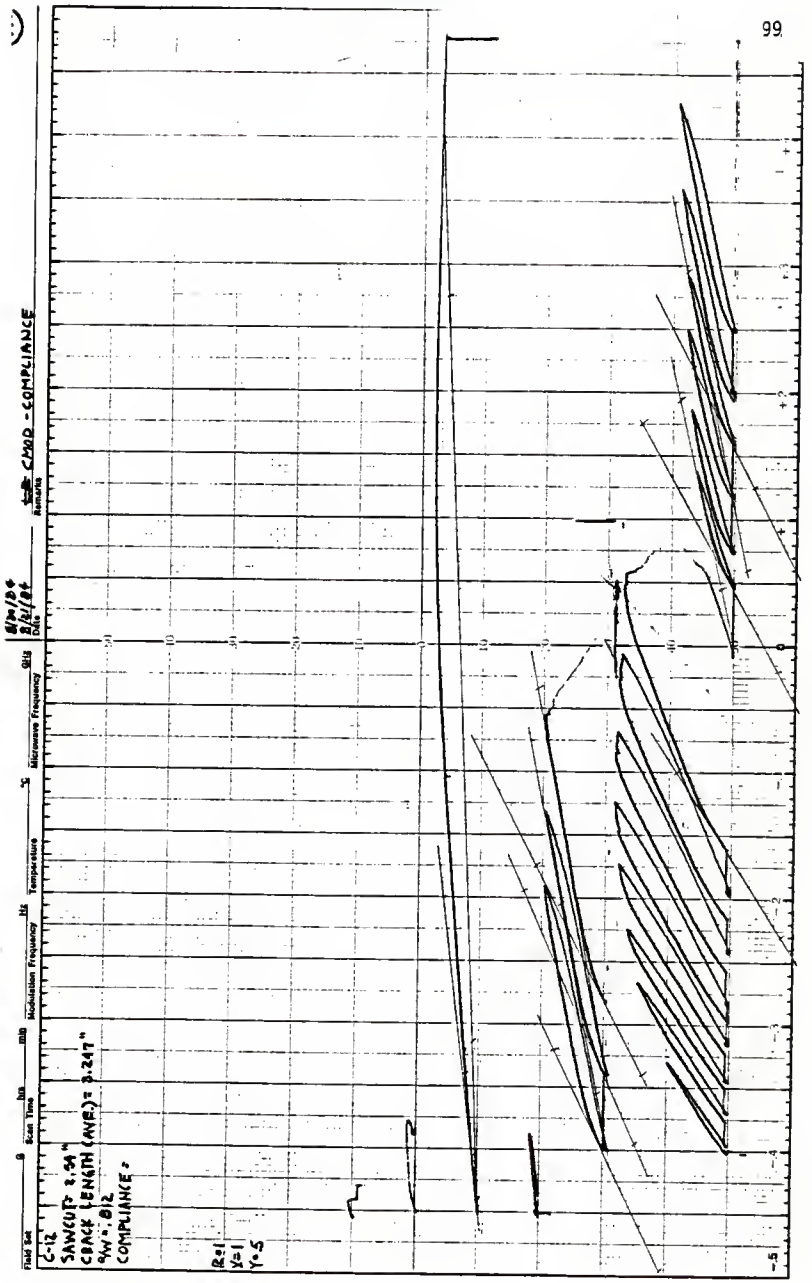
Scale Time

Plot Set

SAW/CUT = 2.24"  
 SPACE LENGTH (AWG) = 7.986"  
 RW = 7.46  
 COMPLIANCE

R=1  
 X=25  
 Y=5





CMWD - COMPLIANCE

dBm/100  
dB/100

Microwave Frequency

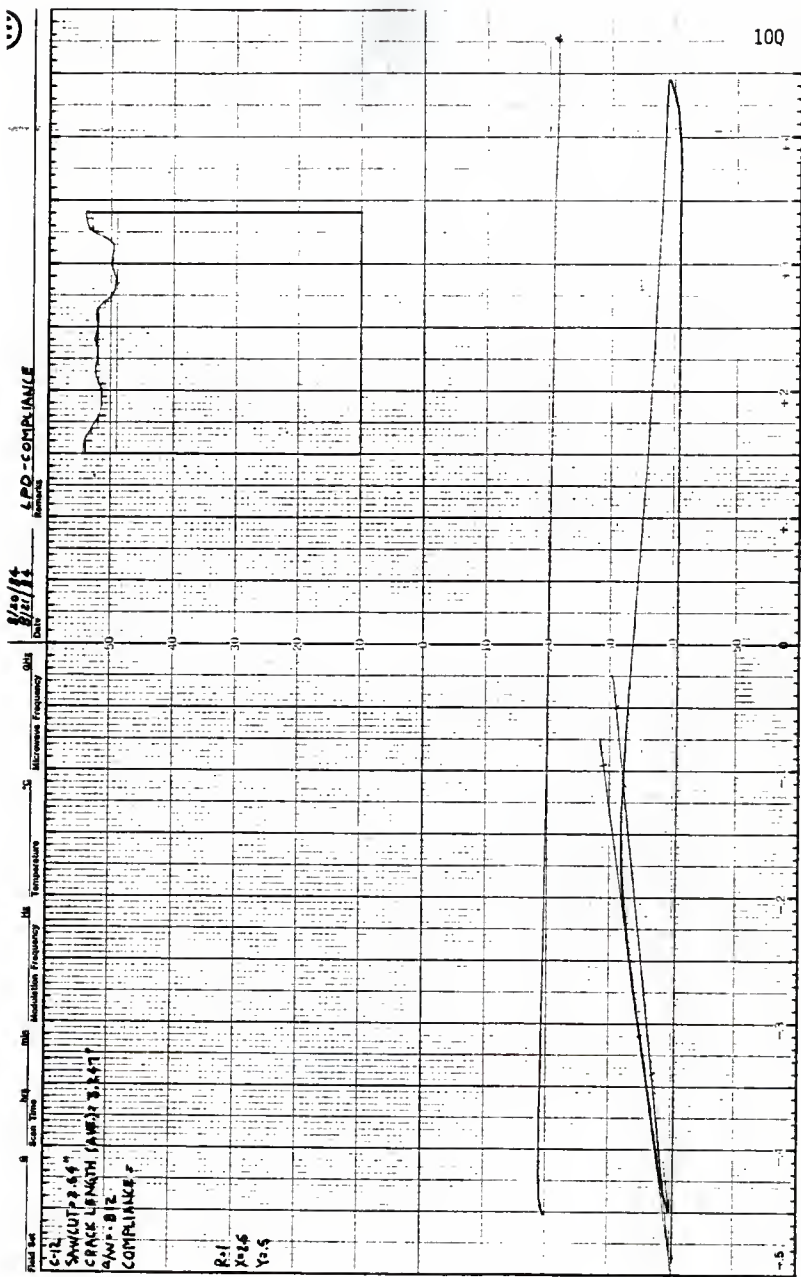
Temperature

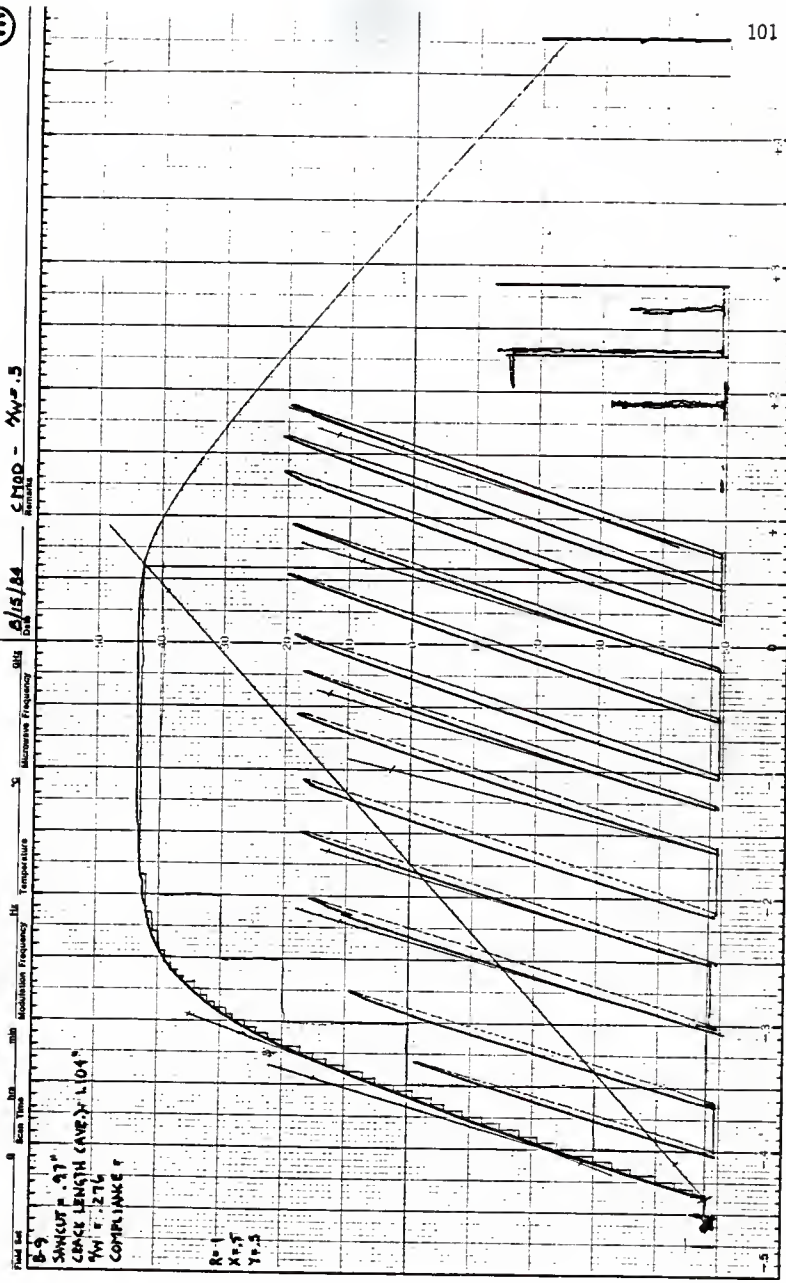
Modulation Frequency

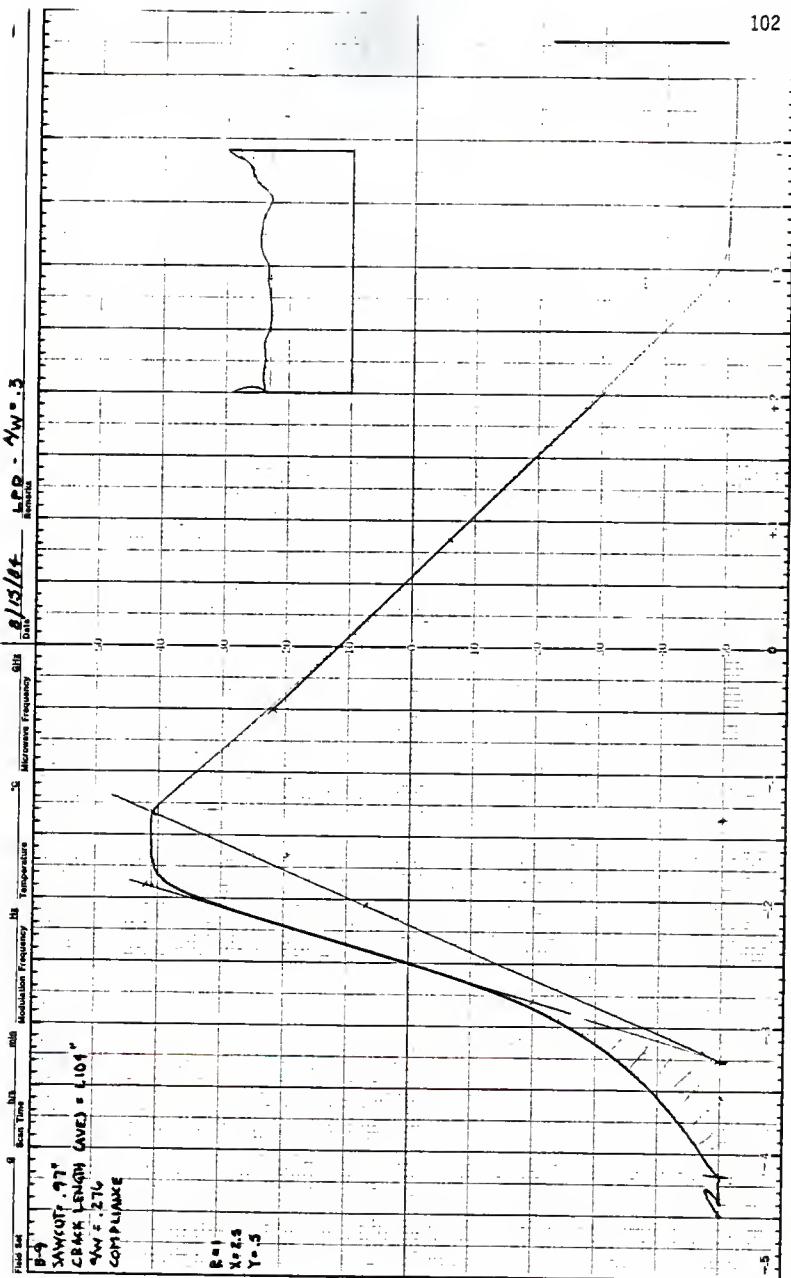
Scan Time

C-12  
 SWEEP: 3.9A  
 TRACE LENGTH (AVE) = 3.247"  
 W = .812  
 COMPLIANCE =

Rel  
 J=1  
 Y=5







CMED - AW 5, B

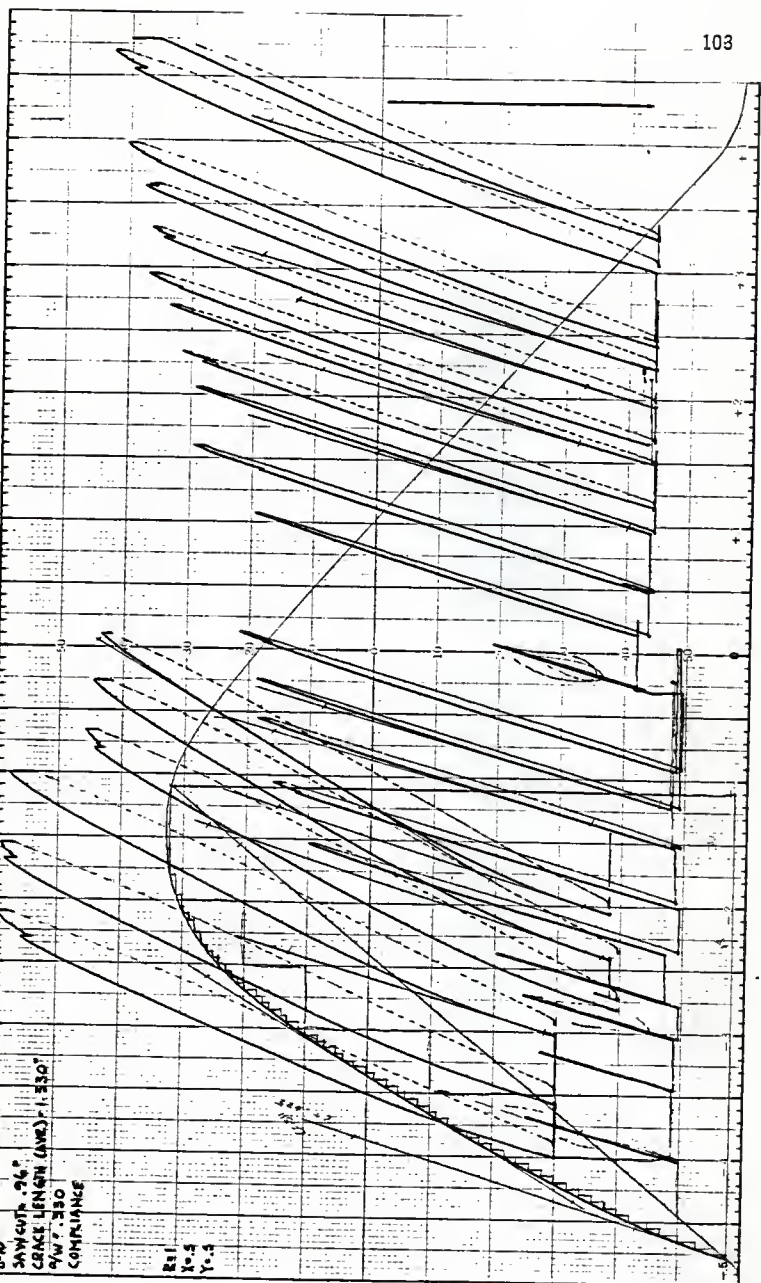
8/13/68

Microvise Frequency

Temperature

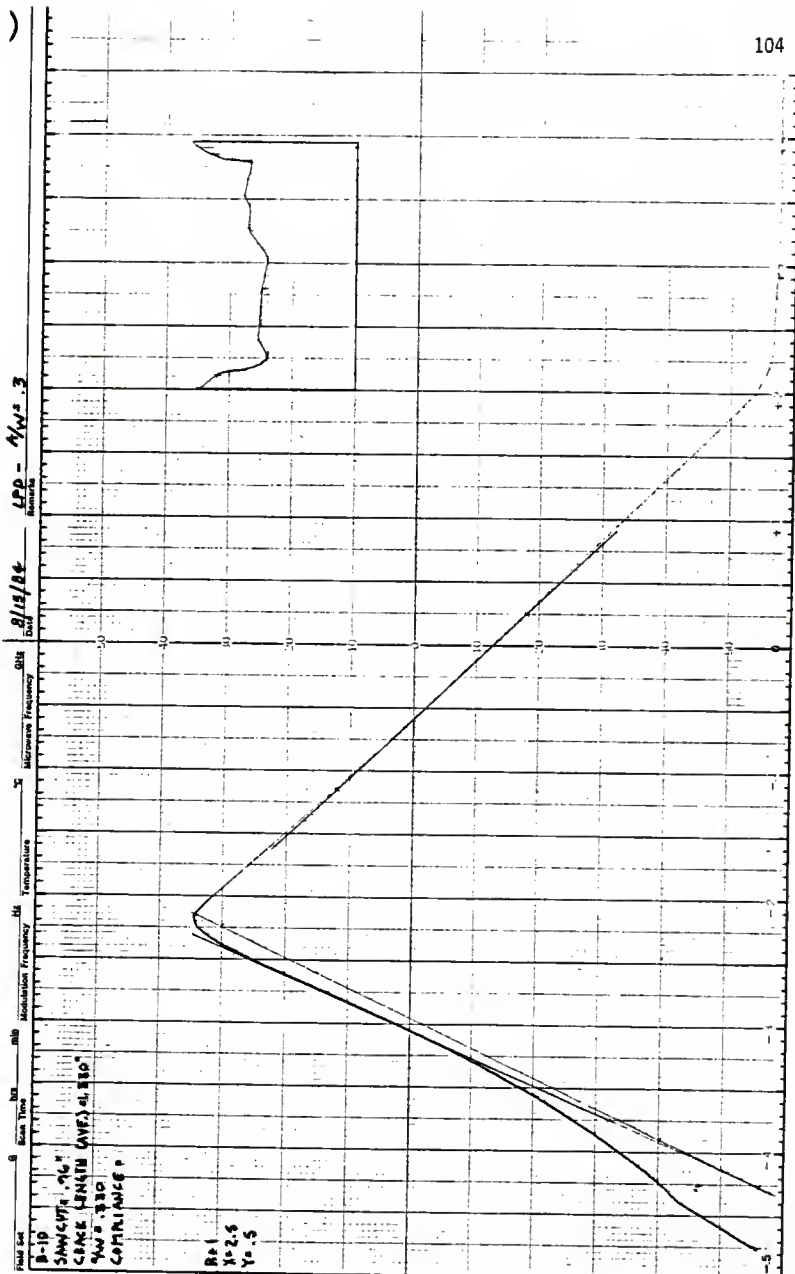
Scan Time

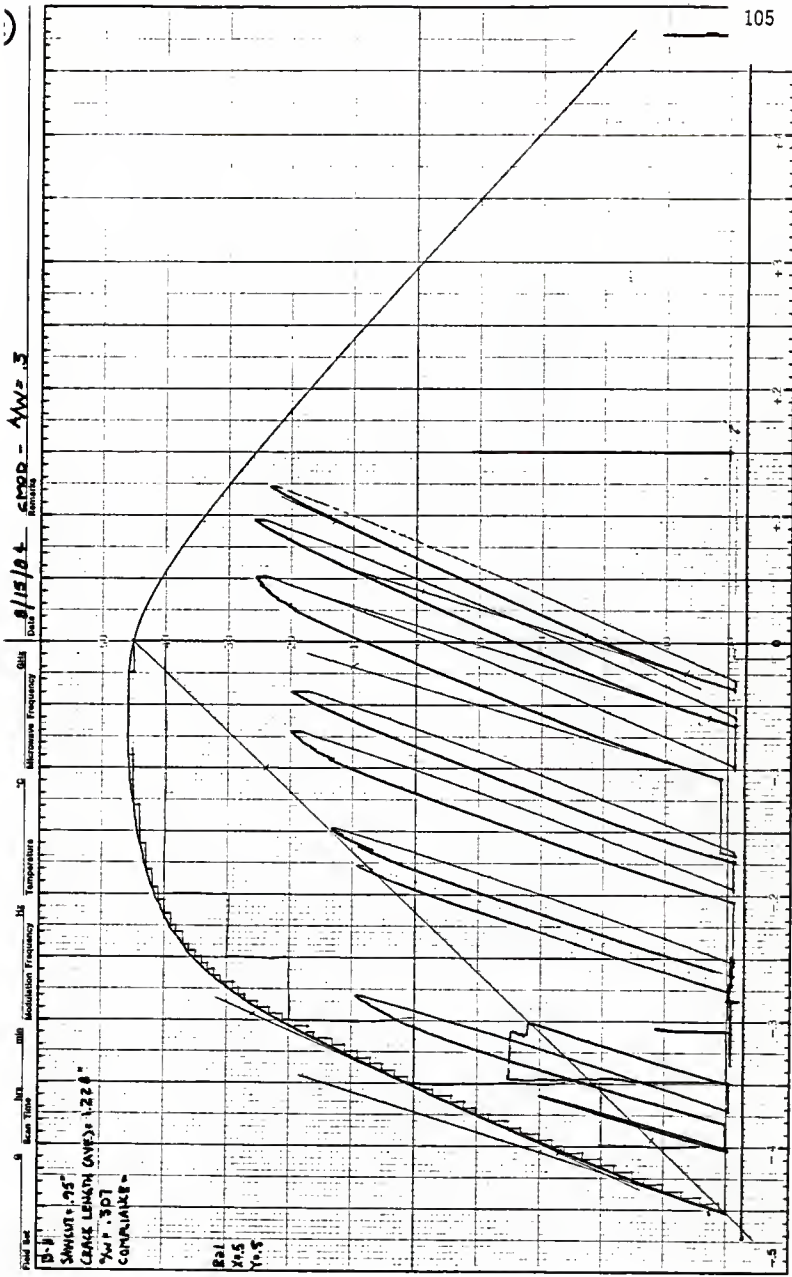
8-10



SAW/CUT  $\approx 76^\circ$   
 CRACK LENGTH (AVG) = 1.530"  
 P/W = .330  
 COMPLIANCE

R1  
 N=5  
 Y=3





01/15/84  
 DATE

CH1

Microphone Frequency

30

Temperature

30

Modulation Frequency

30

Temperature

30

Modulation Frequency

30

Temperature

30

Modulation Frequency

30

Temperature

30

Modulation Frequency

30

Temperature

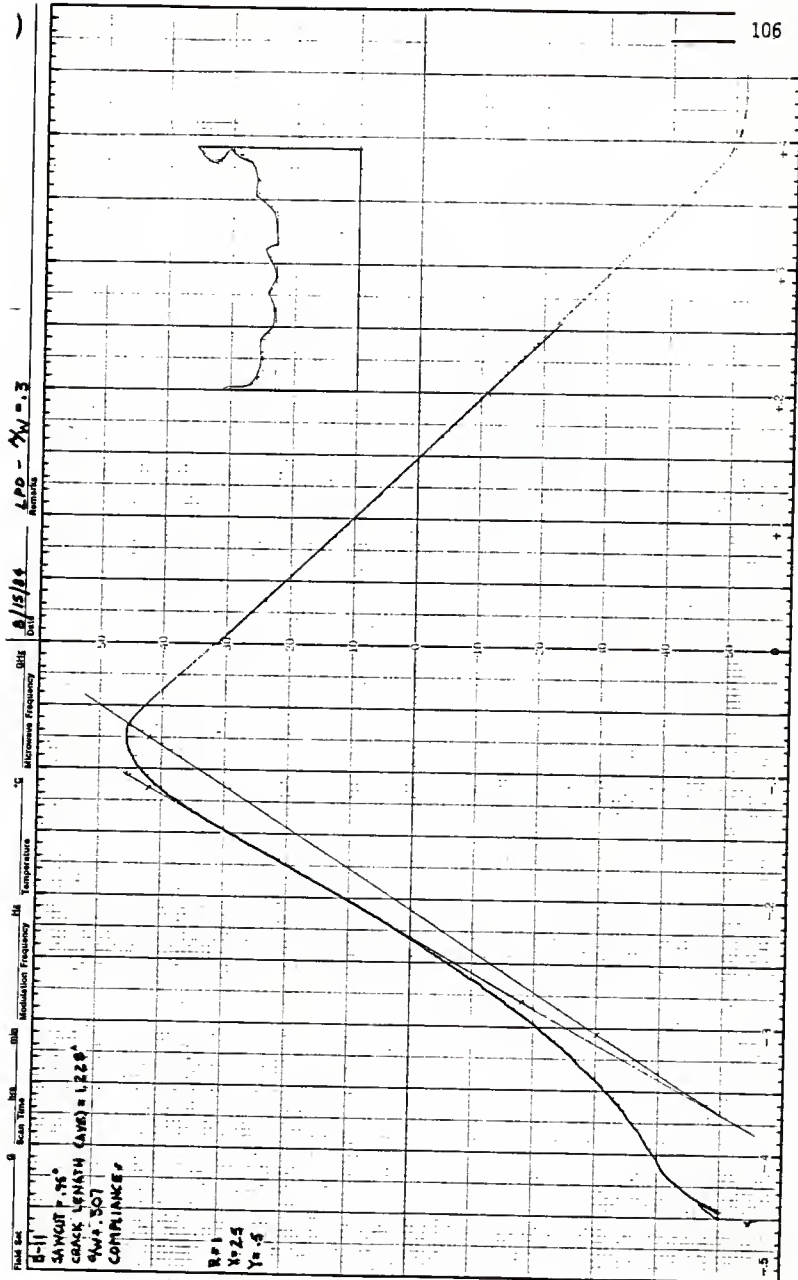
30

Modulation Frequency

30

SWITCH = 95"  
 CABLE LENGTH (VSWR) = 1.226"  
 W/P = 907  
 COMPLAINE =

Bal  
 X6.5  
 Y6.5





CHAD - 4/1/53

8/16/54

50

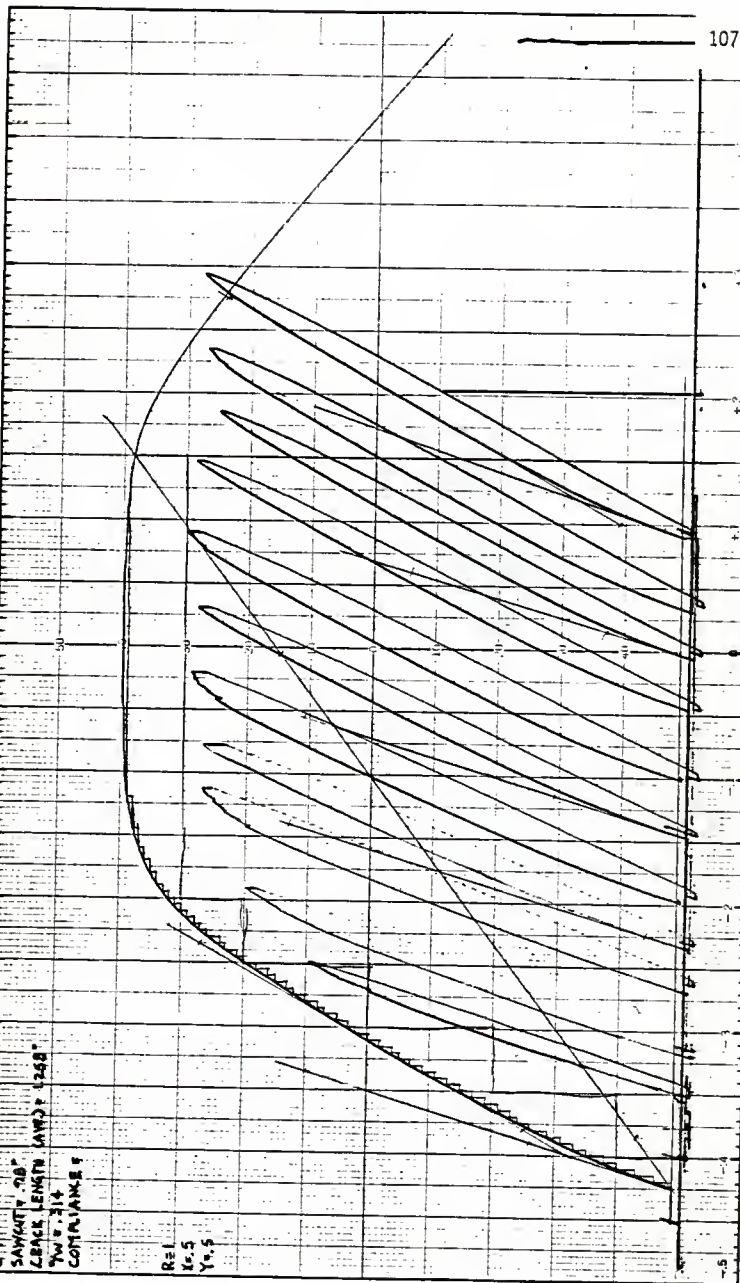
20

Temperature

Modulation Frequency

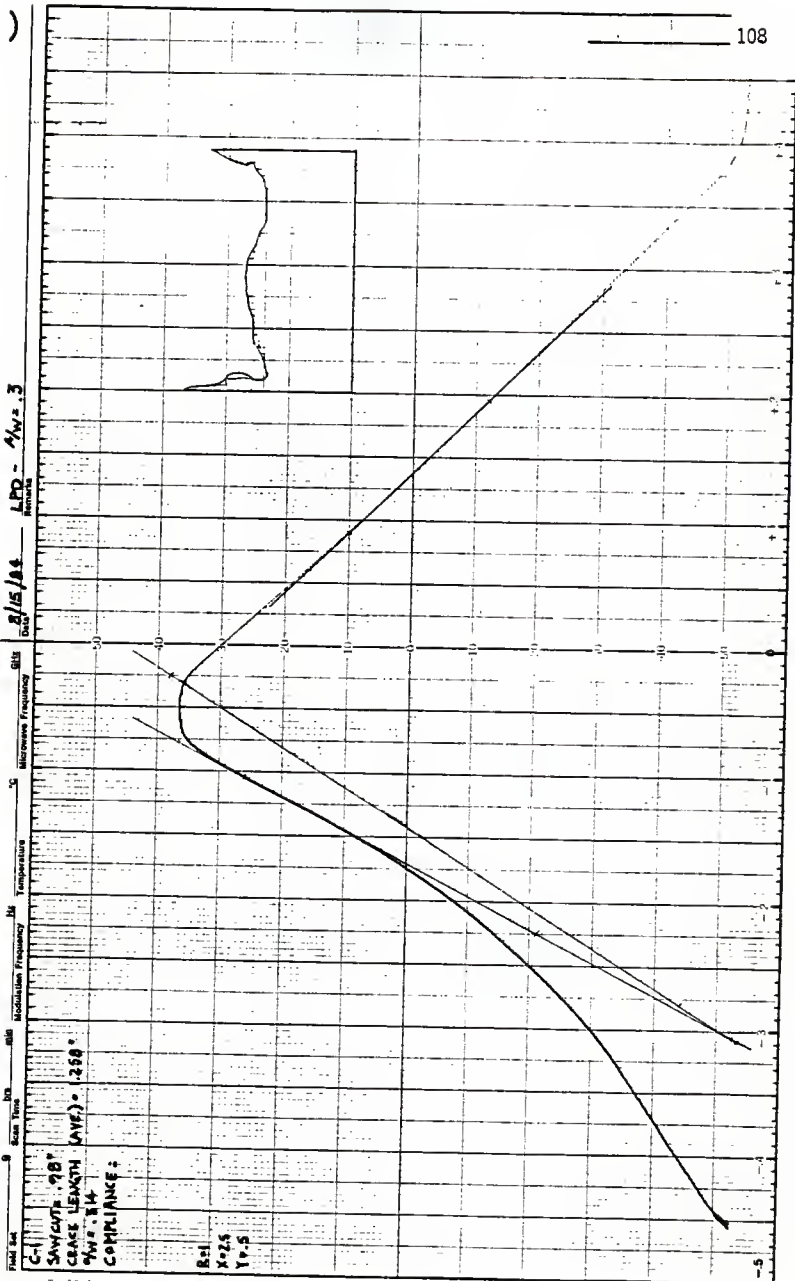
Scan Time

0



SAWTOOTH - 70°  
 TRACE LENGTH SAWTOOTH  
 70° - 114  
 CONTINUED

Re 1  
 Ex 5  
 Y 5



CHOD - 4W. 3

8/2/54  
8/2/54

GHz  
Microwave Frequency

Mc  
Magnetron Frequency

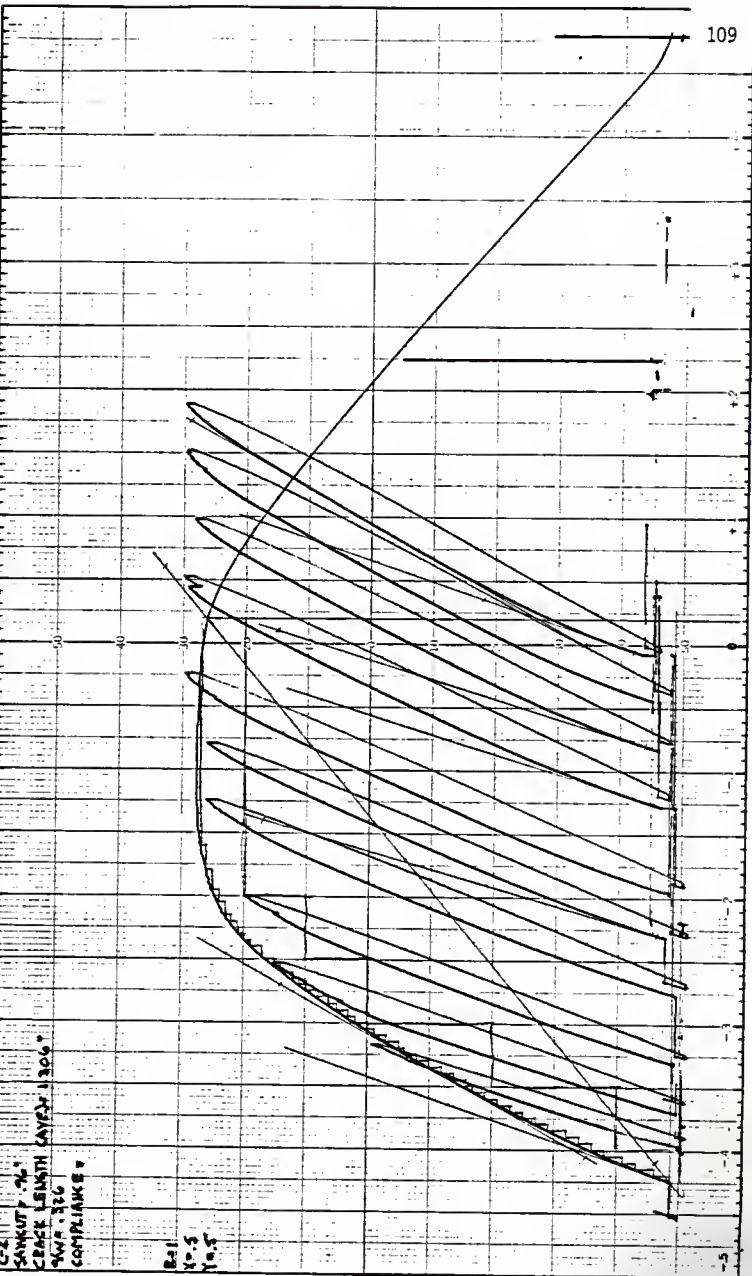
Temperature

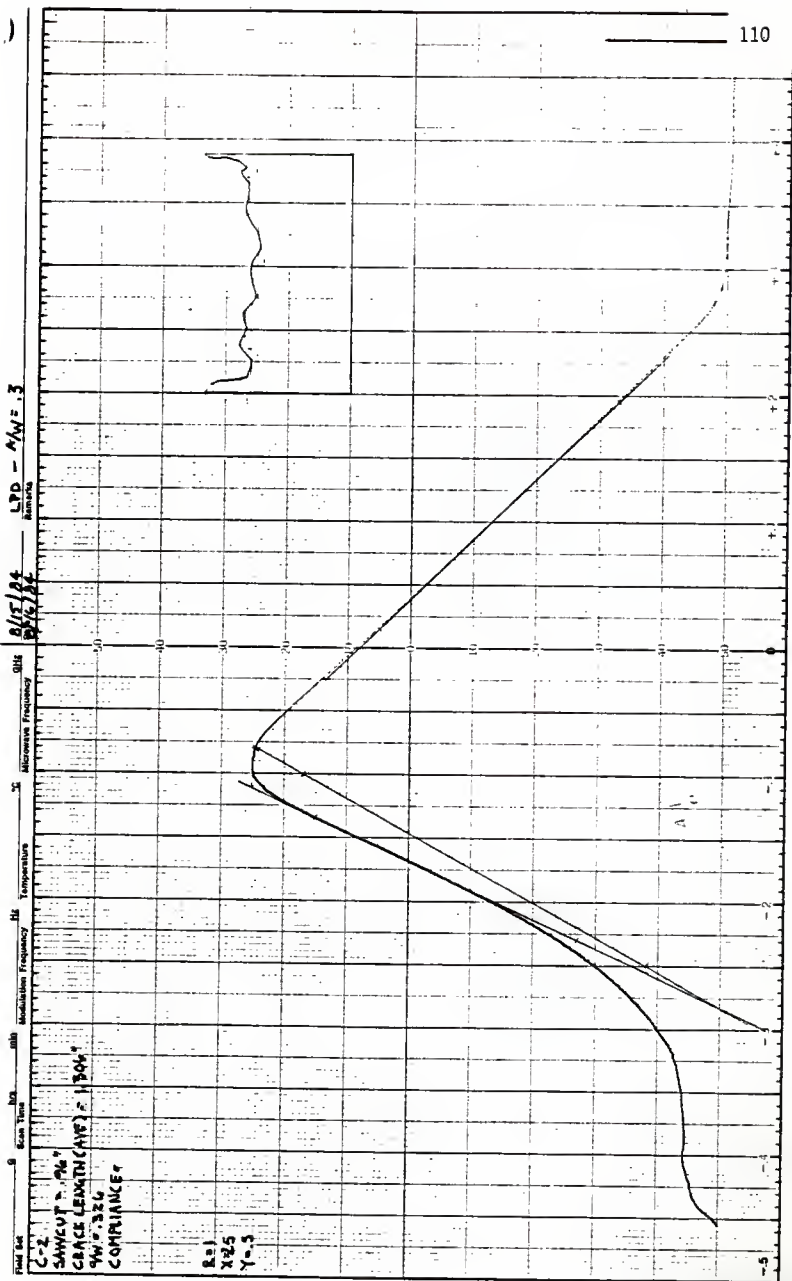
Scan Time

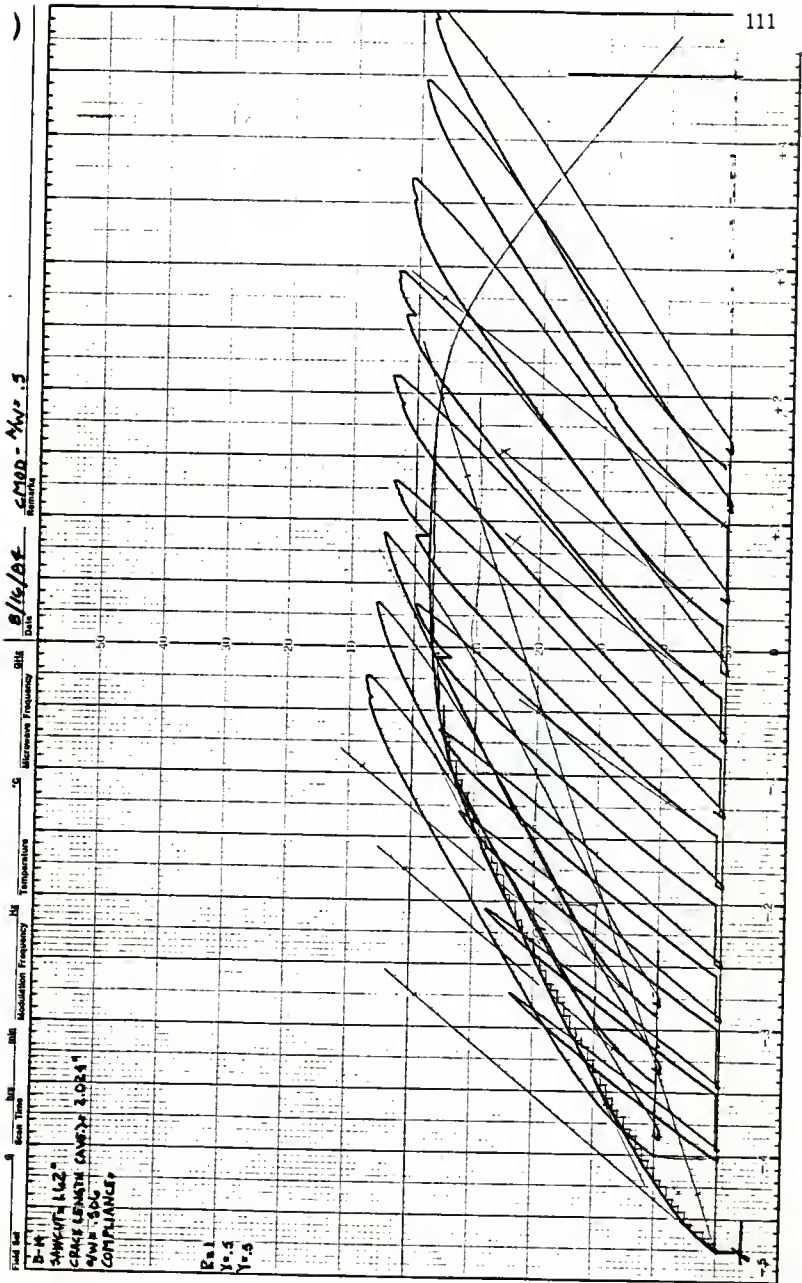
File No

C-2  
SAMPLING %  
CERCE LENGTH LAYER 1306°  
WAVE 326  
COMPLIANCE

Ball  
No. 5  
No. 5



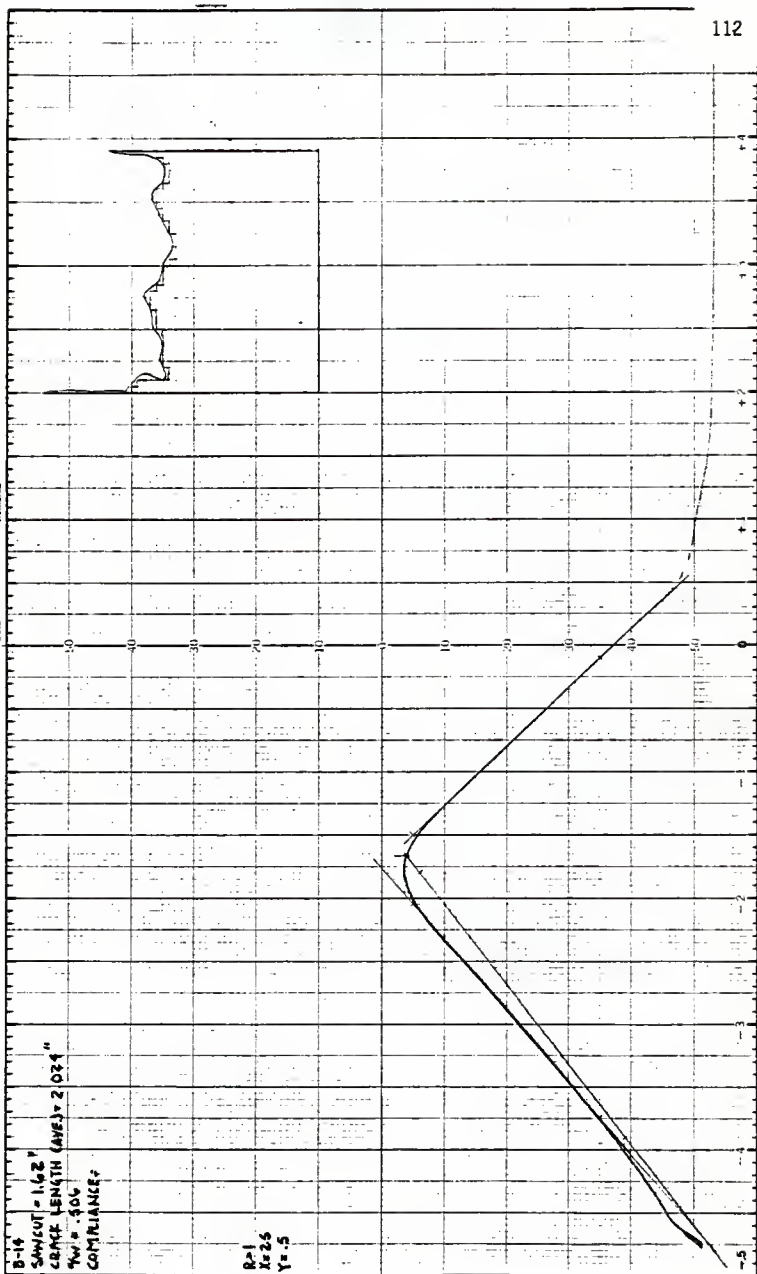




8/16/64  
 Date  
 CMED - Mr. S

8-14  
 SAMPLE 112  
 CRACK LENGTH GAGE 3.0541  
 WAVE 300  
 COMPLIANCE

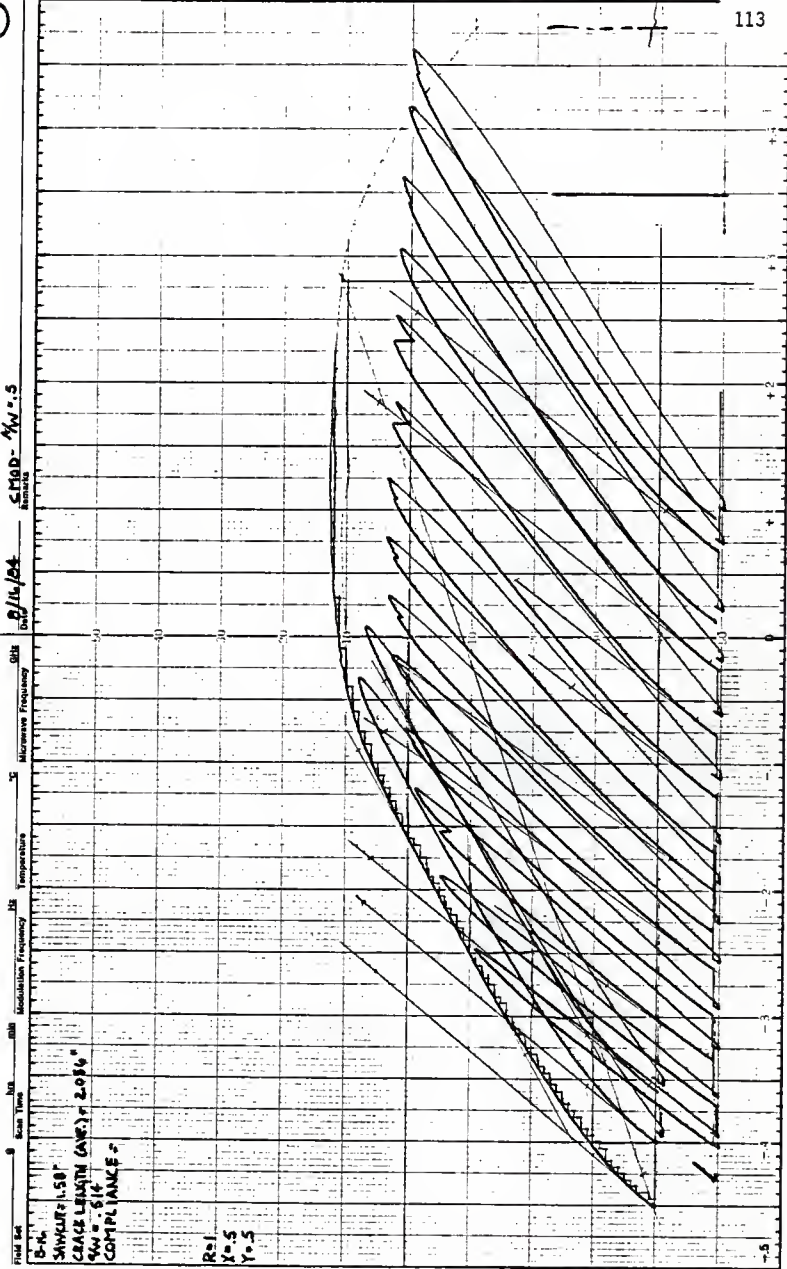
R=1  
 I=3  
 Y=5

$\frac{P}{K/BS}$   $\frac{LPP}{LPP} = \frac{44}{1.5}$ 


B-16  
 SAWCUT = 1.62"  
 CRACK LENGTH (AVE) = 2.034"  
 $\eta_w = 506$   
 COMPLIANCE

$R=1$   
 $X=2.5$   
 $Y=5$

12/14/64 S.M.H.D. - 4W = 5



MHz  
Modulation Frequency

Temperature

dBm  
Modulation Frequency

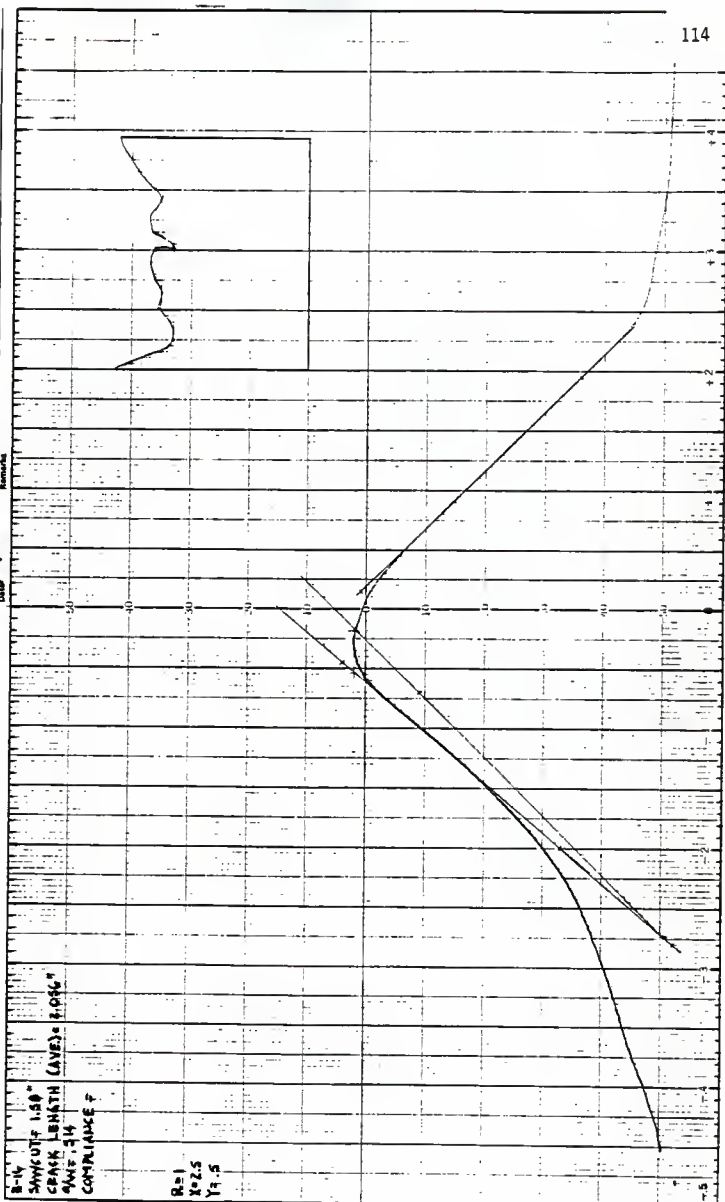
Scan Time

Field Mtg

SWITCH: 1.58°  
 TRACE LENGTH (Ave) = 2.056°  
 4W = 5 (4)  
 COMPLIANCE =

R = 1  
 4 = 5  
 1 = 5

$\frac{g}{W} / \delta l$       LPP -  $W \times 5$







06/16/84  
8/11/84

C-700 - YW-5

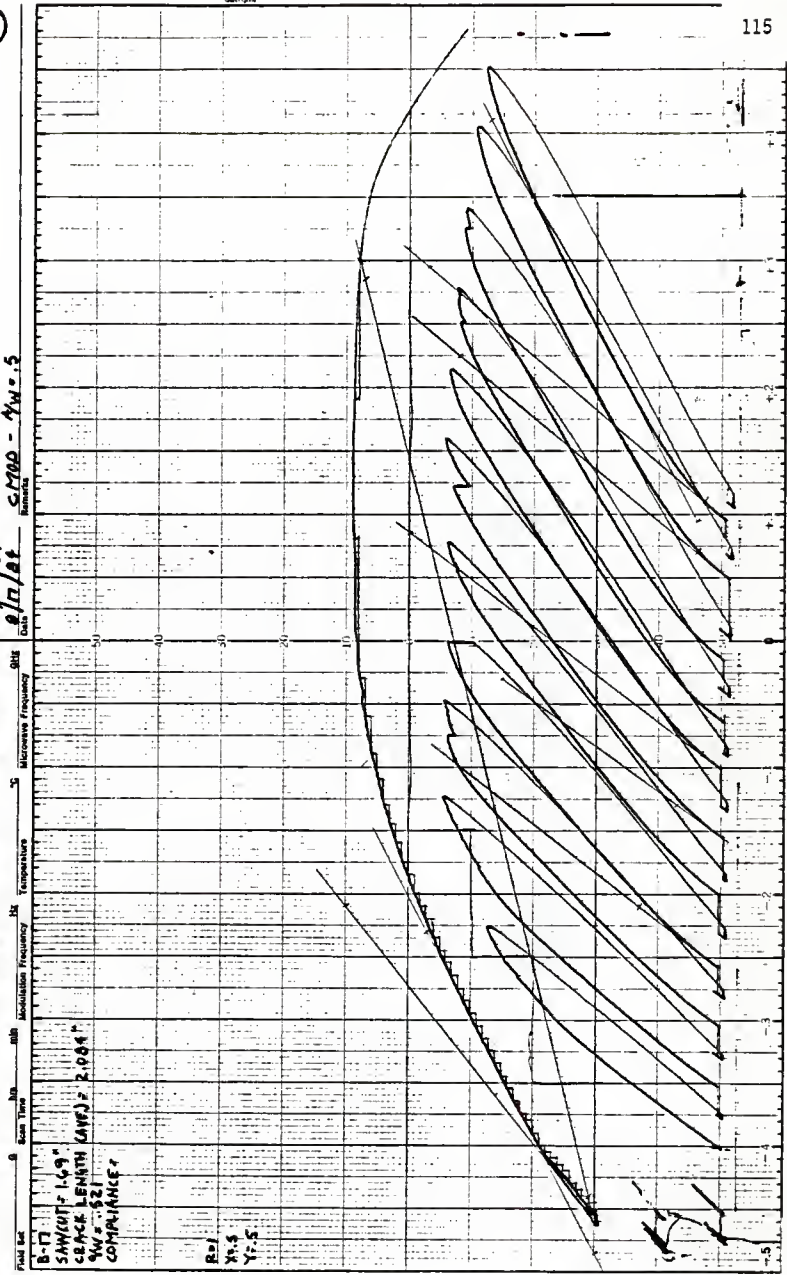
Microphone Power

Receiver Gain

Modulation Amplitude

Time Constant

Scan Range



Field Set

B-17  
SANGUIT-1.49"  
CEPAC LENGTH (AWP) = 2.004"  
NW = 52  
COMPLIANCE

R=1  
X=5  
Y=5

5

Original  
 8/16/84  
 10/17/84  
 LPD - MW-5

Microphone Power  
 Microphone Frequency

Receiver Gain  
 Frequency

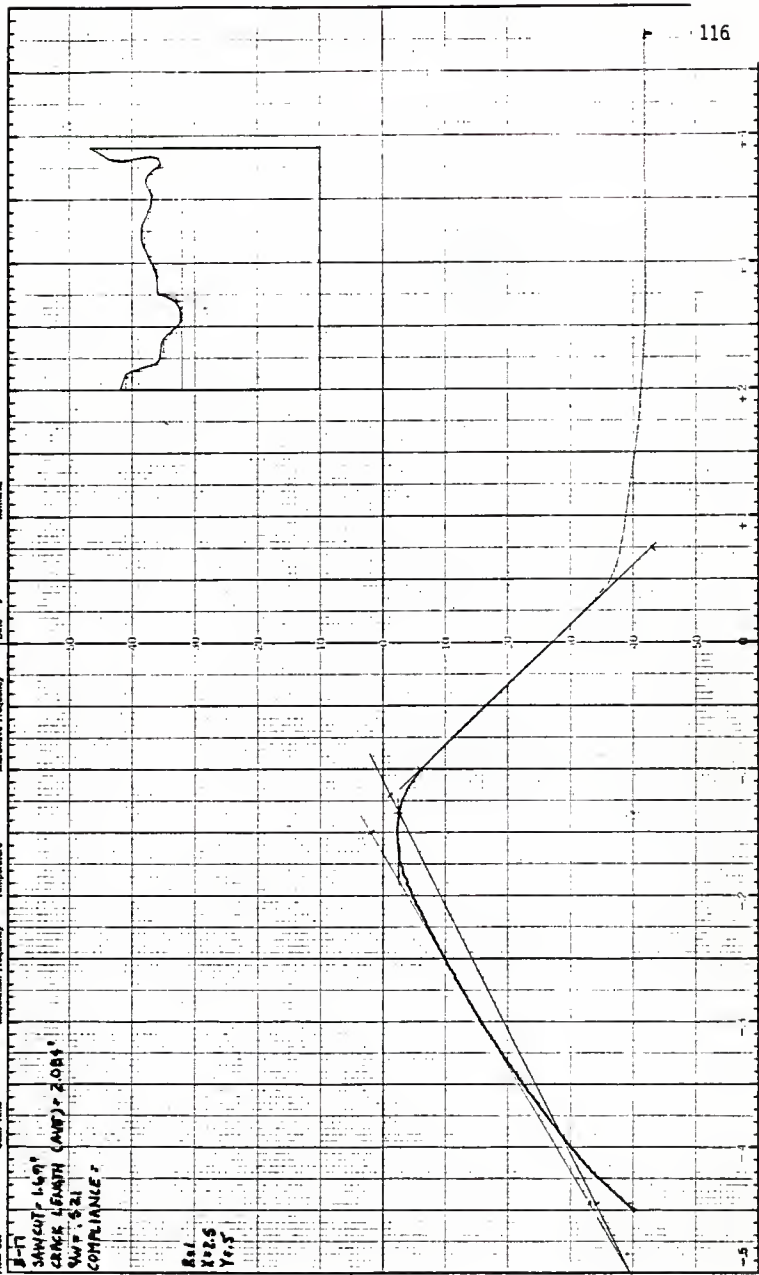
Isolation Amplitude  
 Isolation Frequency

Time Lockout  
 Scale  
 dB

Scale range  
 0 50 100 150 200 250 300 350 400 450 500 550 600 650 700 750 800 850 900 950 1000

8-17  
 SAMPLED - 1.69"  
 CABLE LENGTH (AMB) = 2.08"  
 MW = 5.21  
 COMPLIANCE ?

Rel  
 102.5  
 Yr. 5



CMOD -  $\Delta W = 1.5$

0/17/84

01E

Microstrain Frequency

5

Temperature

10

Modulation Frequency

100

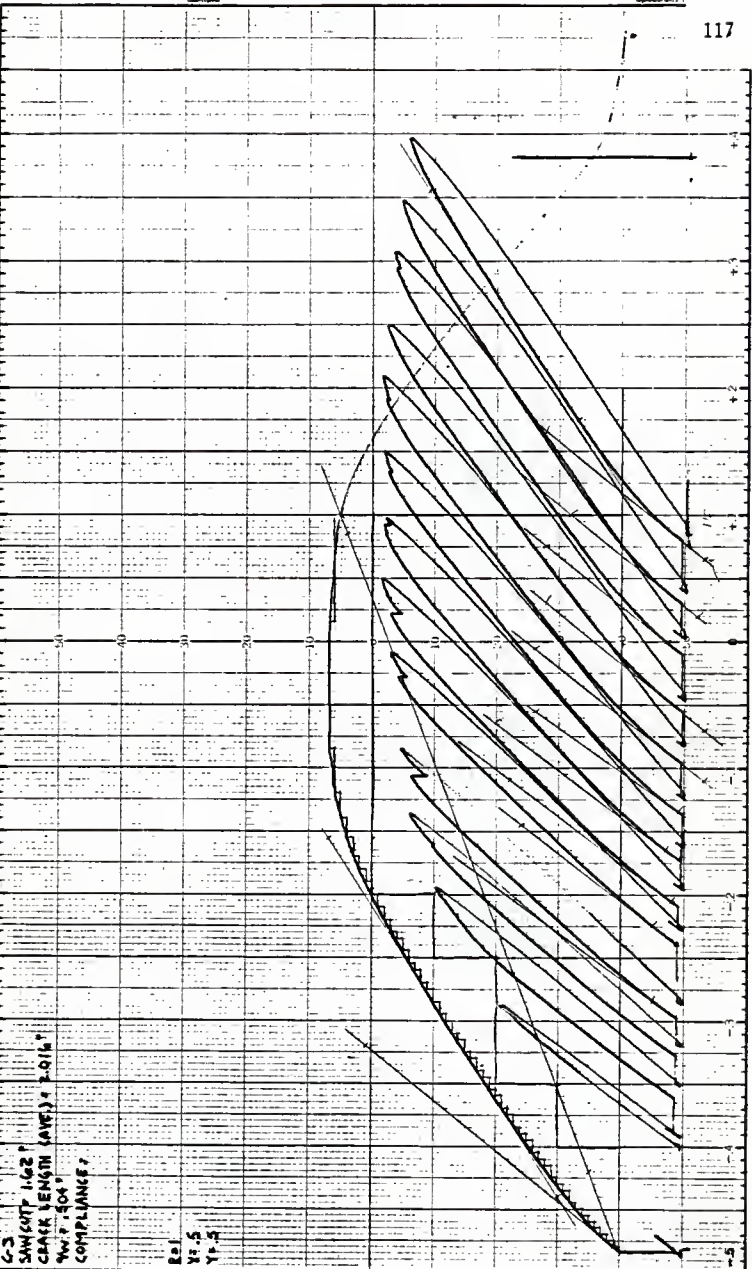
Hz

Scan Time

0

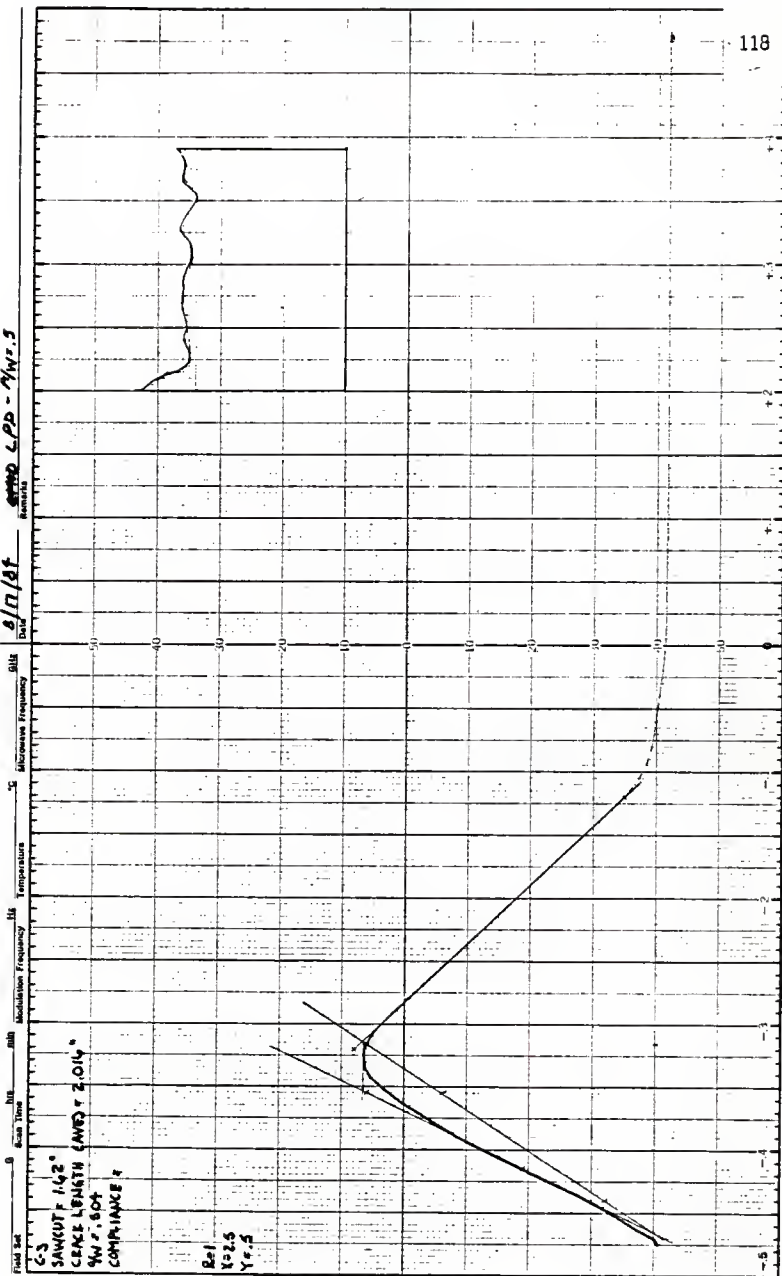
C-3  
 SAW CUT 162 P  
 CRACK LENGTH (AVE) = 0.014"  
 $\Delta W = 1.504$   
 COMPLIANCE =

Re:  
 V1.5  
 Y1.5



)

9/17/81 4000 L.P.D. - 7W.5

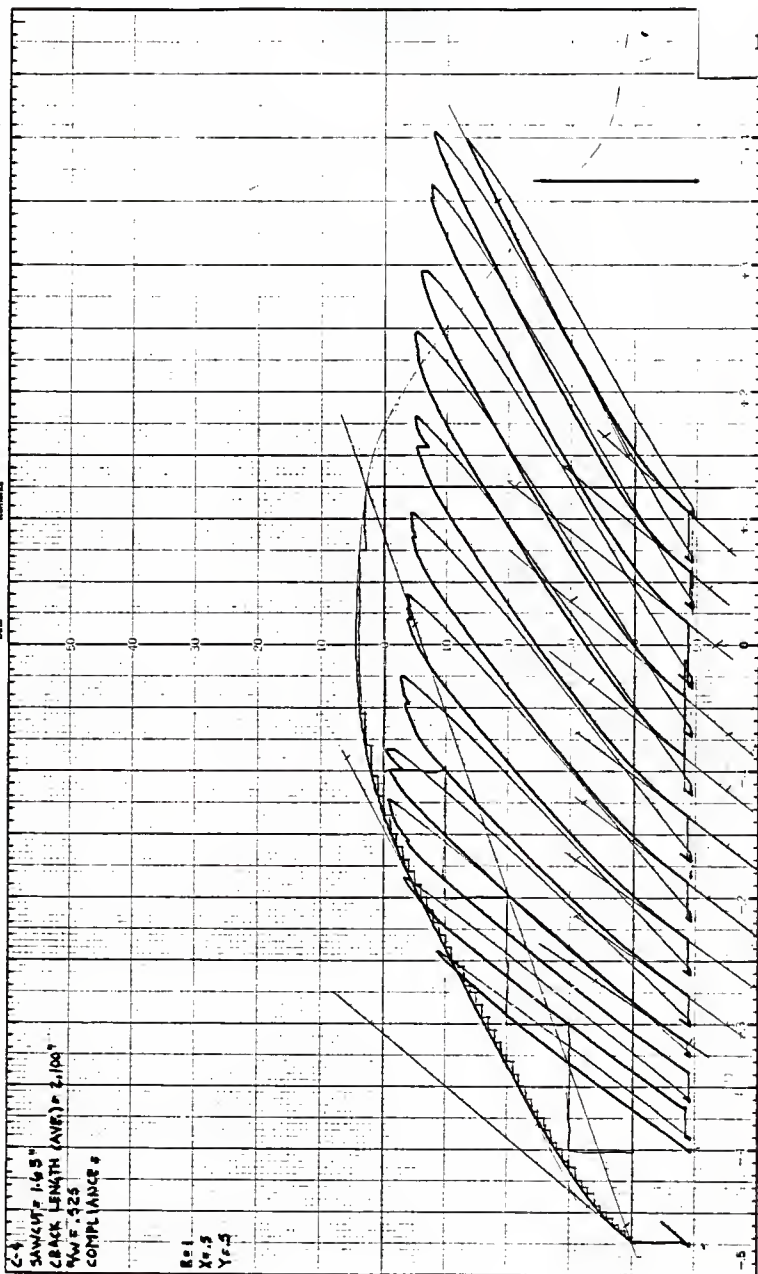


0 Span Time MHz Modulation Frequency MHz dBm  
 INCREASING FREQUENCY DBM  
 TEMPERATURE

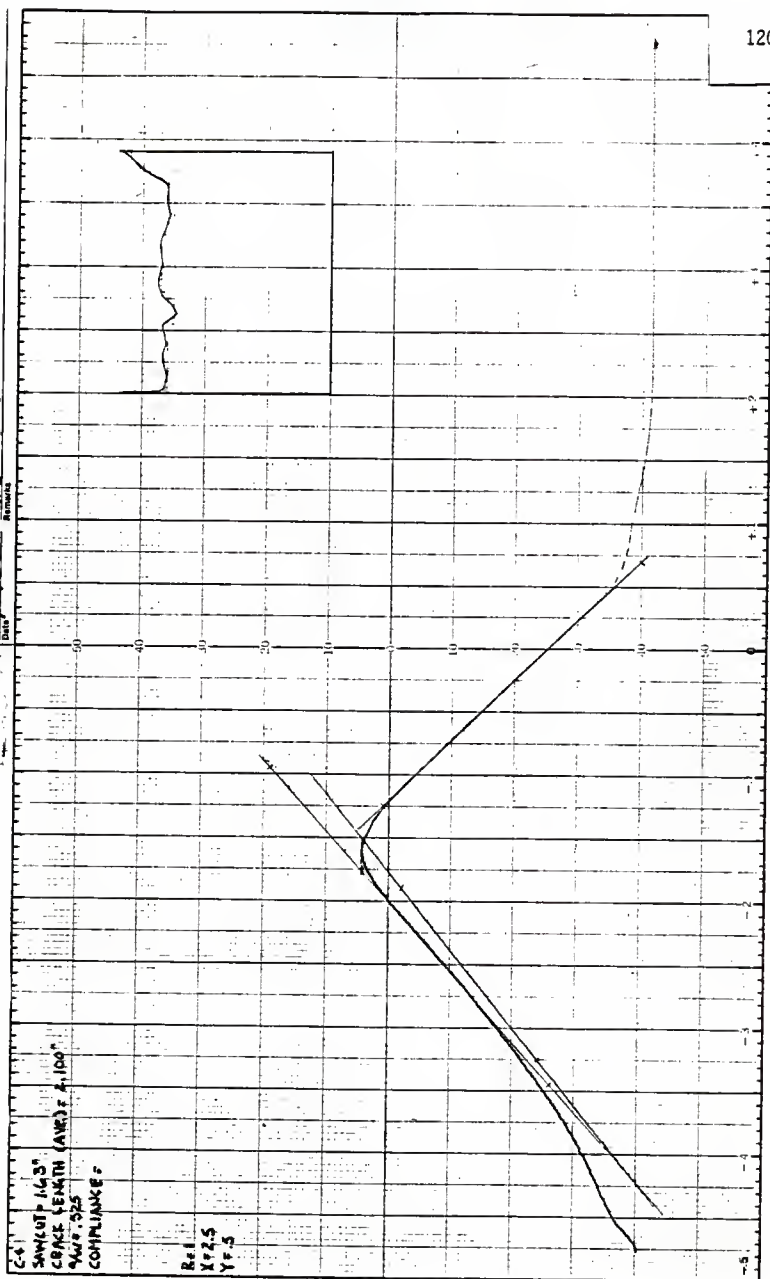
CS  
 SANGCUT F 1.62°  
 CABLE LENGTH (AWG) 2.014°  
 7W.5 804  
 COMPLIANCE 4

Ref  
 N22.5  
 Yr. 5

8/17/81 C-MOD -  $\gamma_W = 5$



DATE: 8/17/64 LPD - YW-5



8/17/84 CMOB - MW-7

8/17/84

816

Microphone Frequency

5

Temperature

10

Acquisition Frequency

100

Scan Time

0

8-10

SAW/COT = 2.24"

CRACK LENGTH (AVE.) = 2.714"

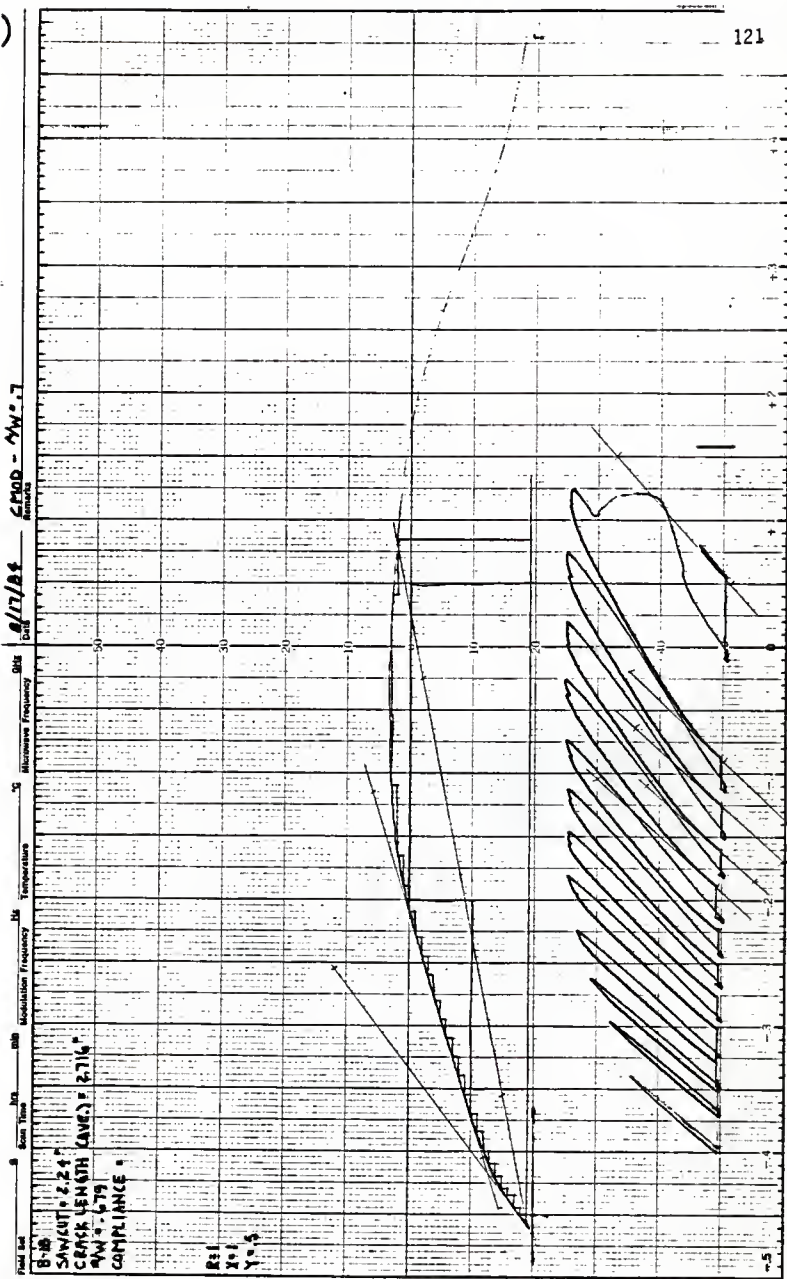
PM = 0.79

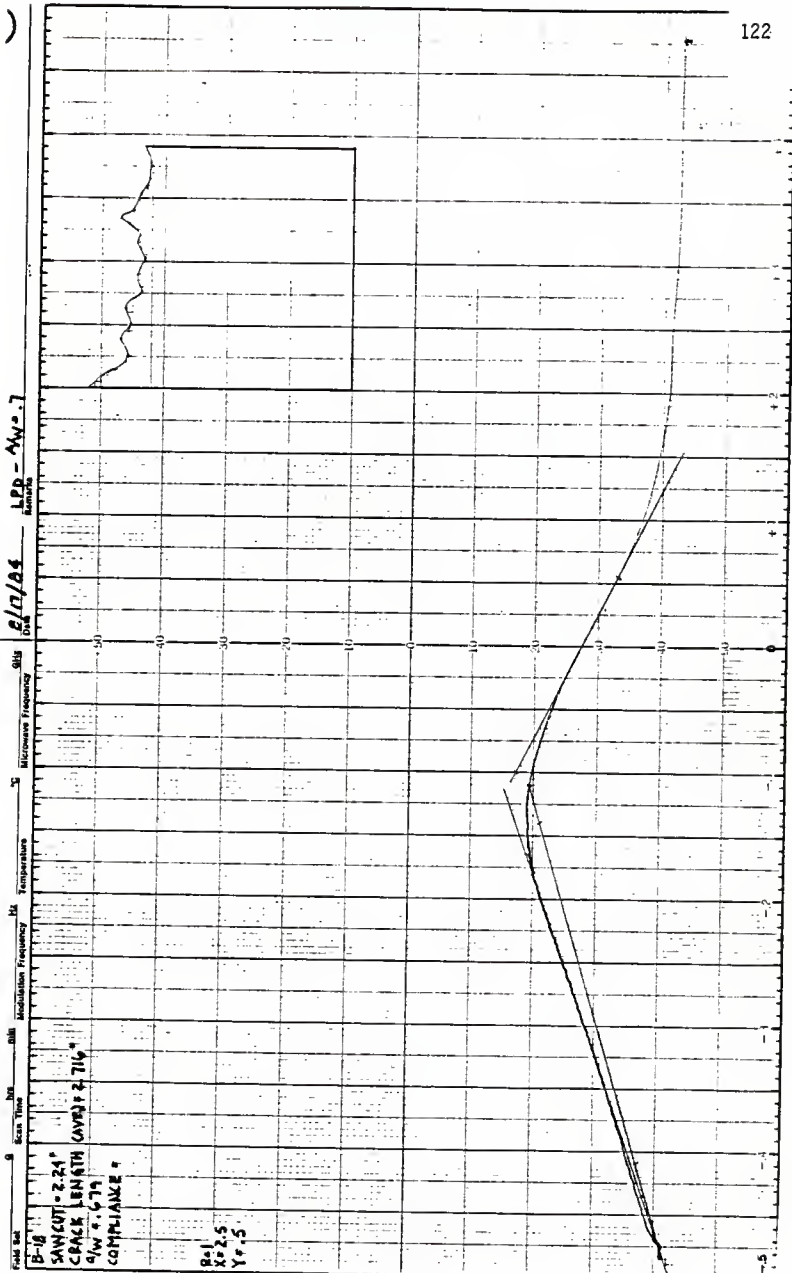
COMPLIANCE =

R1

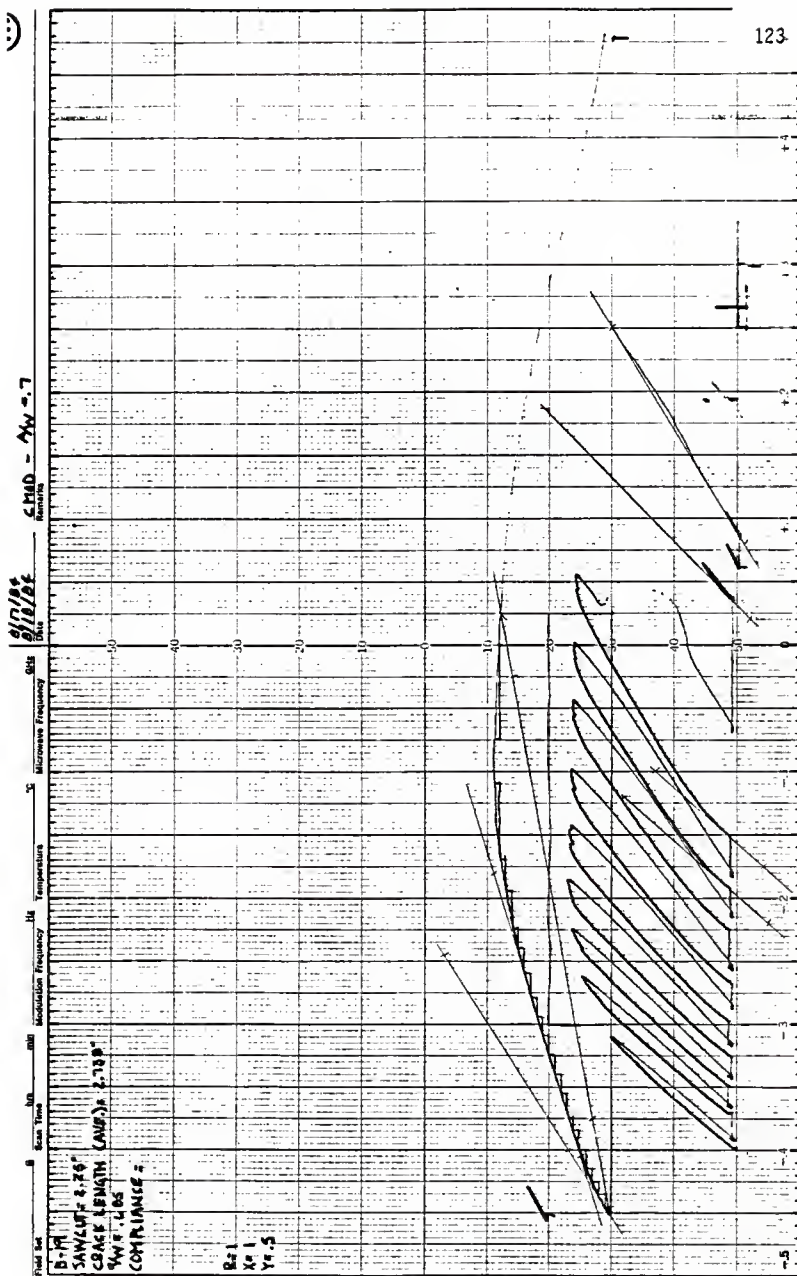
X1

Y=5











LPD - 1/12.7  
Remarks

9/7/84  
9/18/84  
Date

GHz  
Microwave Frequency

Temperature

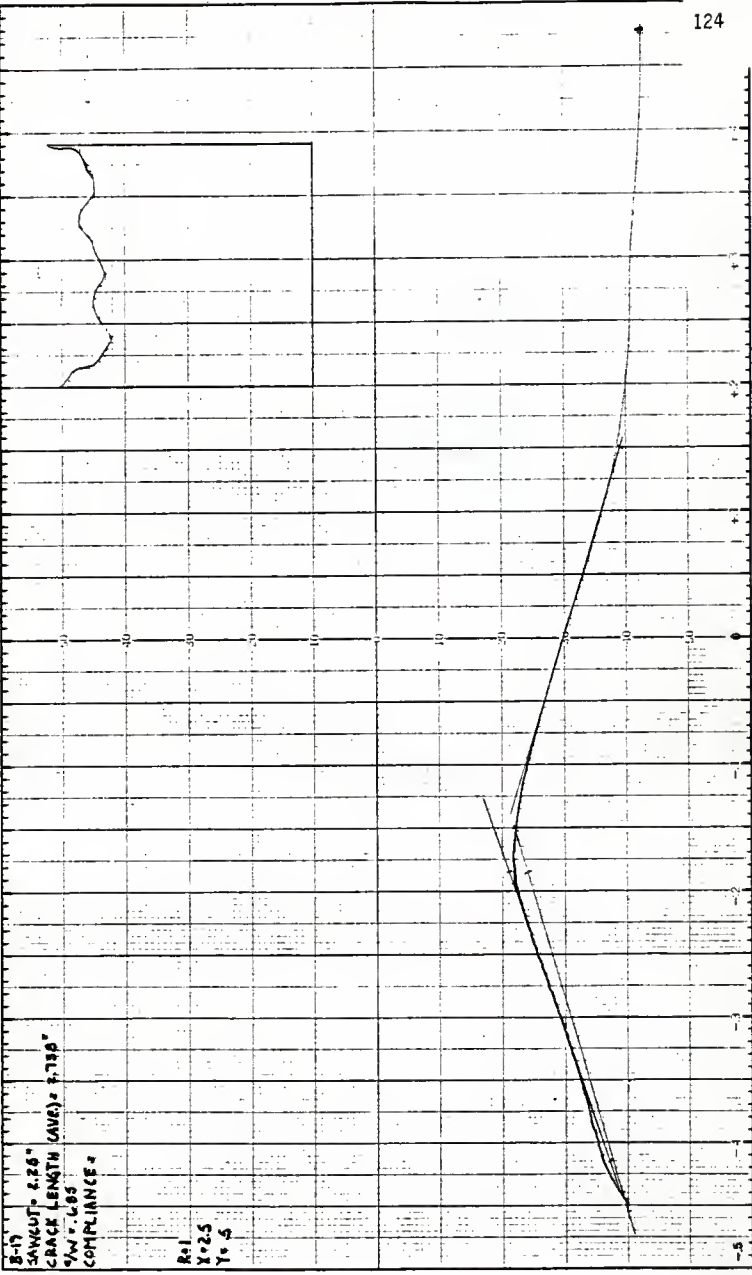
MHz  
Modulation Frequency

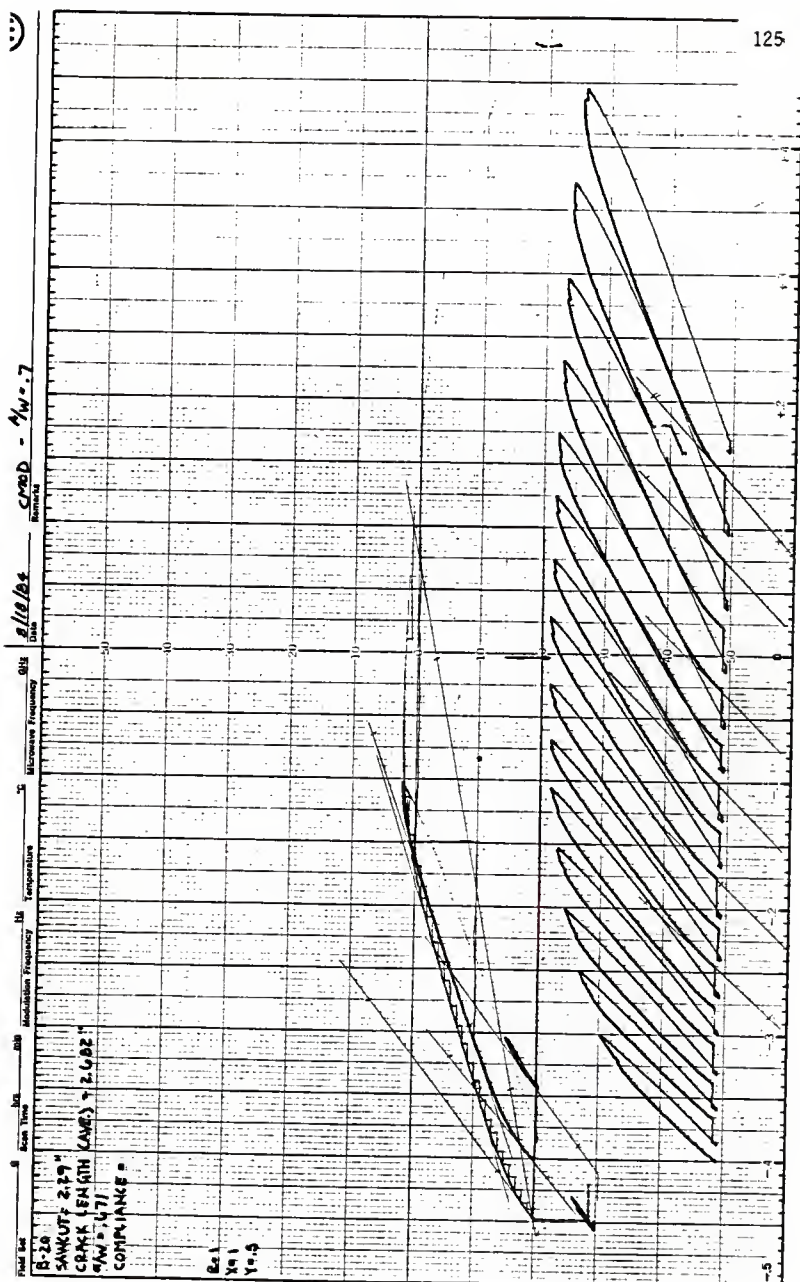
mm  
Scan Time

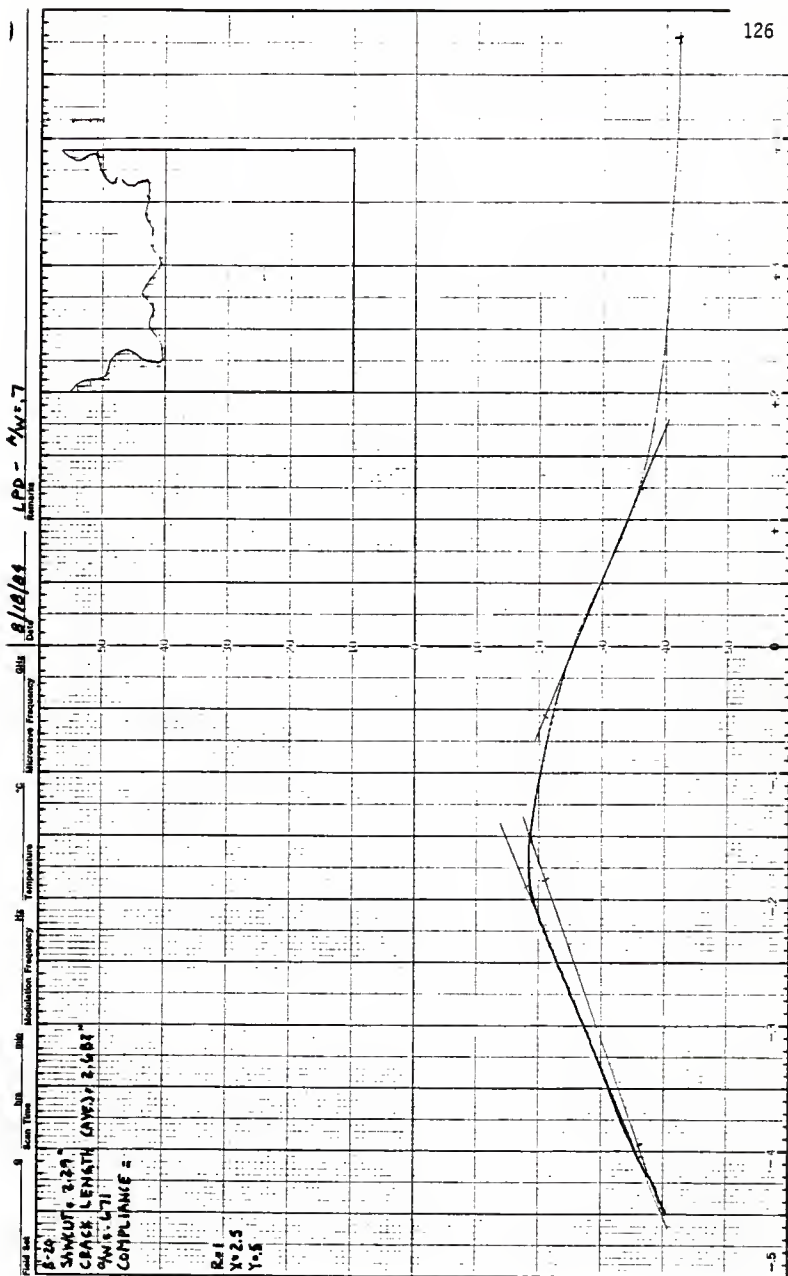
Field Set  
8-17

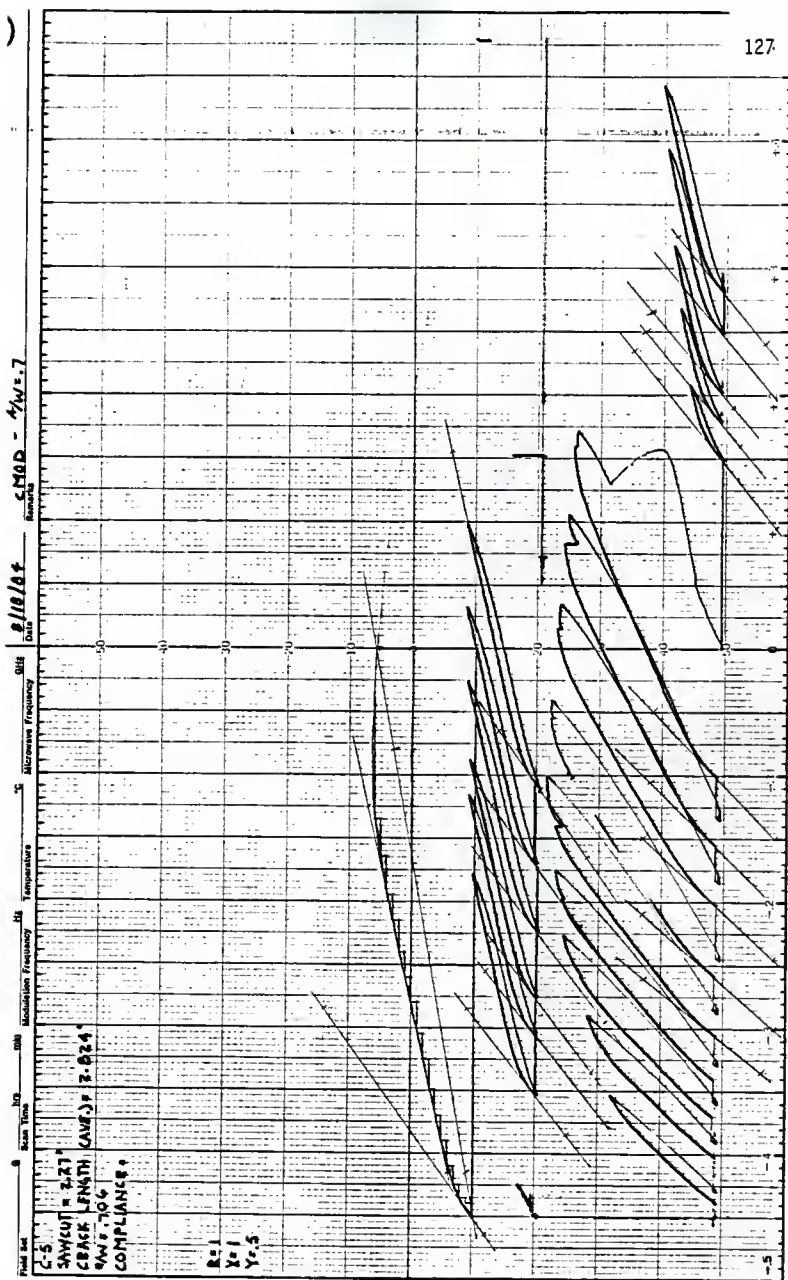
SAWGUT = 4.28"  
CRACK LENGTH (AVE) = 2.780"  
W = .695  
COMPLIANCE =

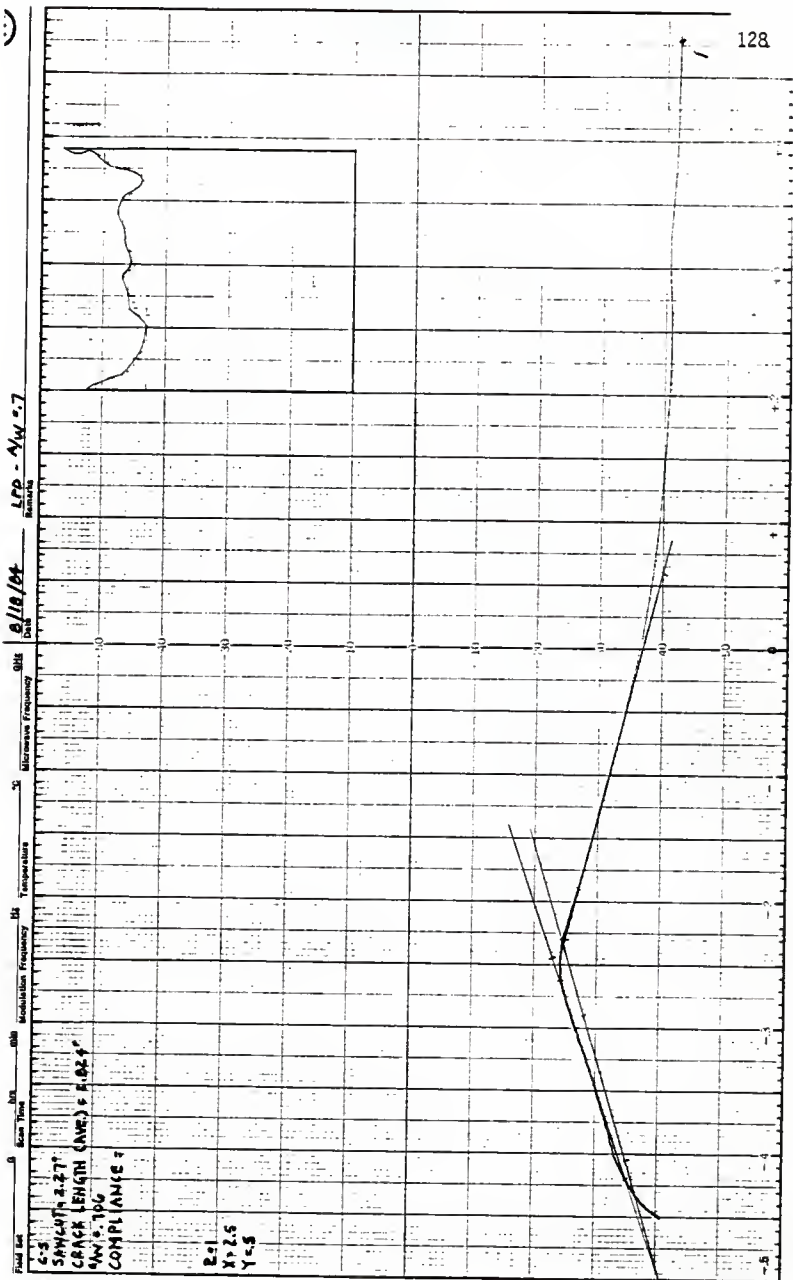
R = 1  
X = 2.5  
Y = 5











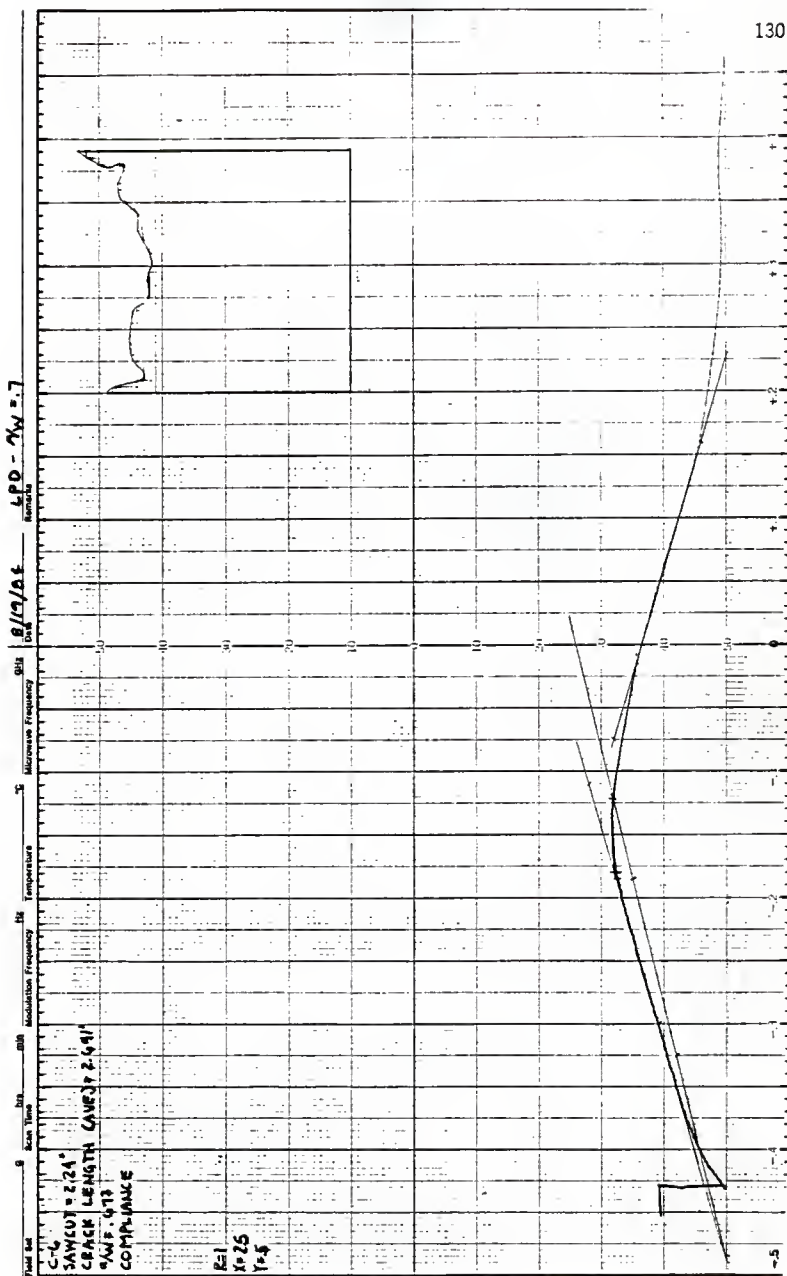
LFD -  $M_W = 7$

8/18/84

4-5  
 SAWCUT 3.2"  
 CRACK LENGTH (AVE) = 0.025"  
 MW = 7.0  
 COMPLIANCE ?

R=1  
 X=LS  
 Y=5







C-15  
A/W# 293

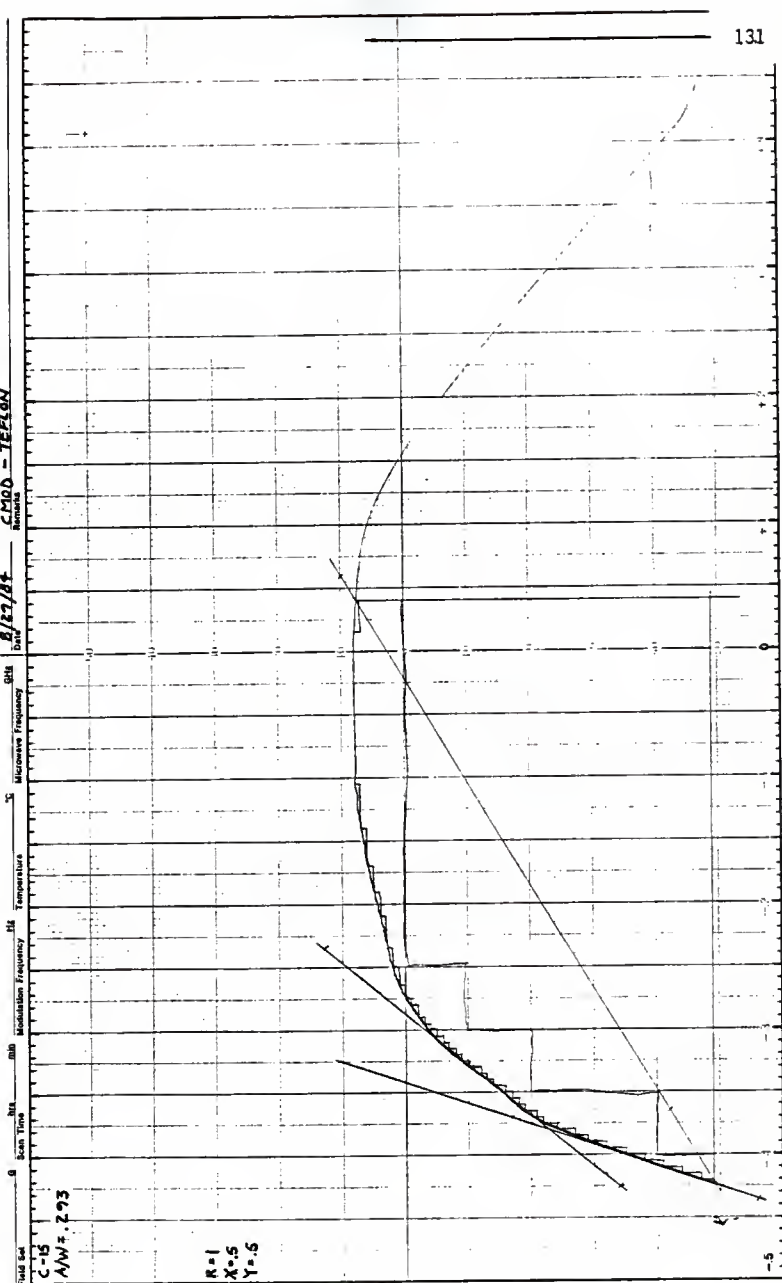
8/12/44

C-1500 - TELEPH

0 Scan Time  
 dB Modulation Frequency  
 dB Temperature  
 % Microwave Frequency  
 dB

Field No  
 C-15  
 A/W# 293

R=1  
 X=5  
 Y=5



LPD - TEFLON

8/28/81  
Date

GHS

MicroWave Frequency

Hz

Temperature

dB

Modulation Frequency

mb

Scan Time

0

10

20

30

40

50

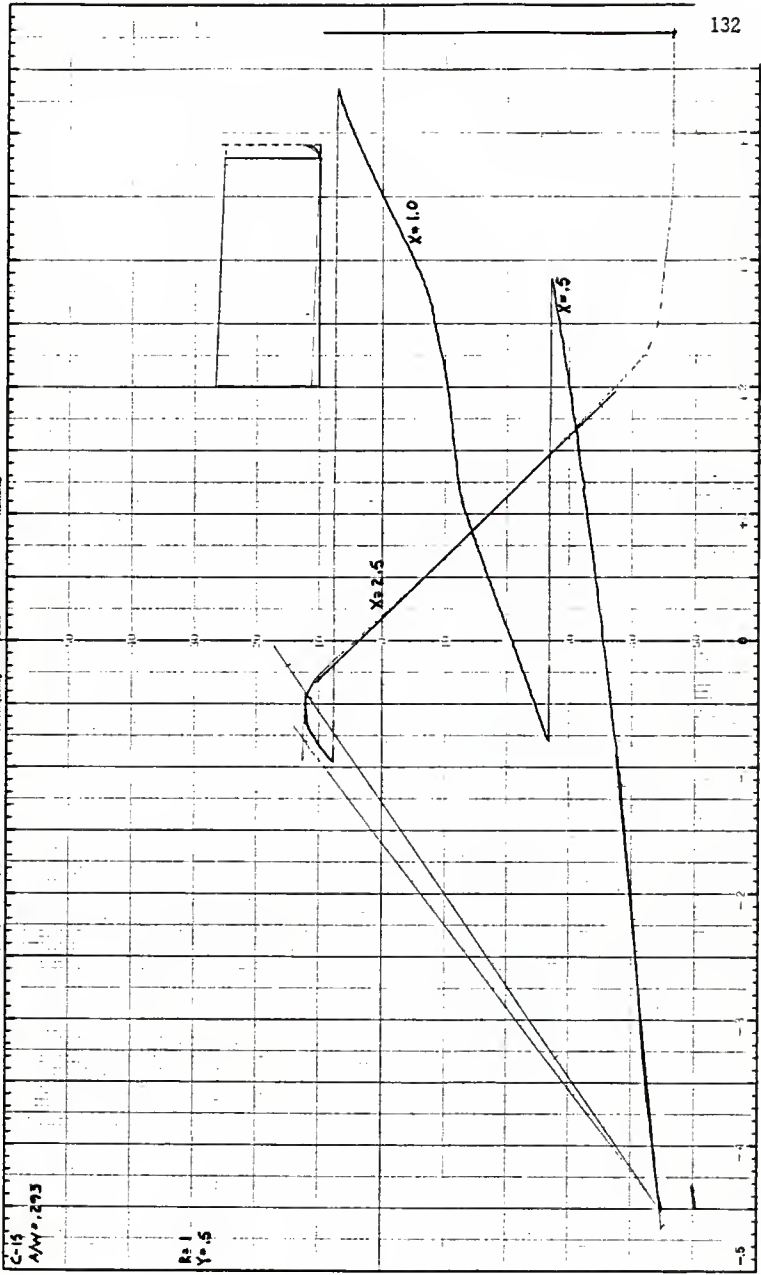
60

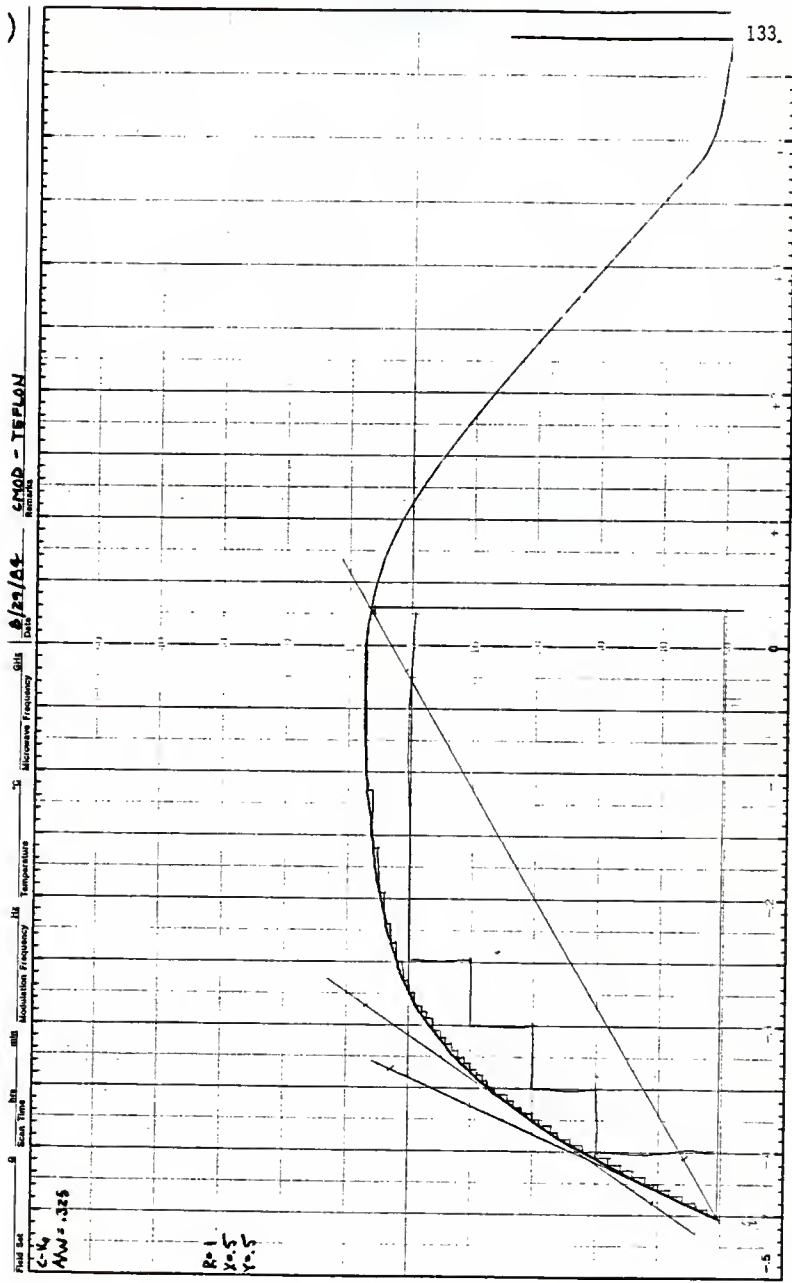
70

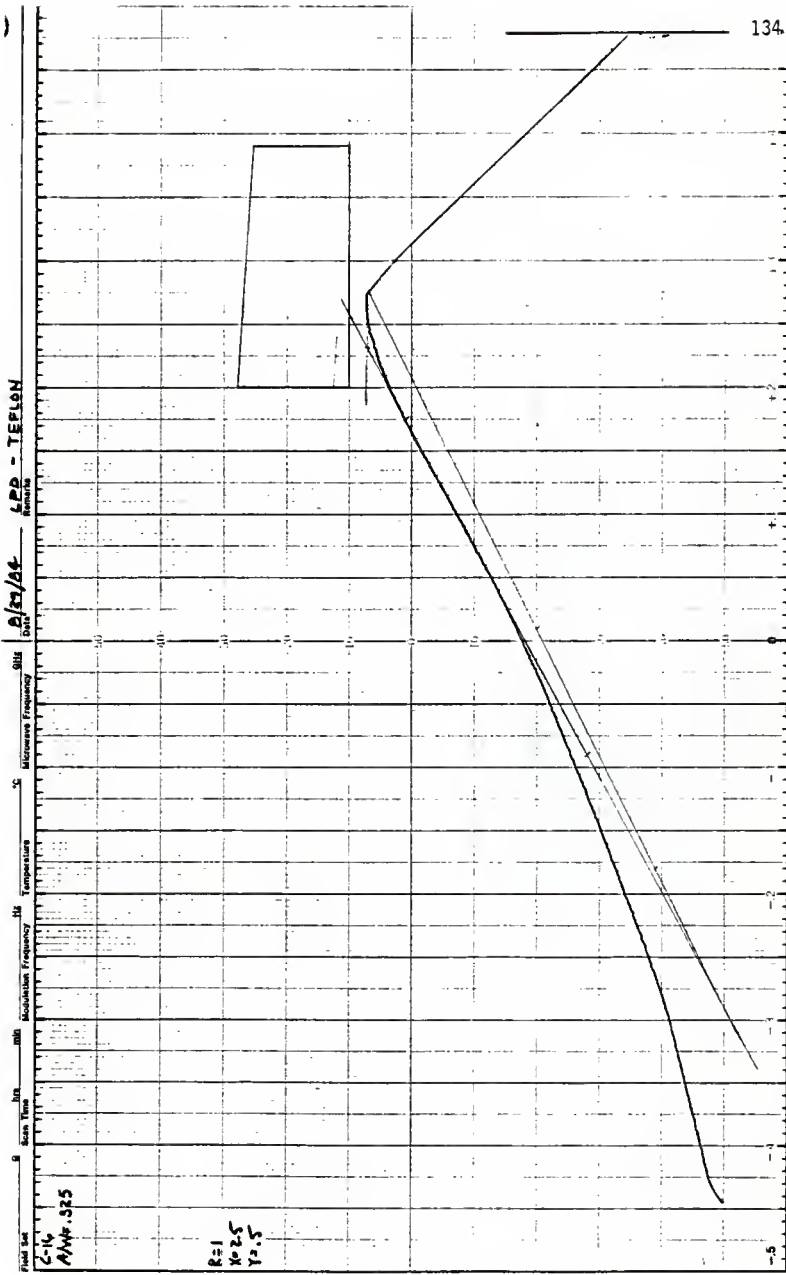
80

C-15  
AW-293

R=1  
Y=5







SP-5000 - TELEON

$\Delta/\Delta t$

dB

Microwave Frequency

°C

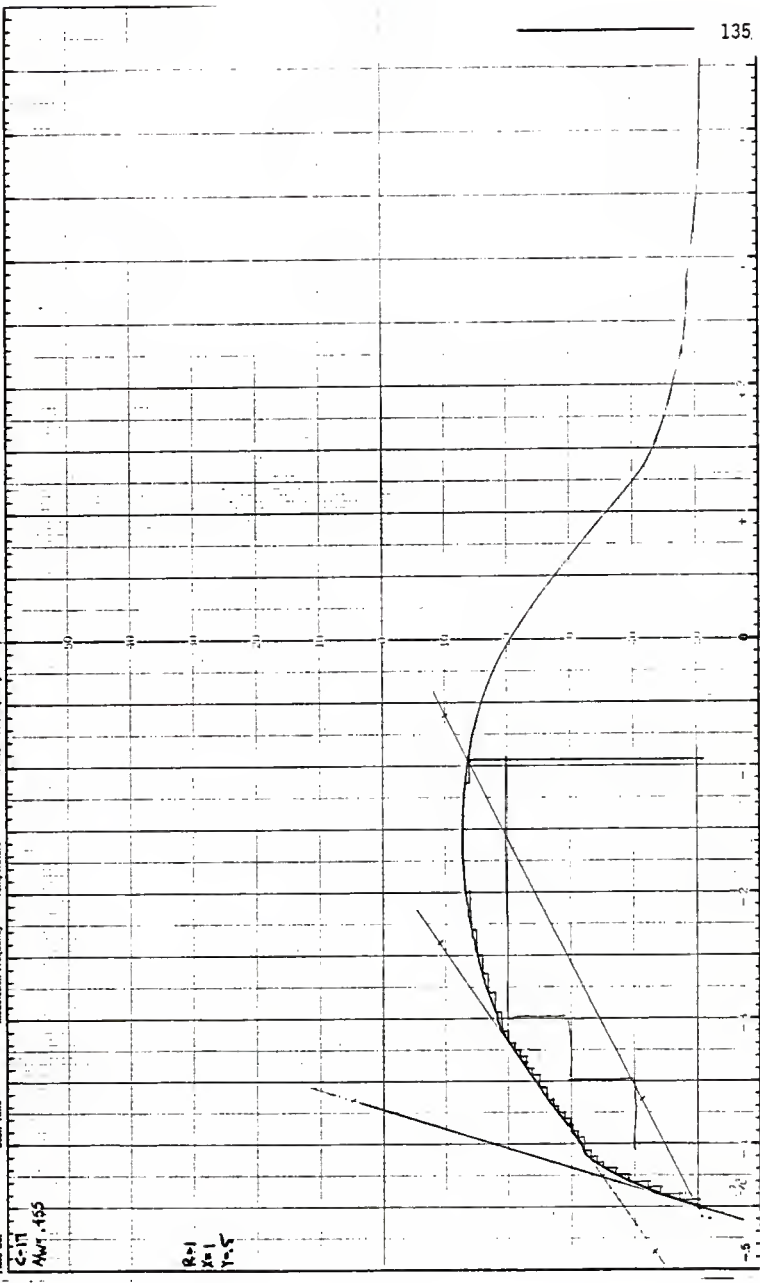
Temperature

Modulation Frequency

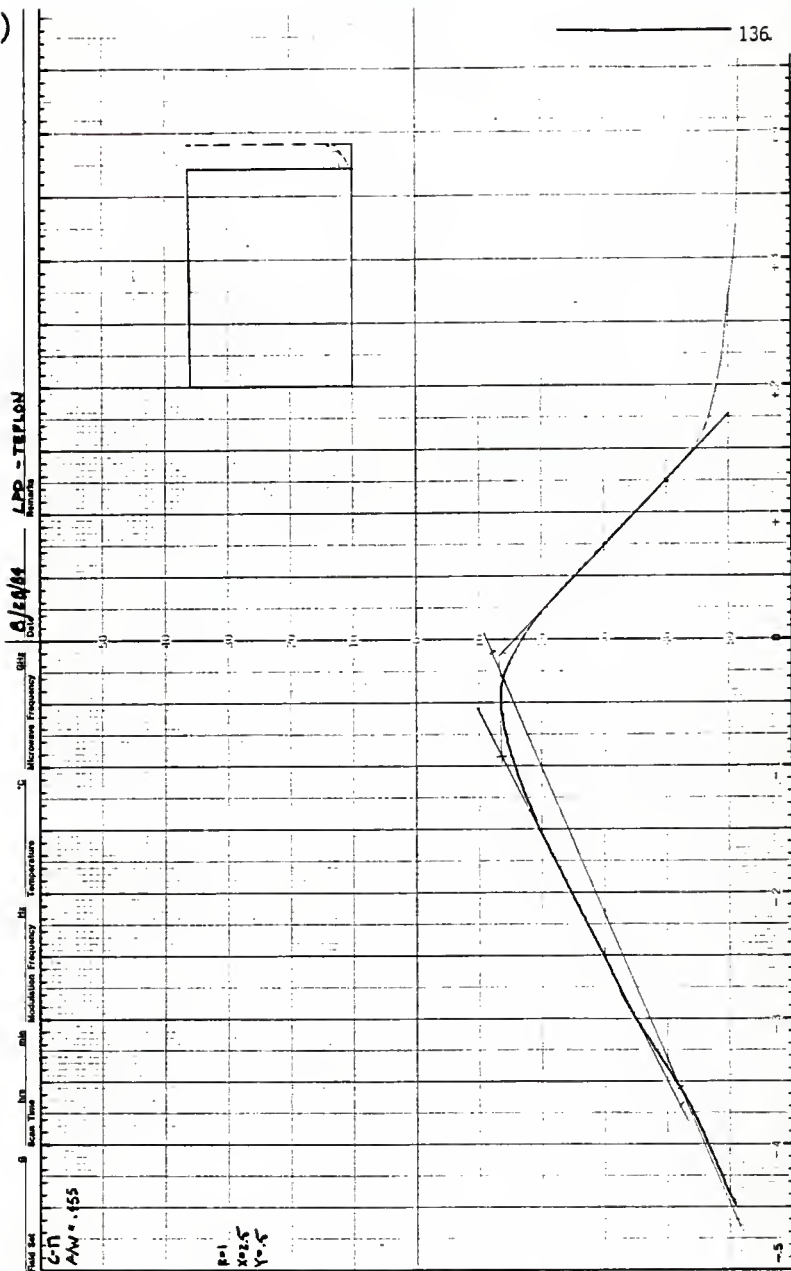
dB

Scale Time

Peak Set



)



CMRD - TEFLON

8/27/04

GHz

Microwave Frequency

Temperature

MHz

Modulation Frequency

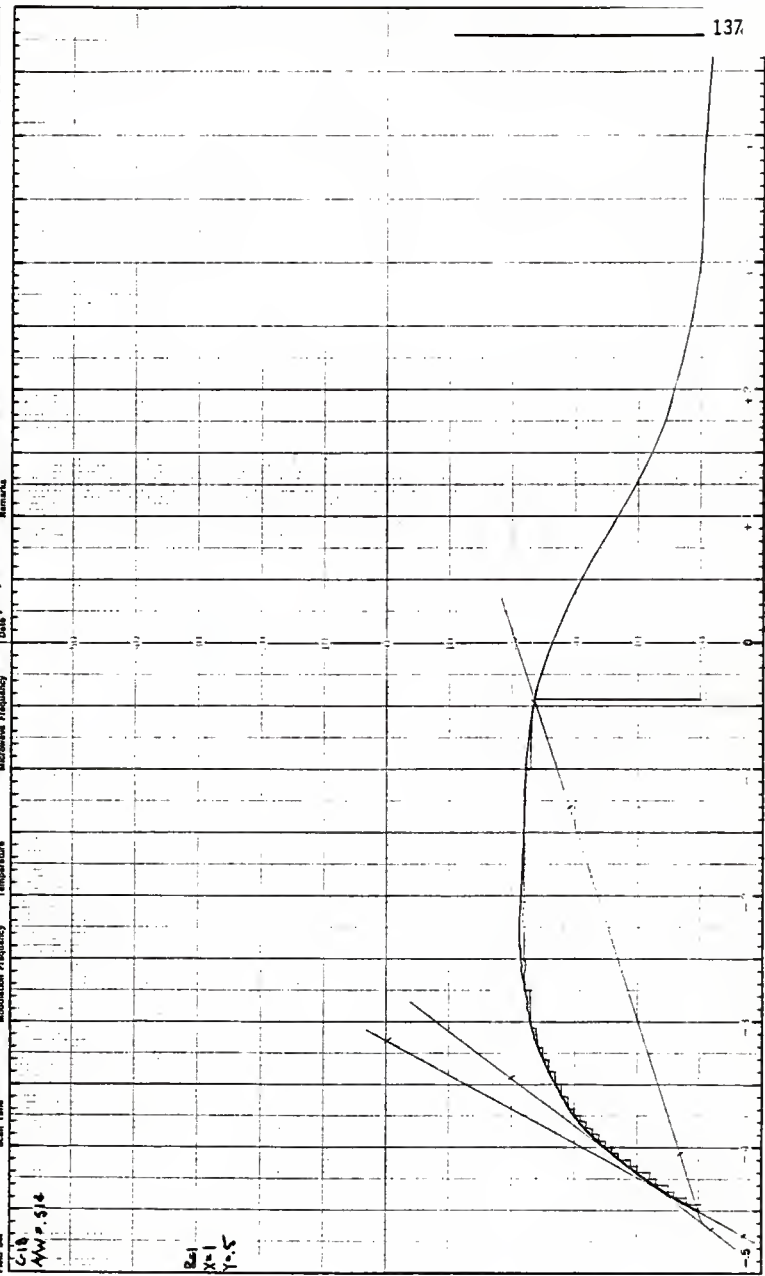
Scan Time

0

Feed 54

C-18  
MW # 514

B=1  
X=1  
Y=5



LPS - TELEON

8/25/84

GHE

MICROSECONDS

GHE

TEMPERATURE

MHz

Modulation Frequency

MHz

MHz

MHz

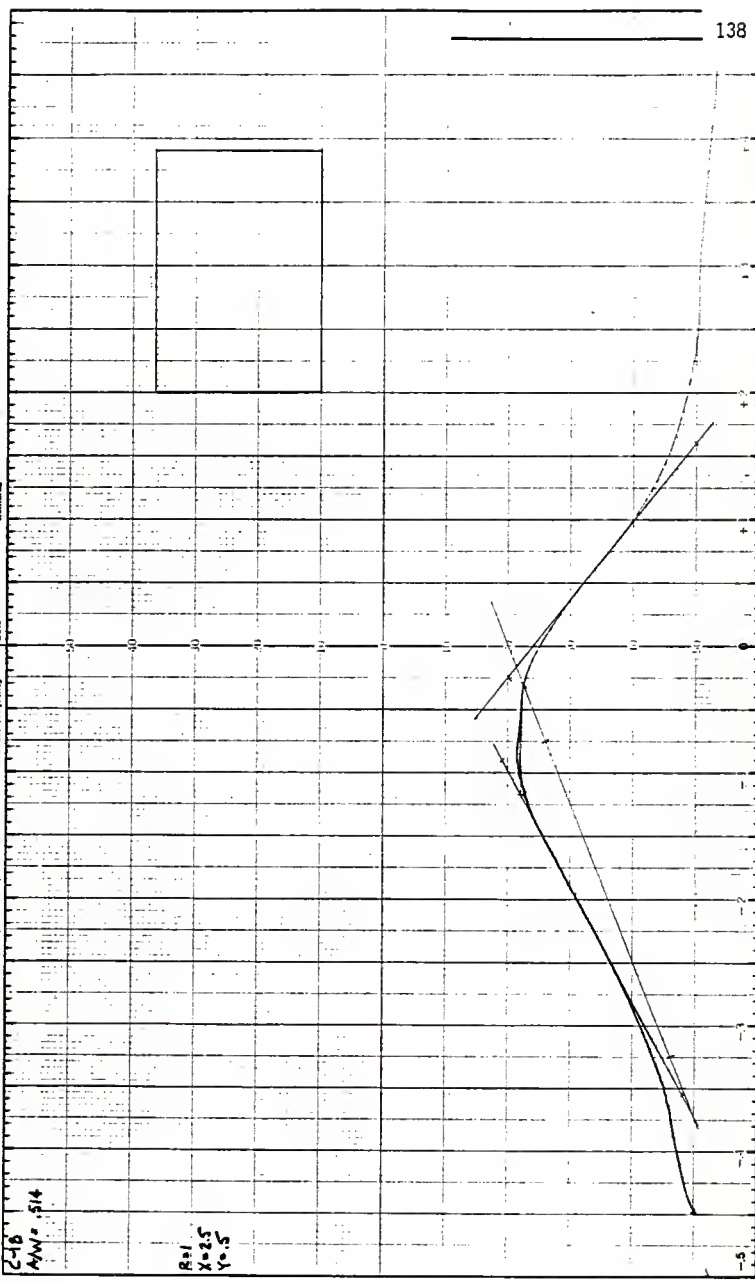
MHz

MHz

MHz

2-18

AW = .514

R = 1  
X = 2.5  
Y = 1.5



CHOP - TELEOP

6/20/64

0811

Microwave Frequency

Temperature

Modulation Frequency

Mill

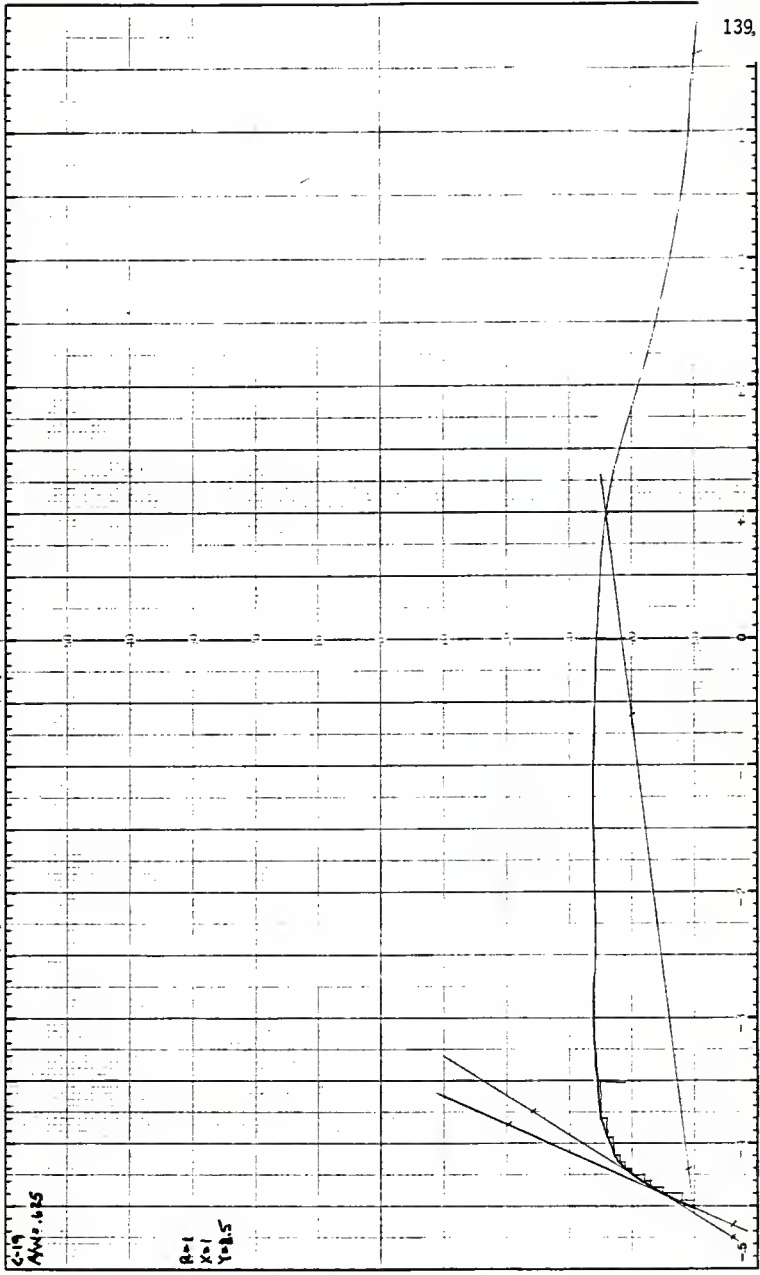
Scan Time

0

Field Unit

6-19  
444.625

R-1  
X-1  
Y-2.5



LPD-TEFLON

8/29/64

Date

GHz

Microwave Frequency

°C

Temperature

MHz

Modulation Frequency

dB

Sweep Time

dB

dB

dB

dB

dB

dB

dB

dB

dB

FWD 64

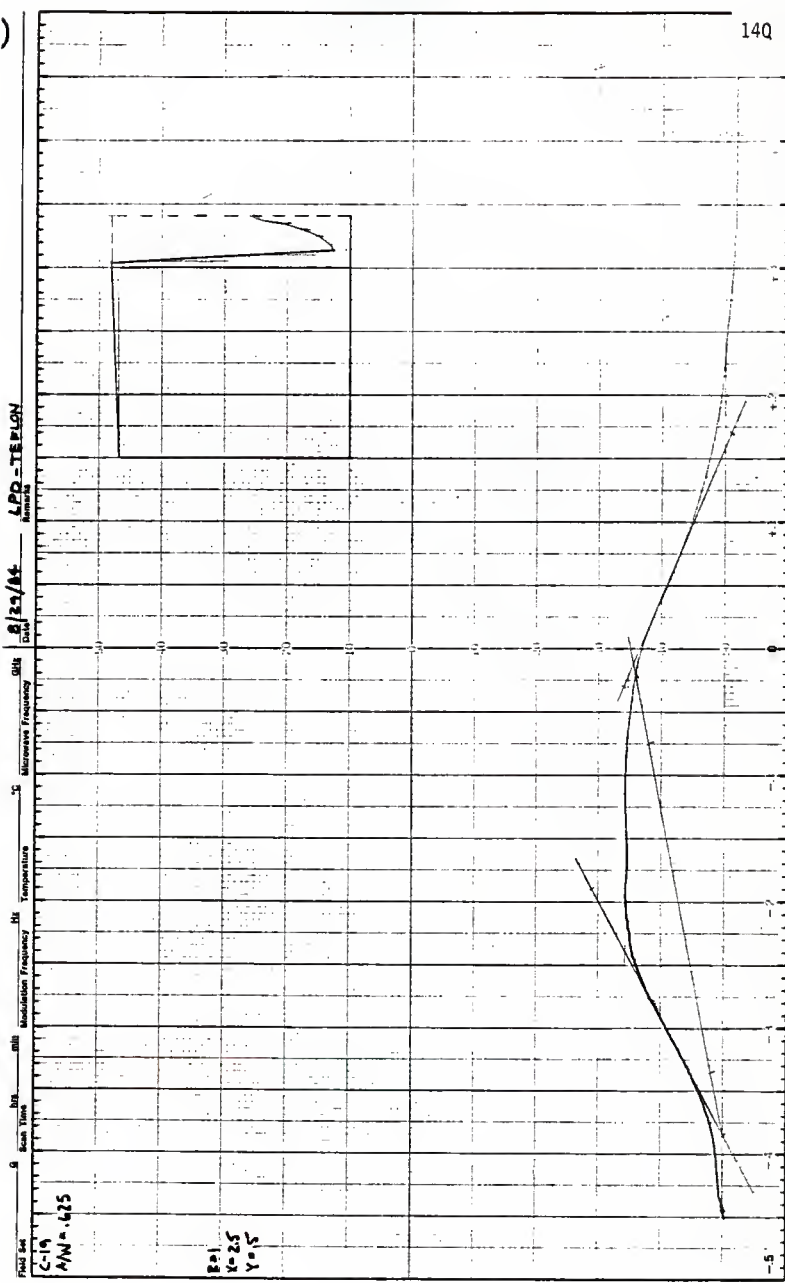
C-19

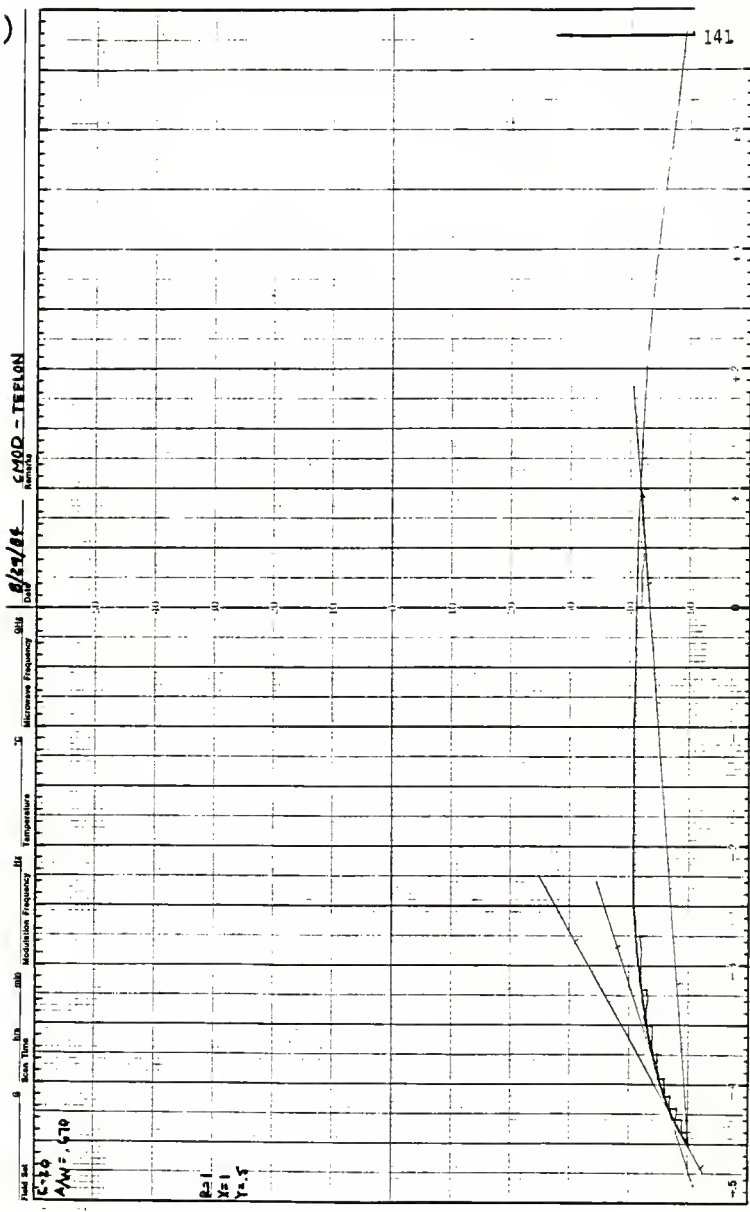
A/N = 425

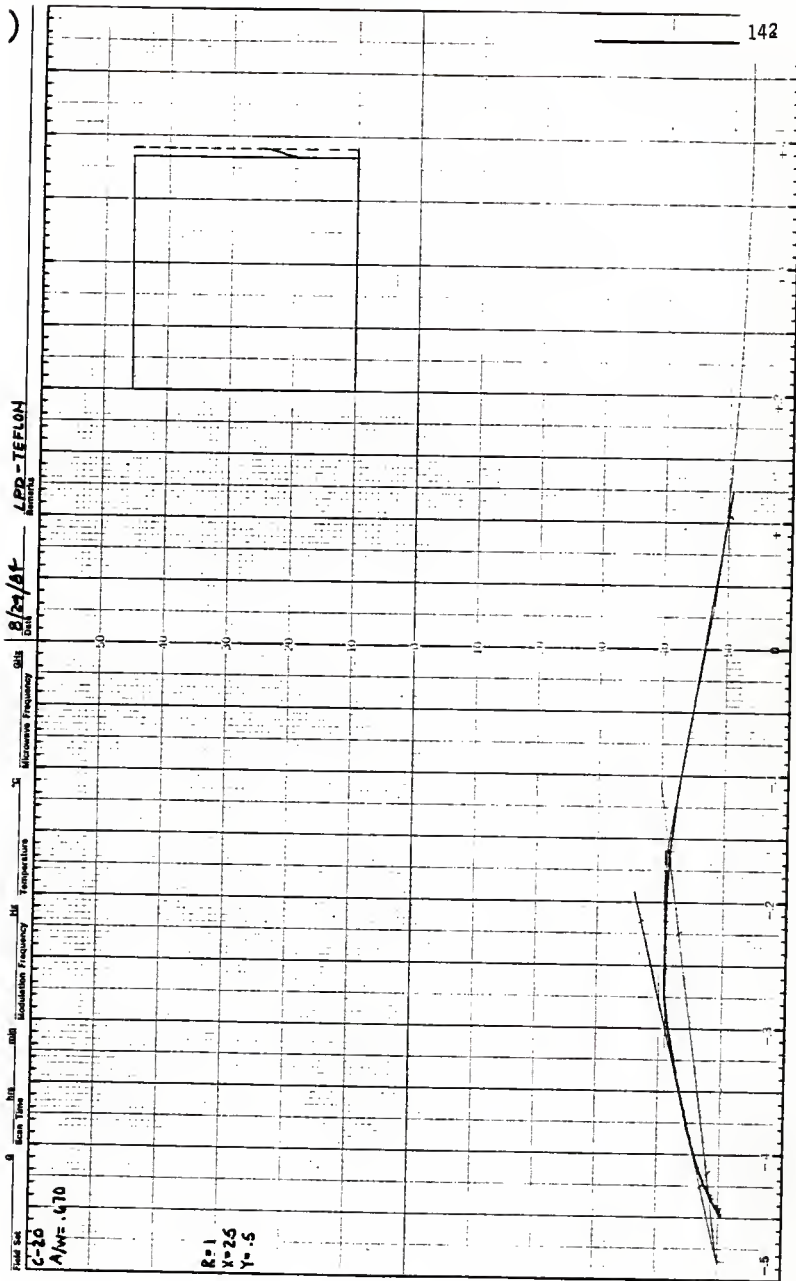
R=1

X=25

Y=15







LPP-TEFLON  
Material

8/24/84  
Date

GHz  
Microwave Frequency

dB  
Attenuation

MHz  
Square Root Frequency

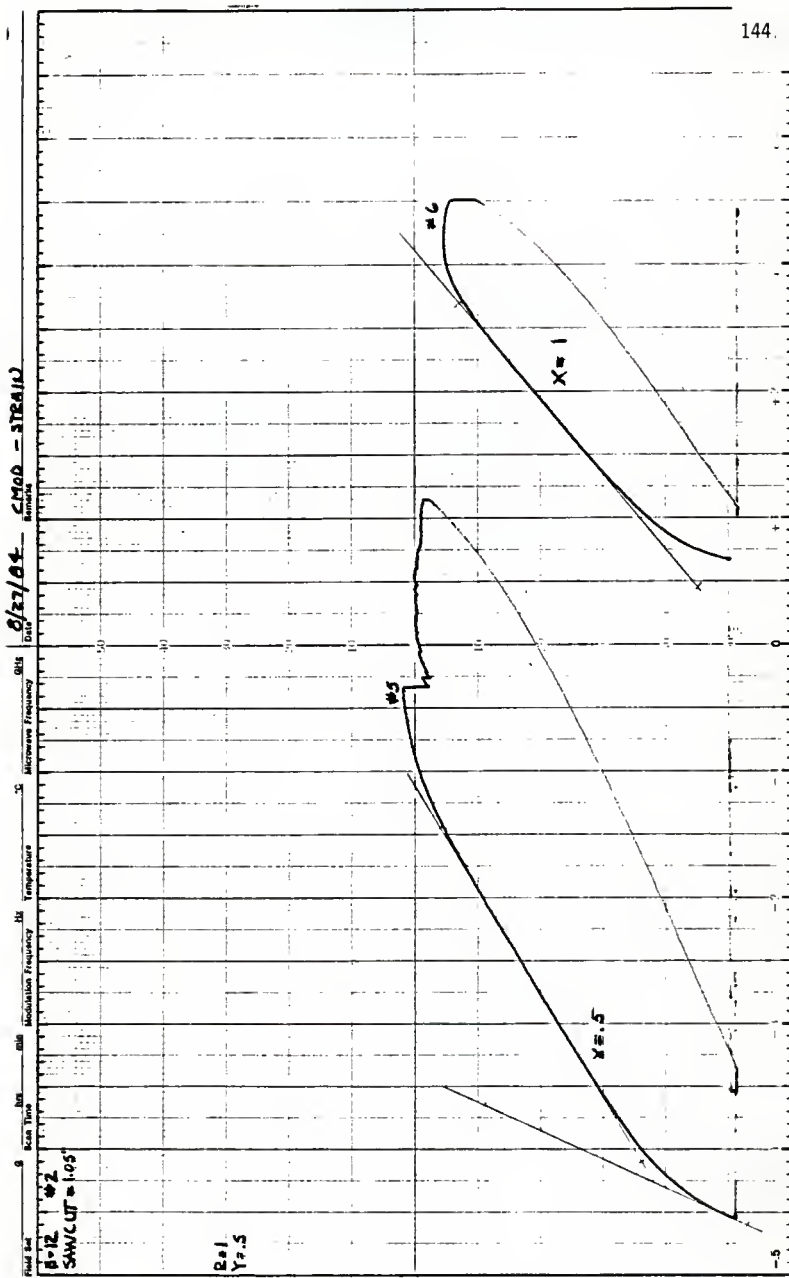
MHz  
Main Tone

Field Set  
C-25

A/W = 670

R = 1  
V = 25  
Y = .5





CMOD- STRAIN

8/27/84

MHz

Microwave Frequency

°C

KHz

Modulation Frequency

mb

Scan Time

sec

min

hr

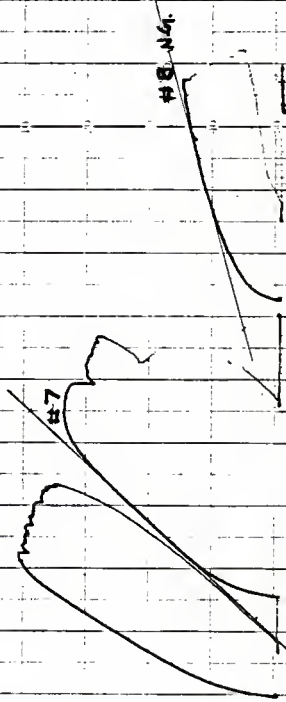
day

month

year

B-12  
W-3  
SAW CUT F 105

Re 1  
X=2.5  
Y=5



CMOD - STRAIN

8/24/84

Obs  
Microstrain Frequency

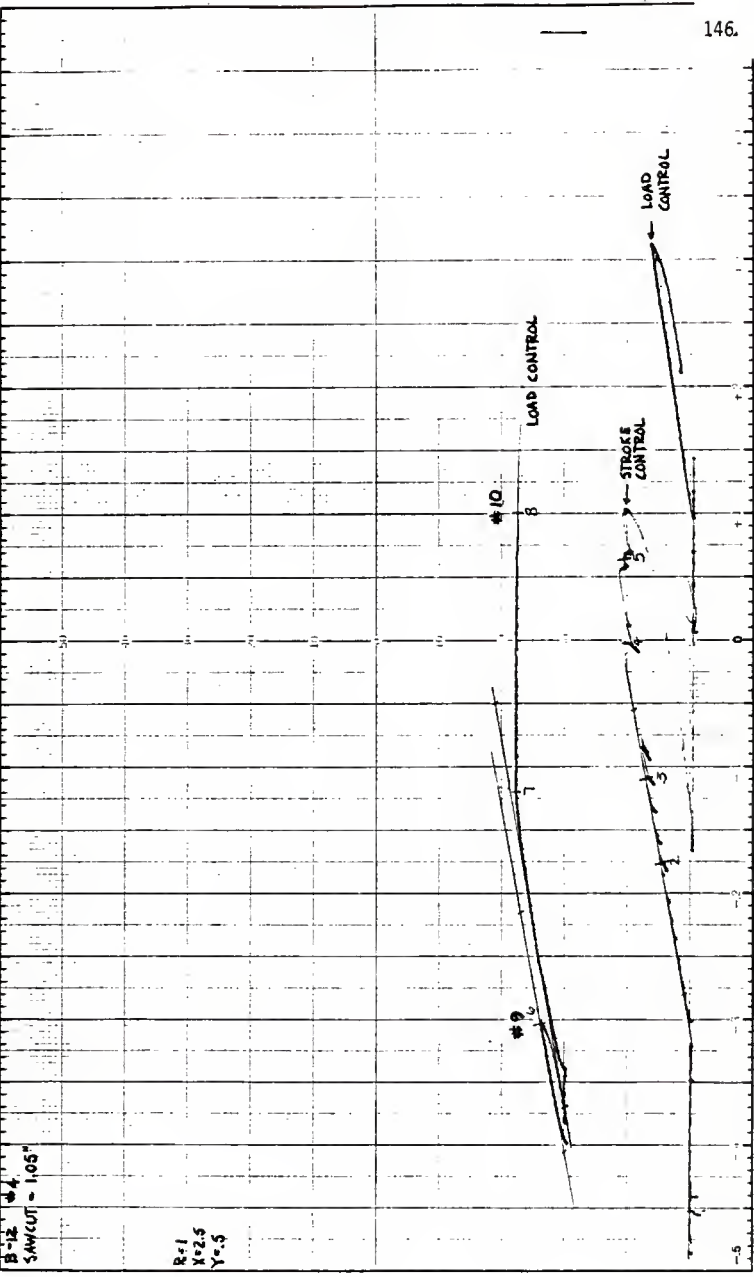
Temp

Hz  
Resonance Frequency

Hz  
Scan Time

Field Set  
B-12  
SW/CUT = 1.05"

R=1  
X=2.5  
Y=5





FRACTURE TOUGHNESS TESTING OF SMALL  
CONCRETE BEAMS

by

Sheryl Rood

B.S., Kansas State University, 1983

---

AN ABSTRACT OF A MASTER'S THESIS

submitted in partial fulfillment of the  
requirements for the degree of

MASTER OF SCIENCE

Department of Civil Engineering

KANSAS STATE UNIVERSITY

Manhattan, Kansas

1984

## Abstract

An extensive experimental program has been started in an attempt to verify the relationships between fracture parameters for plain concrete in bending. Results of a pilot program indicated promising results if the crack lengths at the onset of unstable crack growth were considered in the evaluation of the parameters. It was also demonstrated that the crack tip opening displacement (CTOD) may be a valid fracture criterion. This study attempts to verify these relationships with statistical confidence for three sizes of beams. The program presented here includes only one size of beam, 3 in. wide, 4 in. deep with a 15 in. span. Future studies will be made on larger beams.

These small beams were precracked using a modified compliance calibration technique and loaded to failure. Plots of load versus crack mouth opening displacement (CMOD) and load versus load point displacement (LPD) were obtained simultaneously. Five beams of each crack depth to beam depth ratio ( $a/w$ ) of 0.3, 0.5, and 0.7 were tested in three point bending. Two teflon-insert (prenotched) beams were loaded to failure. Additionally, one beam was instrumented with strain gages in order to obtain strain profiles ahead of the crack tip.

Results presented include stress intensity values ( $K_I$ ), energy release rates ( $G_I$ ) based on three methods of analysis, and CTOD values. Comparisons are made between these values based on unextended crack lengths and on extended crack lengths.